Seminar Report

On

EXPERIMENTAL INVESTIGATION OF MACHINING ASPECTS AND SURFACE MODIFICATION DURING SILICON, GRAPHITE AND TUNGSTEN POWDER MIXED EDM FOR DIFFERENT DIE STEELS

Submitted in partial fulfillment of the requirement for the award of the degree of

Master of Engineering

IN

PRODUCTION & INDUSTRIAL ENGINEERING

Submitted By

NAVEEN KUMAR

Roll No. 800982015

Under the Guidance of

Anirban Bhattacharya

Assistant Professor

Thapar University, Patiala

DEPARTMENT OF MECHANICAL ENGINEERING

THAPAR UNIVERSITY

PATIALA-147004, INDIA

JULY -2011

DECLARATION

I hereby declare that the thesis entitled **"EXPERIMENTAL INVESTIGATION OF MACHINING ASPECTS AND SURFACE MODIFICATION DURING SILICON, GRAPHITE AND TUNGSTEN POWDER MIXED EDM FOR DIFFERENT DIE STEELS"** is an authentic record of my study carried out as requirement for the award of degree of **Master of Engineering (Production and Industrial Engineering)** at **Thapar University, Patiala** under the guidance of **ANIRBAN BHATTACHARYA**,Assistant Professor, Department of Mechanical Engineering, Thapar University, Patiala during **July 2010 to June 2011.** The matter embodied in this report has not been submitted in part or full to any other university or institute for the award of any other degree.

Naveen

(Naveen Kumar)
Reg. No. 800982015

This is to certify that above declaration made by the student concerned is correct to the best of my knowledge and belief.

Anirban Bhattacharya

(ANIRBAN BHATTACHARYA)
Assistant Professor,
Department of Mechanical Engineering,
Thapar University,
Patiala - 147004

Countersigned by:

Dr. AJAY BATISH
Professor and Head,
Department of Mechanical Engineering,
Thapar University,
Patiala -147004

Dr. S.K. MOHAPATRA
Dean of Academic Affairs,
Thapar University,
Patiala-147004

ACKNOWLEDGEMENT

With deep sense of gratitude I express my sincere thanks to my guide, ***Mr. Anirban Bhattacharya*** for their valuable guidance, proper advice and constant encouragement during my work on this seminar.

I also feel very much obliged to ***Dr. Ajay Batish***, Professor & Head, of Mechanical Engineering Department.

I am grateful to the Mr. Baljeet Singh for helping for assisting me in my thesis work.

I am also very thankful to my friends for their cooperation.

NAVEEN KUMAR

Roll No: 800982015

ABSTRACT

Electric discharge machining (EDM) is one of most popular machining methods to manufacture dies and press tools because of its capability to produce complicated shapes and machine very hard materials. The present study has been done to study the effect of different input parameters, namely, current, work piece material, dielectric medium, pulse on time, powder concentration and powder on the MRR, TWR, micro hardness, micro structure, surface roughness. Measurement of overcut size and profile/geometric accuracy has been studied. The effect of various input parameters on output responses have been analyzed using Analysis of Variance (ANOVA). Deposition of the powder material either in pure form or in compound form was also studied. Optimization of the process parameters has been studied.

CONTENTS

LIST OF FIGURES

LIST OF TABLES

ABBREVATIONS

ANOVA	Analysis of Variance
DC	Direct Current
DOF	Degree of Freedom
EDM	Electric Discharge Machining
PMEDM	Powder Mixed Electric discharge Machining
HCHCr	High-Carbon High-Chromium
HDS	Hot Die Steel
RC	Relaxation Circuit
MRR	Material Removal Rate
TWR	Tool Wear Rate
WR	Wear ratio
SR	Surface Roughness
OC	Overcut
SEM	Scanning Electron Microscope
X-RD	X-Ray diffraction
S/N	Signal to Noise Ratio

NOTATIONS

OA	Orthogonal Array
A	Dielectric
B	Workpiece Material
C	Electrode Material
D	Powder concentration
E	Current
F	Pulse on Time
G	Powder
Si	Silicon
Gr	Graphite Electrode
W	Tungsten
W-Cu	Tungsten-Copper Electrode
CI	Confidence Interval
SS	Sum of Squares

CHAPTER 1

INTRODUCTION

1.1 INTRODUCTION TO NON-CONVENTIONAL MACHINING

Traditional machining processes work on the principle that the tool is harder than the work-piece. Some materials, however, are too hard or too brittle to be machined by conventional methods. The use of very hard nickel-based and titanium alloys by the aircraft engine industry, for example, has stimulated nonconventional machining methods. By conventional methods their machining is not only costly but also results into poor surface finish and shorter tool life. Production of complex shapes with better surface finish, precise tolerances and higher production rates in such materials by traditional methods is even more difficult. To overcome these difficulties, a number of newer machining methods have been developed which are termed as non-traditional machining processes or advanced machining processes. Such processes which can accurately and easily machine the most difficult-to-machine materials to intricate and accurate shapes. These methods are not conventional in the sense that material removal does not occur due to plastic deformation and with the formation of chips.

These methods have found successful applications in several important industries for machining of components having complicated shapes made of hard materials like tungsten carbides, super-alloys, ceramics, refractory materials etc. Newer machining methods can be classified on the basis of the type of energy they employ for purpose of metal removal. Broadly speaking they can be classified as below:

1. Mechanical Metal Removal Processes.

2. Electro-chemical Metal Removal Processes.

3. Thermal Metal Removal Processes.

Some of them can be used only for electrically conductive materials, while others can be used for both electrically conductive and electrically non-conductive materials.

In mechanical advanced machining methods, (abrasive jet machining, ultrasonic machining, and water jet machining) kinetic energy of either abrasive particles or water jet is utilized to remove material from the work piece.

In electro-thermal methods, (laser beam machining, electron beam machining, and plasma arc machining), the energy is supplied in the form of heat and energy is concentrated onto a small area of work piece resulting in melting, or vaporization and melting both.

Electrochemical (electro chemical machining), is a process which is reverse of electroplating. In some of above mentioned above cases, productivity can be increased as compared to conventional methods either by performing the operations faster or by reducing the total number of manufacturing operations.

In nonconventional machining methods, there is no direct contact between the tool and the work piece; hence the tool need not be harder than the work piece. The conventional machining processes are inadequate to produce complex geometrical shapes in the hard and temperature resistant alloys and die steels.

1.2 INTRODUCTION TO ELECTRICAL DISCHARGE MACHINING (EDM)

Electrical discharge machining (EDM) is one of the earliest non-traditional machining processes. This process enables machining of any material, which is electrically conductive, in any shape, irrespective of its hardness or strength. Even highly delicate sections and weak materials can be machined without any fear of distortion because there is no direct contact between the tool and the work piece. But its low efficiency and poor surface finish have been the key problems restricting its further development. The tool electrode and the work are held at an accurately controlled distance from one another, which are dependent on the operating conditions and referred to as spark gap based on thermoelectric energy between the work piece and an electrode. A pulse discharge occurs in a small gap between the work piece and the electrode and removes the unwanted material from the parent metal through melting and vaporising. The electrode and the work piece must have electrical conductivity in order to generate the spark. Electrical discharge machining (EDM) is been widely used to produce dies and molds [1-3].

1.3 HISTORY OF ELECTRIC DISCHARGE MACHINING

The origin of electrical discharge machining (EDM) takes place in 1770 when English scientist Joseph Priestly discovered the erosive effect of electrical discharges. More than hundred years elapsed before some practical use was affected. In the 1930s, attempts were made for the first time to machine metals and diamonds with electrical discharges. Erosion was caused by intermittent arc discharges occurring in air between the tool electrode and workpiece connected to a DC power supply. These processes were not very precise due to

overheating of the machining area and may be defined as “arc machining” rather than “spark machining” [4]. In 1943, Soviet Scientists B.R. Lazarenko and N.I. Lazarenko decided to exploit the destructive effect of an electrical discharge and developing a controlled process for machining materials that are conductors of electricity. The first British patent was granted to Rudorff in 1950. USA, Japan and Switzerland developed their machines around 1952. In 1960, EDM discharge analysis, mono discharge modeling and physical mathematical modelling came into existence. In 1975 to 1985, multi arc analysis, discharge classification, adoptive control optimizations [ACO] and adoptive control constraints were studied and used for EDM Process. Jeswani [5] reported the effect of addition of graphite powder to kerosene used as a dielectric fluid in EDM and researchers tried many other additives to improve and modify the EDMed surface. In 1980, the event of computer numerical control (CNC) in EDM brought tremendous advances in improving efficiency of the machining operation. In 1985-1990 brought revolution in improvement of the process. During this period pulse recognition, real time analysis, A.C. tool wear analysis, controls and expert systems for wire EDM machine [WEDM] touched the new heights of performance. In 1990-95 brought the parametric approach, Neutral networks and Fuzzy controllers. Modern era brought in various new aspects in EDM machining such as micromachining by EDM and machining without liquid dielectric. EDM of new conductive materials changed the total scenario. Now EDM is much accepted technique for material removal next to CNC Milling. This process enables machining of any material, which is electrically conductive, irrespective of its hardness, shape or strength [6].

1.4 WORKING PRINCIPLE OF EDM

When a difference of potential is applied between two conductors immersed in a dielectric fluid, the fluid will ionize if the potential difference reaches a high enough value and a spark will occur. If the potential difference is maintained, then the spark will develop into an arc. If the potential difference decreases, the fluid will de-ionize and the discharge will cease. In electric discharge machining process (Figure 1.1), the control of erosion of the metal is achieved by the rapidly recurring spark discharges produced between two electrodes, one tool and the other workpiece, and spark impinging against the surface of the workpiece which must be an electrically conductive body. A suitable gap known as “spark gap” is maintained between the tool and the workpiece by a servomotor which is actuated by the difference between a reference voltage and the gap breakdown voltage, which feeds the tool downwards towards the workpiece.

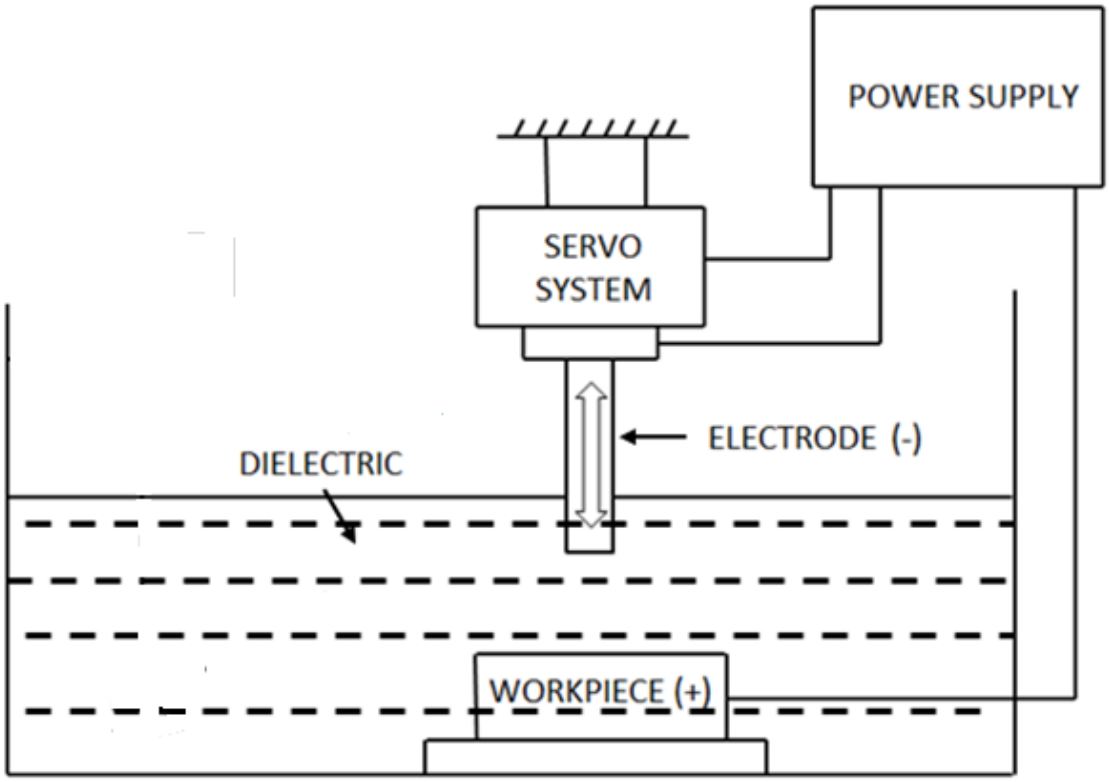

Figure 1.1: Schematic Diagram of EDM Process

The dielectric fluid fills up spark gap. The dielectric fluid may be typical hydrocarbon oil or de-ionized water which helps in cooling down the tool and the workpiece, cleans the inter-electrode gap, and concentrates the spark energy into small cross-sectional area under the electrode. Each electric discharge or spark causes a focused stream of electrons to move with a very high velocity and acceleration from the cathode towards the anode, and ultimately creates compression shock waves on both the electrode surfaces, particularly at high spots on the workpiece surface, which are closest to the tool (Figure 1.2). The generation of compression shock waves, develops a local rise in temperature. The whole sequence of operation occurs within a few microseconds. However, the temperature of spot hit by the electrons is of the order of 10,000°C. This temperature is sufficient to melt a part of the metals. The force of electric and magnetic fields caused by a spark produce a tensile force and tear off particles of molten and softened metal from this spot in the work piece.

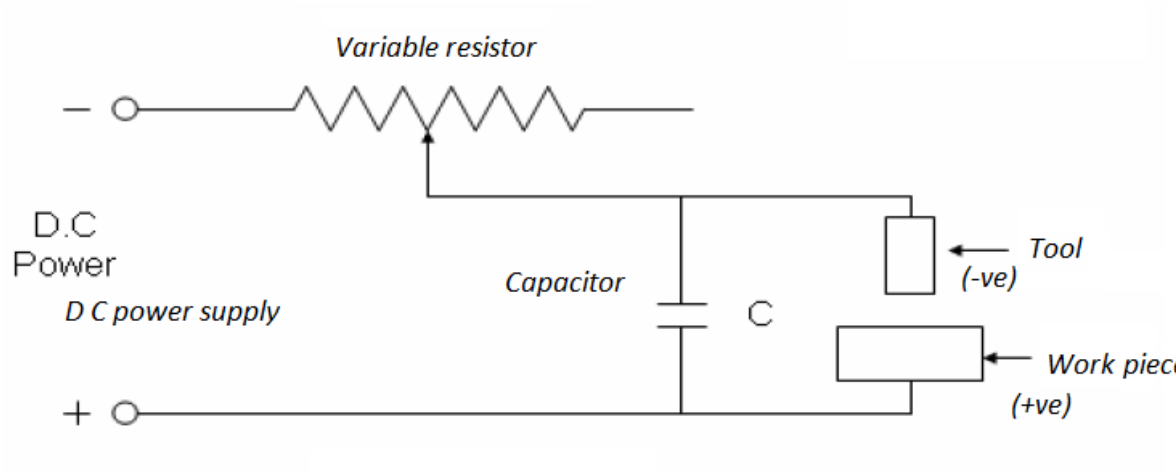

Figure 1.2: Working Principle of EDM

A part of the metal may vaporize and fill up the gap. The metal is thus removed in this way from the work piece. The electric and magnetic fields on the heated metal cause a compressive force to act on the cathode tool so that metal removal from the tool is at a slower rate than that from the work piece.

Comparatively less metal is eroded from the tool as compared to the workpiece due to following reasons:

a) The momentum with which positive ions strike the cathode surface is much less than the momentum with which the electron stream impinges on the anode surface.

b) A compressive force is generated on the cathode surface by spark which helps reduce tool wear [2].

Hence, the work piece is connected to the positive terminal and the tool to the negative terminal.

The variation of capacitor voltage with time in above circuit is shown in Figure1.3. A major portion of the time of machining is spent on charging the capacitors.

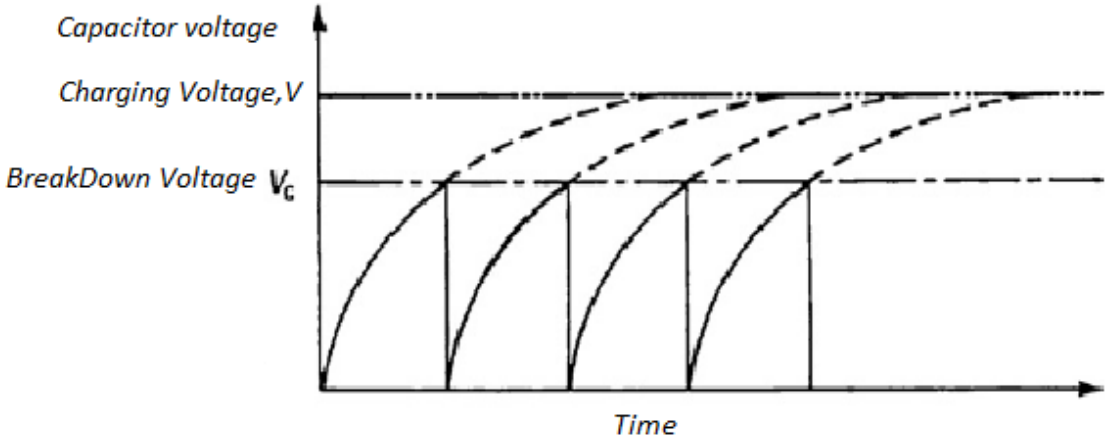

Figure 1.3: Variation of capacitor voltage with time [7]

1.5 PROCESS PARAMETERS OF EDM

1.5.1 Discharge Voltage

Discharge voltage in the EDM is related to the spark gap and breakdown strength of the dielectric Current will flow into the system and before it happen the open gap voltage increases until it has created a path that will go through the dielectric. The path that is mentioned before is called the ionization path. When the current is flowing, voltage drops and stabilizes at the working gap level. The pre-set voltage determines the width of the spark gap between the leading edge of the electrode and the work piece [9]. If we set the voltage to a high value then the gap will increase, increasing the gap will improve the flushing conditions and helps to stabilize the cut. The open circuit voltage also have an impact to the system, as we increase the open circuit voltage tool wear rate (TWR) and surface roughness increases because the field strength increases. The variation of discharge voltage with time is shown in Figure 1.4.

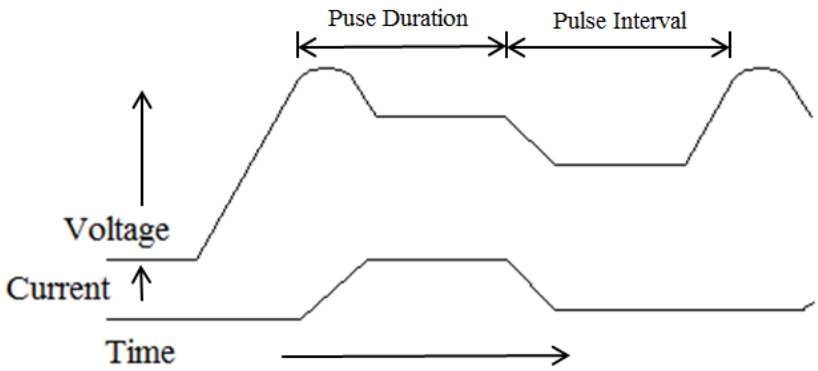

Figure 1.4: Actual profile of single EDM pulse

1.5.2 Electrode Polarity

Polarity means the electric condition determining the direction of the current flow relative to the electrode. The polarity of the electrode can be either positive or negative depending on the application. Some electrodes give better results when the polarity is changed. There are types of polarity.

- Straight or normal polarity
- Reverse polarity

Straight or normal polarity is that in which the tool is positive and the workpiece is negative, while in reverse polarity, tool is negative and the work piece is positive. The concept of normal and reverse polarity is shown in Figure 1.5.

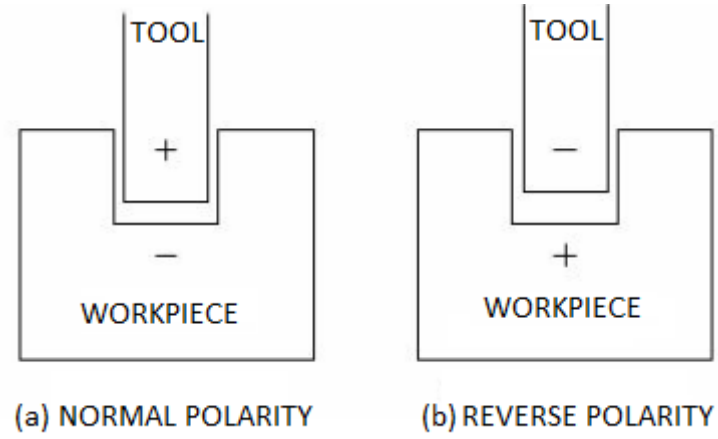

Figure 1.5: Diagram showing Electrode Polarity

Polarity can affect processing speed, finish, wear and stability of the EDM operation. It has been proved that MRR is more when the tool electrodes are connected at positive polarity(+) than at negative terminal(-).This may be due to transfer of energy during the charging process is more in this condition of machining. When a electrical discharge is generated electrons dispatch from the negative polarity collides with neutral molecules between the work piece and electrode which is responsible for ionization process in EDM. However, ionization is taken because the electron arrives at the positive terminal of the surface. The negative polarity is more desirable as compared to positive polarity [10]. The researcher concluded this is because the MRR is higher and better surface finish is produced as MRR is dependent on anode potential drop.

1.5.3 Pulse on Time (T_{on})

Each cycle has an on-time and off-time .Pulse on time is the time period during which machining is performed. Pulse on time is also referred as pulse duration. Metal removal is directly proportional to the amount of energy applied during the on-time [9]. The energy is controlled by the peak current and the length of the pulse on-time. The resulting crater will be deeper and broader than a crater produced by a shorter on-time. When the pulses with small on time are used, material removal by electron bombardment is predominant due to higher response rate of less massive electrons. However, when the longer pulses are used, energy sharing by positive ions is predominant and material removal rate decreases. When the electrode polarities are reversed, longer pulses are found to produce higher MRR. When the optimum on-time for each electrode-work material combination is exceeded, material rate starts to decrease. The pulse on time is shown in Figure1.6.

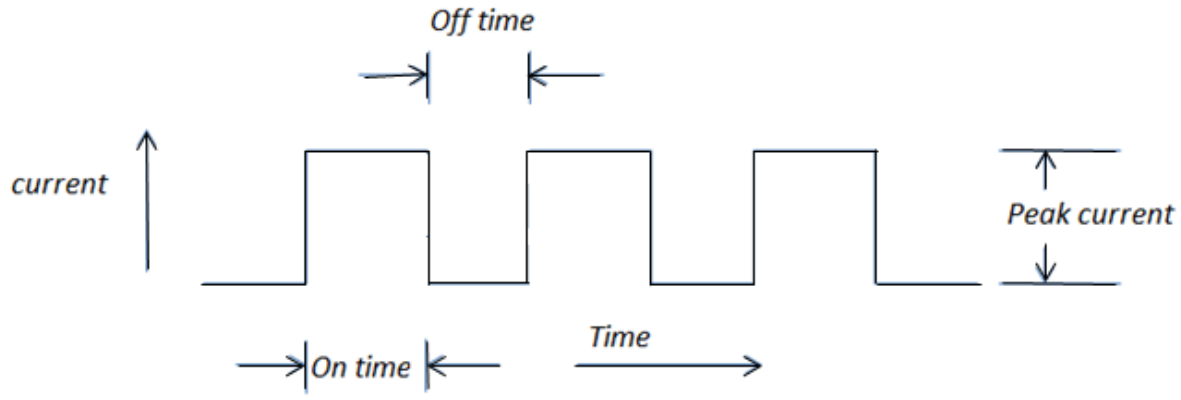

Figure 1.6: Diagram of pulse on time and pulse of time

1.5.4 Pulse off Time (T_{off})

The 'pulse off time' is the time during which re-ionization of the dielectric takes place. The more is the off time, the greater will be the machining time. The cycle is completed when sufficient off-time is allowed before the start of the next cycle [9]. Pulse off-time will affect the speed and stability of the cut. If the off-time is kept shorter, then faster will be the machining operation. If the off-time is too short, the ejected work piece material will not be swept away by the flow of the dielectric and the fluid will not be deionized. This will cause the next spark to be unstable. Unstable conditions cause erratic cycling and retraction of the advancing servo thereby slowing down the operation cycle. Off-time must be greater than the deionization time to prevent continued sparking at one point. The surface roughness is found to depend strongly on the spark frequency. When high frequency sparks are used lower

values of roughness average (Ra) are observed, because the energy available in given amount of time is shared by large number of sparks leading to shallower discharge craters. The pulse off time can be seen in Figure 1.6.

1.5.5 Peak Current

It is one of the most important parameter in EDM process and it is the amount of power used in discharge machining. The current is an average of the amperage in the spark gap measured over a complete cycle. This is read on the ammeter during the process. During each pulse on-time, the current increases until it reaches a pre-set level, which is expressed as the peak current. An increase in current, results in increased MRR as well as increased surface roughness (SR) and tool wear rate (TWR). In die-sinking and wire EDM applications, the maximum amount of amperage is governed by the surface of the cut.

1.5.6 Electrode Gap (Spark Gap)

It is the distance between the electrode and the part during the process of EDM. To obtain good performance and gap stability a suitable gap should be maintained. It should neither be less nor should it be more than the desirable. The tool servo-mechanism is of considerable importance in the efficient working of EDM and its function is to control responsively the working gap of the set value. Servo head is incorporated in EDM to maintain gap voltage since the dielectric parameters constantly fluctuate. Servo mechanism affecting the movement of the electrode may be either electric motor driven, solenoid operated or hydraulically operated or a combination of these. The servo feed control maintain the working gap at proper width [2]. Mostly electromechanical (DC or stepper motors) and electro-hydraulic systems are used, If the gap is less then the short circuit may occur. The most important requirements for good performance are gap stability and the reaction speed of the system; the presence of the backlash is practically undesirable. Gap width is not measurable directly, but can be inferred from the average gap voltage [11].

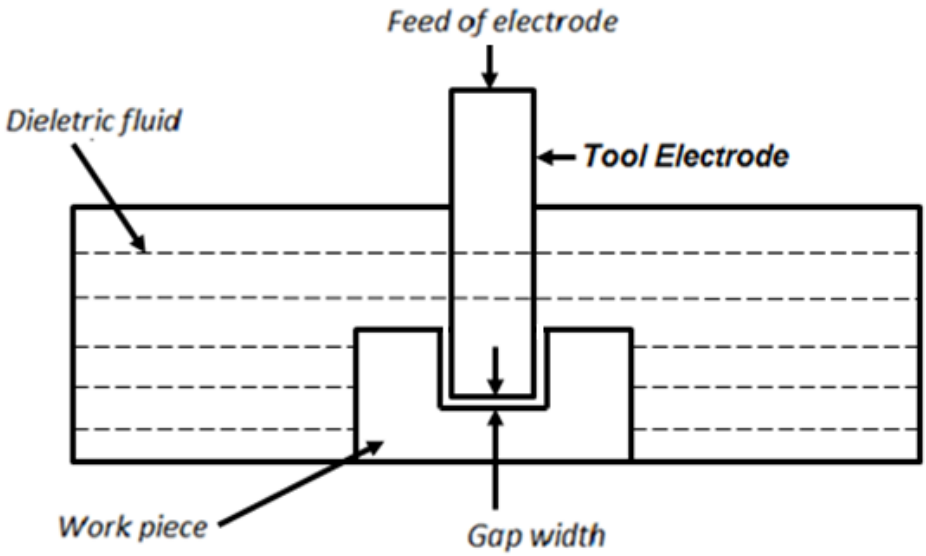

Figure 1.7: Diagram of electrode gap in EDM

1.5.7 Pulse Wave Form

The pulse shape is generally rectangular. But different generator has different waveform. Some generator can produce trapezoidal pulses. This waveform succeeded in reducing relative tool wear to very low values.

In relaxation generator, the spark oscillation is reduced. TWR will be less and charging time is equal to ignition delay, so the ionization process is slower and depends on charging time.

In case of rotating impulse generators the rectified sinusoidal voltage wave form is given across the spark gap to produce the spark.

Due to the inductive circuitry there is a spark oscillation even after the pulse is withdrawn give rise to extremely high tool wear and arcing become frequent if the second pulse comes before complete dampening of the oscillation.

Pulse wave form, generated by the square pulse generators, is much more defined and easily controllable. Using a generator, which can produce trapezoidal pulses, one can reduce relative tool wear to very low values [9]. Pulse waveform of pulse generator is shown in Figure 1.8.

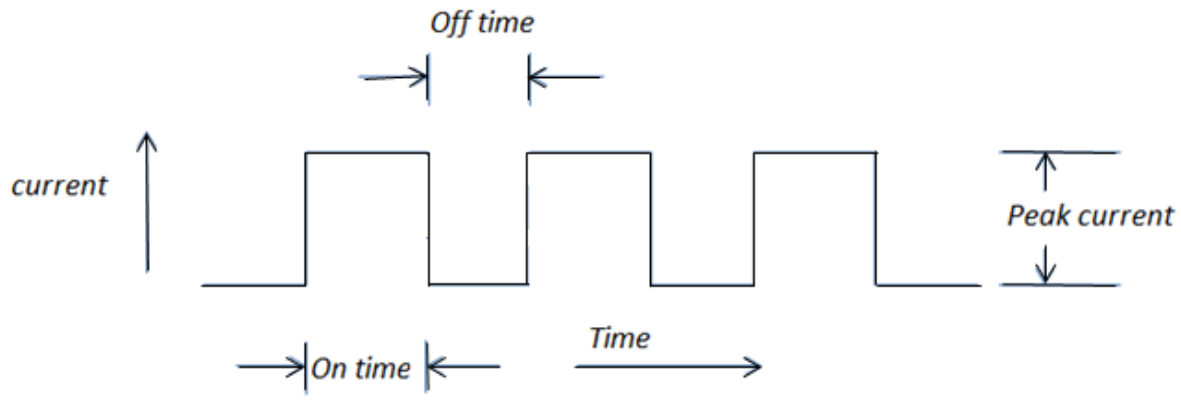

Figure 1.8: Pulse wave form of pulse generator

1.5.8 Dielectric Fluids

Selection of dielectric medium is an important parameter in EDM. The dielectric fluids are used to flush away the eroded particles from the gap between electrode and work piece, otherwise they can form bridges, which may cause short circuits. Such arcs can burn big holes in the work piece and the electrode. Light hydro-carbon oils seem to adequately satisfy these requirements. The common fluid that are used are kerosene paraffin oil, lubricating oils, transformer oil. Mineral oils are exhibit high dielectric strength and a low viscosity is preferred because of their better performance. Water based dielectric are used almost extensively for wire EDM operations. Water has a high specific heat capacity which leads to better cooling effect required for wire cut operations. To prevent chemical reactions, deionized water is used in such applications. The deionised water gives high MRR and TWR [3]. Although most of the commercially available hydrocarbons, siloxanes, alcohols and ordinary water possess the properties of a good dielectric to a greater extent but, kerosene has found widest application for fine and medium fine machining. During machining, the dielectric temperature rises and it gets contaminated with erosion debris. This may consist of resolidified metal particles from electrodes, together with carbon rich solid particles produced due to the breakdown of the dielectric fluid during the spark. If kerosene is cooled and the solid debris is removed by settling or filtration it may be reused over a long period of time without any appreciable loss in machining efficiency [12].

For using a dielectric fluid in EDM process it is essential that they should have following characteristics:

- Remain electrically non-conducting until the required breakdown voltage has been reached.

- Breakdown electrically in the shortest possible time once the breakdown voltage has been reached.
- Rapidly quench the spark or deionize the spark or spark gap after the discharges have occurred.
- Provide an effective cooling medium.
- Deionize the gap immediately after the spark has occurred.
- Have good degree of fluidity.
- Should be cheap and easily available.

1.5.9 Tool Electrode

The EDM is basically a copying process and therefore the shape and accuracy of the machined part would largely depend upon the shape and accuracy of the cutting tool electrode. Metals with a high melting-point and good electrically conductivity is usually chosen as tool materials for EDM. They should be cheap and readily shaped by conventional methods. Electrodes for discharge machining are highly expendable because each erosive spark removes a certain amount of the material from the tool electrode as well [13-14]. . In some cases, a series of slightly differing tool shapes may have to be used to achieve the desired result. This obviously increases the machining cost. Consequently, materials that are cheap, easy to fabricate, and give high cutting rate with minimum self-erosion are preferred for tool electrode manufacturing.

1.5.10 Types of Flushing

Flushing is defined as the correct circulation of the dielectric fluid between electrode tool and work piece during operation. A dielectric in EDM must have a basic characteristic of high dielectric strength and quick recoveries after breakdown also have an effective quenching and flushing ability. In order to obtain highest machining efficiency, suitable flushing conditions are necessary.

In order to understand the significance of flushing it is important to understand the phenomenon which occurs in the machining gap when flushing is absent. During the machining operation, debris is produced in the gap and decreases the dielectric strength of the dielectric fluid. If the amount of debris in the gap becomes too high, the particles can form “bridges” between the electrodes which causes abnormal discharges and damage the tool as well as work electrode. This debris can be eliminated by the process of flushing. Using flushing will give optimum results.

In EDM, flushing can be achieved by the following method:

1. Injection Flushing

In this method, dielectric is injected through either the work piece or the tool in to the working gap. A hole is provided either in tool or work piece to accommodate the flow. The amount of dielectric flowing through is more important than the pressure of flushing. When calculating the smaller than specified dimension of the electrode, it must be remembered that in this type of flushing particles rising up through the lateral gap are continuously causing additional erosion.

2. Suction Flushing

In this method of flushing, dielectric is sucked through either the work piece or the tool. This technique is used to avoid any tapering effect due to sparking via machining debris along the side walls of the electrode. Suction flushing through the tool is more effective rather than through the work piece.

3. Side Flushing

When the flushing holes cannot be drilled either in the work piece or the tool, side flushing is employed. If there is need of flushing of entire working area, special precautions must be taken for the pumping of dielectric fluid.

4. Flushing by Dielectric Pumping

Flushing is achieved by using the electrode pulsation movement. When the electrode is moved upward, the gap increases, resulting in clean dielectric being sucked into mix with contaminated fluid, and as the electrode is moved downward the particles are flushed out[7, 9].

1.6 ADVANTAGES OF EDM

The popularity of EDM process is due to the following advantages:

- The process can be readily applied to electrically conductive materials. Physical and metallurgical properties of the work material, such as strength, toughness, microstructure, etc., are no barrier to its application.
- During machining, the work piece is not subjected to mechanical deformation as there is no physical contact between the tool and work. This makes the process more versatile. As a result, slender and fragile jobs can be machined conveniently.

- Although the metal removal in this case is due to thermal effects, yet there is no heating in the bulk of the material.
- Complicated die contours in hard materials can be produced to a high degree of accuracy and surface finish.
- The surface produced by EDM consists of a multitude of small craters. This may help in oil retention and better lubrication, especially for components where lubrication is a problem. The random distribution of the craters does not result in an appreciable reduction in fatigue strength of the components machined by EDM.
- The overall production rate compares well with the conventional processes because it can dispense with operations like grinding, etc.
- The process can be automated easily thereby requiring very little attention from the machine operator.

1.7 POWDER MIXED EDM (PMEDM)

Electrical discharge machining (EDM) can be successfully employed to machine electrically conductive parts regardless of their hardness and toughness. But on the other hand low machining efficiency and poor surface quality are the major drawbacks of this process that restricts its use in mechanical manufacturing. Researchers did a lot of work to overcome these drawbacks and to enhance process capabilities. Rotating of electrode, orbiting of electrode, application of ultrasonic vibrations and addition of powders in dielectric fluid of EDM are some of the techniques suggested by researchers to enhance process capabilities. PMEDM has more complex mechanism than conventional EDM. Powder particles play an important role during machining. Powder mixed EDM (PMEDM) has emerged as one of the advanced techniques in the direction of the improvement of the capabilities of EDM [15, 16]. In this process, an additional material in fine powder form is mixed into the dielectric fluid of EDM. The added powders can aluminium, chromium, graphite, silicon or titanium etc. The spark gap is filled up with additive particles. The added powder significantly affects the mechanism of EDM process. The electrically conductive powder reduces the insulating strength of the dielectric fluid and increases the spark gap distance between the tool electrode and work piece. As a result, the process becomes more stable, thereby improving machining rate (MR) and surface finish. The principle of PMEDM is shown in Figure 1.9.

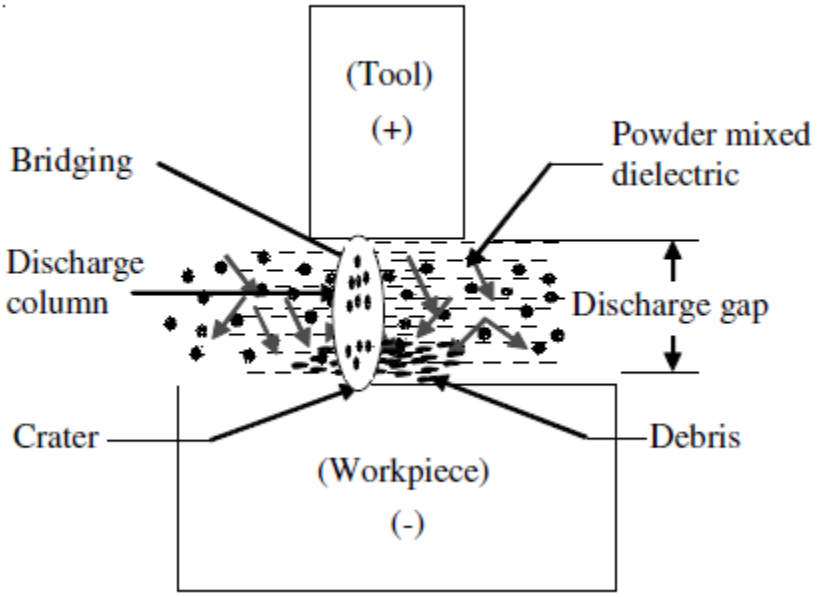

Figure 1.9: Principle of Powder Mixed EDM [17]

In this process, the material in powder form is mixed into the dielectric fluid in a tank. When a voltage of 80-320 V is applied between the electrodes, an electric field in the range $10^5$to 10^7 V/m is created. The spark gap is filled up with additive particles, and the gap distance between tool and the work piece increases from 25 μm to 50μm to many times larger. The powder particles get energized and behave in a zig-zag fashion. The grains come close to each other under the sparking area and gather in clusters. Under the influence of electric forces, the powder particles arrange themselves in the form of chains at different places under the sparking area as shown in figure. The chain formation helps in bridging the gap between both the electrodes. Due to the bridging effect, the gap voltage and insulating strength of the dielectric fluid decreases. The easy short-circuit takes place, which causes early explosion in the gap. As a result, the 'series discharge' starts under the electrode area. Due to the increase in the frequency of discharging, the faster sparking within a discharge takes place, which causes faster erosion from the work piece surface. At the same time, the added powder modifies the plasma channel. The plasma channel gets enlarged [15]. The electric density decreases; hence, sparking is uniformly distributed among the powder particles. Hence even and more uniform distribution of the discharge takes place, which causes uniform erosion on the work piece. This results in improvement in surface finish.

From above discussion we come to know that the addition of powder in the dielectric fluid result in increase in material removal rate (MRR) and surface finish. It also reduces tool wear rate.

1.8 EDM SURFACE LAYERS

The examination of a section of the surface layer produced by EDM (Figure 1.10) reveals that there is a top white layer which crystallizes from the liquid cooled at high speed. The depth of this top melted zone depends on the pulse energy and duration. Below the top layer is a chemically affected layer with changes in the average chemical composition and possible phase changes. After this, there is a plastically deformed zone with micro and macro strains characterized by the presence of twinning, slip and phase changes.

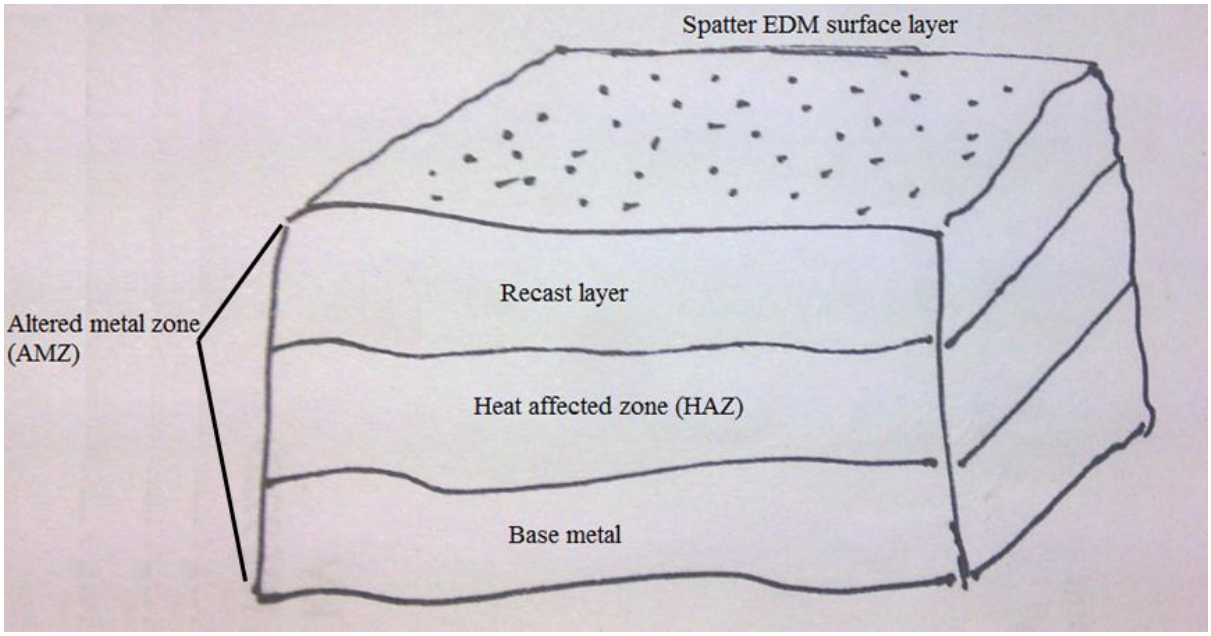

Figure 1.10: Surface layers after electrical discharge machining [18]

The EDM process changes not only the surface of the work piece metal, but also the subsurface.

Three layers are created on top of the unaffected work piece metal.

- The spattered EDM surface layer is created when expelled molten metal and small amounts of electrode material form spheres and spatter on the surface of the work piece. This spattered material is easily removed.
- The next layer is the recast (white) layer. The action of EDM has actually altered the metallurgical structure and characteristics in the recast layer. This layer is formed by the unexpelled molten metal solidifying in the crater. The molten metal is rapidly quenched by the dielectric. Micro-cracks can form in this very hard, brittle layer. If this layer is too thick or is not reduced or removed by polishing, the effects of this layer can cause premature failure of the part in some applications.

- The last layer is the heat affected zone (HAZ) or annealed layer, which has only been heated, not melted. The depth of the recast layer and the heat affected zone is determined by the heat sinking ability of the material and the power used for the cut. This altered metal zone influences the quality of the surface integrity. Automatic finishing circuits available on CNC machines greatly reduce the recast layer, but do not eliminate the heat affected zone.

1.9 OVERCUT IN EDM

An overcut in EDM is that dimension by which the hole is in the workpiece exceeds the electrode size. Overcut in EDM is due to the side sparks and is dependent on the gap length and crater dimensions. Lazarenko[2] has been shown experimentally that overcut O can be expressed by the relationship

$$O = AC^{1/3} + B$$

Where A and B are constants and their value depend upon the tool work pair.

C is the capacitance.

It has been found that when the wear particles are present in the gap, the magnitude of the overcut is increased by the diameter of the wear particle (d_W) [2].

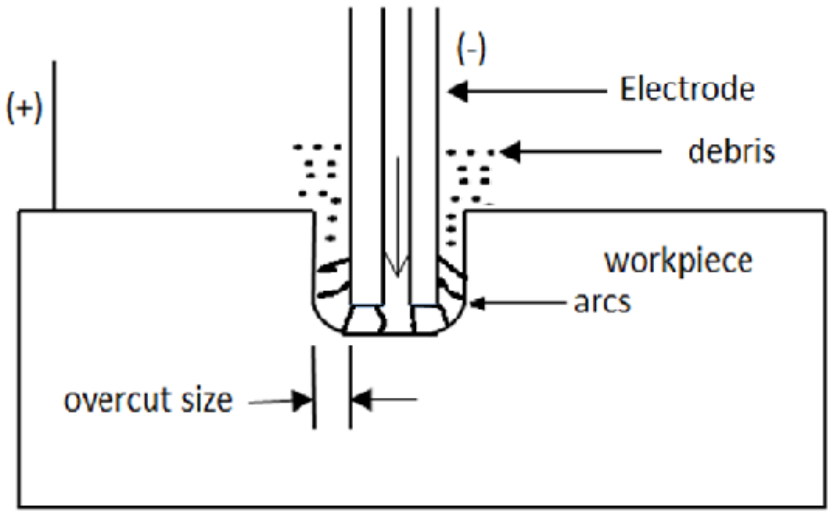

Figure 1.11: Overcut in EDM

CHAPTER 2

LITERATURE REVIEW

2.1 INTRODUCTION

A large work has been done on different aspects of EDM. This chapter covers the literature on Powder Mixed EDM and its effects on Material removal Rate and Tool Wear rate along roughness and hardness and of the surface.

2.2 LITERATURE SURVEY

There are various literature available on Powder Mixed EDM. Given below is the work of some of the researchers.

Ho and Newman [4] have reported the state of the art EDM. In this paper, experimental research has been conducted on the machining efficiency and surface roughness of PMEDM in rough machining. The result shows that PMEDM improves the machining efficiency. It is resulted that PMEDM makes discharge breakdown easier, enlarges discharge gaps and passages and lastly forms evenly distributed and large and shadow shaped etched cavities. The machining efficiency of PMEDM is much better than conventional EDM. The result for surface roughness is also same as that of machining efficiency. Because of much of loss of discharge energy in discharge gaps and reduction of ejecting force on the melted material, the surface roughness becomes smaller in PMEDM than that of conventional EDM.

Sanjeev et al. [9] studied the Surface modification by electrical discharge machining and concluded the following. Most of the available research works on powder-mixed dielectric have studied the impact of such machining on MRR, surface roughness and TWR etc. with normal polarity.

Zhao et al. [15] performed experimental research on powder mixed EDM (PMEDM) in rough machining to assess machining efficiency and surface roughness. In this work, they confirmed that PMEDM machining can improve the machining and surface roughness efficiency at the same time by selecting proper discharging parameters.

Wong et al. [16] reported that near-mirror-finish phenomenon is achieved by using semi conductive Si and C powder-mixed dielectrics. Powder additives can cause higher material removal rates (MRR) by lowering the breakdown strength of the insulating dielectric fluid

and increasing the discharge probability. Machining was performed on various types of steel with different types of powder suspension at a peak current of around 1A. Particular combination of powder mixed dielectric and workpiece have been found to produce mirror surface or glossy machined surface.

Kansal et al. [17] have carried out a study to optimize the process parameters of Powder Mixed Electric Discharge Machining (PMEDM). Pulse on time, duty cycle, peak current and concentration of silicon powder added into the dielectric fluid of EDM was chosen as variables to study the process performance in terms of material removal rate and surface roughness. Silicon powder was suspended into the dielectric fluid of EDM and an enhanced rate of material removal and surface finish has been achieved. The results identify the most important parameters to maximize material removal rate and minimize surface roughness. The silicon powder suspended in the dielectric fluid of the EDM effects both MRR and Surface roughness.

Narumiya et al. [19] reported that under specific working conditions aluminium and graphite powders yield a better surface finish than the silicon powder. The best results (Ra less than 2 μm) are obtained for aluminium and graphite powder particles having diameters less than 15 μm and powder concentration is varied from 2 to 15 g/l.

Mohri et al. [20] reported the effect of silicon powder on the surface finish of H-13 die steel when added into the dielectric fluid. Machining with addition of silicon powder produces the fine and corrosion-resistant surfaces having roughness of the order of 2 μm were produced. However, this performance could only be achieved at controlled machining conditions (even distribution of powder into dielectric, short discharge time, work piece composition, etc.).

Pecas and Henriques [21] investigated the influence of silicon powder mixed dielectric on conventional EDM. They used silicon powder and assessed the improvement through quality surface indicators and process time measurements over a set of different processing areas. They observed that silicon powder showed a positive influence in the reduction of the operating time required to achieve a specific surface quality, and in the decrease of the surface roughness, allowing the generation of mirror-like surfaces. The surface quality is assessed through quality surface indicators and process time measurements over a set of different processing areas. The results show that by the addition of 2 g/l silicon powder, the operating time and surface roughness decrease. The average surface roughness depends on machining area and machining time. The surface roughness varies from 0.09 to 0.57 μm for the area range of $1cm^2$ to 64 cm^2.

Uno and Okada [22] investigated the effect of silicon powder mixing on the surface generation mechanism. The EDM with silicon powder mixed fluid produced glossier surfaces as compared to those produced by conventional EDM with kerosene fluid. It was argued that EDM with silicon powder mixed fluid led to smaller undulation of a crater because the impact force acting on the work piece is smaller. This results in the stable machining without a short circuit between the electrode and the work piece.

Klocke et al. [23] reported a work where the influence of the suspended powder in the white-layer and in the heat-affected zone is qualitatively discussed. The use of silicon powder promotes a softer transition from the white-layer into the matrix material than the observed with powder-free dielectric.

The authors attribute this behaviour to the balancing of the heat introduced by the silicon particles with the rapid cool down of the molten surface. The physical properties of the powder additives play an important role in changing the recast layer composition and morphology. It was found that the Si powder produces a grey zone beneath the actual "white zone". That phenomenon can be explained by means of the Si-high heat of fusion property. The EDS analysis furthermore shows a lower Ni concentration in that area.

Wu et al. [24] found that the use of surfactant contributes to the particles separation and to their homogeneous distribution in the dielectric. As a result the work piece surface is improved and the white layer thickness is reduced. In spite of the intense research covering the powder-mixed dielectric EDM (PMD-EDM) there is limiting knowledge about its quantitative influence in the white-layer thickness and crater diameter and deepness. In this work, a set of EDM and PMD-EDM tests were performed that allow defining a quantitative relation of those surface characteristics with the electrode area for the two process conditions.

Pecas and Henriques [25] reported that the addition of powder particles to the EDM dielectric fluid modifies some process variables and creates the conditions to achieve a higher surface quality in large machined area. They studied the improvement in the polishing performance of conventional EDM when used with powder mixed dielectric. The analysis was carried out by varying the silicon powder concentration and flushing flow rate over a set of different processing areas and the effects in the final surface is evaluated.The evaluation was done using surface morphologic analysis and measured through some quality surface indicators. The result showed the positive influence of silicon powder in the reduction of crater dimensions, white layer thickness and surface roughness.

Kobayashi et al. [26] investigated the effects of suspended powder in dielectric fluid on surface roughness. It was reported that the surface finish of SKD-61 material is improved with the addition of silicon powder.

Sano et al. [27] reported that in powder-suspended EDM with silicon powder, the surface roughness has been improved because of the discharge dispersion. In addition, a surface has been modified by the defused silicon. Then it was modified to harden the surface of a work piece.

Furutani et al. [28] attempted to make thick titanium carbide (TiC) or WC layer and investigated a surface modification method by EDM with a green compact electrode. Titanium alloy powder or tungsten powder was supplied from the green compact electrode and it adhered on a work piece by the heat caused by discharge. They proposed a surface modification method by EDM with powder suspended in working fluid in order to avoid the production process of the green compact electrode.

According to the investigators, the use of a thin electrode and a rotating disk electrode were expected to keep powder concentration high in the gap between a work piece and an electrode and to accrete powder material on the work piece. Titanium powder was suspended in working oil like kerosene. TiC layer developed a thickness of 150 μm with a hardness of 1600 HV on carbon steel with an electrode of 1 mm in diameter. When a disk placed near a plate rotates in viscous fluid, the disk dragged the fluid into the gap between the disk and the plate. Hence, the powder concentration in the gap between a work piece and a rotational disk electrode could be kept high. A wider area of the accretion could be obtained by using the rotational electrode with a gear shape.

Simao et al. [29] reviewed the published on the deliberate alloying of various work piece materials using EDM. Experiments carried out by powder metallurgy tool electrodes and the use of powders suspended in the dielectric fluid, typically aluminium, nickel, titanium etc.

Erden and Bilgin [30] studied the effect of suspended powder particles (copper, aluminium, iron, and carbon) on the machining rate of a mild steel work piece. It was found that the added powder improves the breakdown characteristics of the dielectric fluid, and the machining rate increases with an increase in the concentration of the added powder. It was further reported that the machining becomes unstable at an excessive powder concentration due to the occurrence of short-circuits. When the brass electrode was used, there was a

significant increase in machining rate. This is due to short time lag in case of copper electrodes and long-time lags in case of brass electrodes.

Kozak et al. [31] reported investigation of electrical discharge machining using powder suspended working fluid instead of pure dielectric fluid. The EDM characteristics obtained using hydrocarbon dielectric and mixtures of deionized water with abrasive powder have been compared. The relationships between surface roughness parameters, material removal rate and operating parameters of EDM have determined for different kinds of powder and concentration in kerosene/water.

Chow et al. [32] studied the EDM process for the micro- slit machining of titanium alloy by adding Silicon Carbide and aluminium powders into kerosene. The addition of both SiC and aluminium powder to the kerosene enhanced the gap distance. The increased gap increases the debris removal rate and material removal depth. Several discharging trajectories formed within a single input impulse and several discharging spots created within a discharging impulse. The effects due to discrete discharging pulse were, minimizing of machined debris, increases the material removal depth and surface roughness.

Uno et al. [33] observed that nickel powder mixed working fluid modifies the surface of aluminium bronze components. Nickel powder was purposely used to deposit a layer on an EDM surface to make the surface abrasion-resistant. It proposed a surface modification technique to obtain high surface wear resistance using EDM with powder mixed fluid. First, a coating application of nickel layer on aluminium bronze for plastic molds and shell molds and then formation of a hard titanium carbide layer on alloy steel is carried out by using carbon powder mixed fluid with titanium electrodes. They investigated that EDMed surface with nickel powder mixed fluid has smaller surface roughness than that in EDM with kerosene type fluid.

Ming and He [34] reported that the additives (conductive and inorganic oxide particles)increase the material rate, decrease the tool wear rate, and improve the surface quality of the work piece quite effectively, especially in mid-finish machining and finish machining phases. They studied the effects of additives in kerosene used as dielectric fluid for EDM.

Jeswani [35] investigated the effect of the addition of fine graphite powder into kerosene oil on the machining of tool steels. It was reported that the addition of 4 g/l of fine graphite powder increased the interspace for electric discharge initiation and lowered the breakdown

voltage. The machining process stability was improved, which caused around a 60% increase in material removal rate and 28% reduction in wear ratio. This effect may be attributed to the reduction in the breakdown voltage of kerosene dielectric caused by the addition of the graphite powder.

Tzeng and Chen [36] conducted experiment on SKD-11 steel with aluminium, chromium, copper and silicon carbide powder. They found that copper powder generated worst surface characteristics whereas aluminium powder gave the best surface finish followed by chromium. Particle size, powder concentration as well as its properties such as thermal conductivity, density and electrical resistivity affected performance.

Tzeng and C.Y. Lee [37] studied the Effects of Powder Characteristics on Electro discharge Machining Efficiency. The additives examined include aluminium (Al), chromium (Cr), copper (Cu), and silicon carbide (SiC) powders that have significant differences in their thermo physical properties. Based on the experimental results, The most important characteristics of powders affecting the EDM performance have been found to be the particle size, the particle concentration, the particle density, the electrical resistivity, and the thermal conductivity.

Kibria et al. [38] from the experimental investigations, it is evident that there is great influence of different dielectrics such as pure dielectrics and additive-mixed dielectrics on micro-EDM performance measures such as material removal rate, tool wear rate, overcut, diameteral variance at entry and exit, machined surface integrity, and micro hole accuracy during micromachining of Ti-6Al-4V super alloy. The accuracy of the micro hole is higher at lower peak current and pulse-on-time using deionized water and at higher peak current and pulse-on-time using kerosene. Using B4C additive, the both dielectrics show larger overcut compared to pure dielectrics.

Yeo et al. [39] studied the effects of powder additives suspended in dielectric on crater characteristics for micro electrical discharge machining and found that even at low discharge energy of 2.5 μJ, the craters produced in dielectric with additive were characterized by a circular build-up of material within an outer material build-up at the crater rim. Craters with smaller diameters and more consistent circular shapes are produced in dielectric with additive than in dielectric without additive. Craters with smaller and more consistent depths are produced in dielectric with additive than in dielectric without additive. The average diameter and depth of craters produced at a discharge energy of 2.5 μJ in dielectric with additive are8.3 μm and 0.56 μm respectively. The presence of additives in dielectric lowers the amount of

charges flowing between the tool electrode and work piece, and slows down the rate at which these charges flow.

Wong et al. [39] observed that machining of SKH-54 tool steel in the presence of graphite powder particles produces higher MR and better discharge dispersion.

Furutani [41] studied the Electrical Conditions of Electrical Discharge Machining with Powder Suspended in Working Oil for Titanium Carbide Accretion Process. The conditions for accretion machining by Ti powder-suspended EDM is investigated with respect to discharge current and pulse duration in this paper. The conditions for deposition machining by Ti powder suspended EDM was investigated with respect to discharge current and pulse duration in this paper. Because the thin electrode was used in the experiments, the TiC layer was deposited under the same conditions as the removal process by the conventional powder-suspended EDM. It was found that the discharge energy affects the accretable condition range. The discharge energy affected the depositable condition range.

Yan and Chen [42] studied the effect of suspended aluminium and silicon carbide powders on EDM of SKD11 and Ti-6Al-4V. Considerable improvement in machining rate (MR) was observed, but at the cost of surface finish.

Prihandana et al. [43] has studied a new method that consists of suspending micro-MoS2 powder in dielectric fluid and ultrasonic vibration is used during micro-electrical discharge machining (μ- EDM) processes. Pareto analysis of variance was applied to analyse the four machining process parameters: ultrasonic vibration of dielectric fluid, concentration of micro powder, tool electrode material and work piece materials. The introduction of MoS2 micro powder in dielectric fluid and using ultrasonic vibration significantly increase the material removal rate and improves the surface quality by providing a flat surface free from black carbon spots.

Kung et al. [44] studied the effect on material removal rate (MRR) and electrode wear ratio (EWR) of powder mixed electrical discharge machining (PMEDM) of cobalt-bonded tungsten carbide (WC-Co). In the PMEDM process, the particles of aluminium powder suspended in the dielectric fluid disperse and make the discharging energy dispersion uniform. The study was carried out taking into consideration the four processing parameters: pulse on time, discharge current, grain size, and concentration of aluminium powder particle. The response surface methodology (RSM) has been employed to plan and analyze the experiments.

Mohri et al. [45] reported a method of surface modification by EDM using composite electrodes on workpieces of carbon steel or aluminium were carried out in hydrocarbon oil. The materials of electrodes which were used are Copper, aluminium, tungsten carbide and titanium. It was revealed that the electrode material existed in the work surface layer and the characteristics of the surface of material are changed. Surfaces have lesser cracks, high corrosion resistance and wear resistance.

Singh et al. [46] carried out experimental investigation to study the effects of machining parameters such as pulsed current on material removal rate, diameteral overcut, electrode wear, and surface roughness in electric discharge machining of En-31 tool steel (IS designation: T105 Cr 1 Mn 60) hardened and tempered to 55 HRC. The work material was ED machined with electrodes such as copper, tungsten copper, brass and aluminium by varying the pulsed current at reverse polarity. The investigation indicated that the output parameters of EDM increase with the increase in pulsed current and the best machining rates are achieved with copper and aluminium electrodes.

Marafona and Wykes [47] used tungsten copper electrode and D2 tool steel workpieces. In this work, the parameters such as MRR, TWR and surface roughness were optimized. It was found that a black layer of carbon was deposited on the tool when low current intensity and long pulse duration was used. This layer formed on the tool inhibits further tool wear and a higher current intensity can then be used to improve the MRR without increase in the TWR. SEM showed that a layer was formed on the surface of tool with high carbon content as well as D2 steel elements such as iron and chromium. The composition of tool was measured with the help of Energy dispersive X-ray analysis.

Muttamara et al. [48] used graphite as an electrode for machining of alumina in EDM. They showed that, when graphite was used as an electrode for machining it gave a significantly higher MRR and low electrode wear than copper electrode. It was found that the value of MRR increase by 60% with positive electrode wears. When investigated with energy dispersive spectroscopy, no element of copper was observed on the conductive layer. Surface roughness was improved by 12% with positive polarity.

Mohri et al. [49] used wires of tungsten, copper and brass of 0.1 mm diameters as electrode on AISI-1049 steel workpiece material to observe the effects of electrode materials on material accretion process using EDM. Tungsten was the deposited on the workpiece, while

the workpiece was drilled with copper and brass electrode under the same machining conditions.

Jeswani and Basu [50] carried out electron microprobe analysis for surface deposition and diffusion of tool material with copper and brass as tool electrodes using kerosene and distilled water as dielectric medium on mild steel, high carbon steel and high speed steel. They found that high energy machining results in lower surface deposition but more depth of diffusion. mild steel showed the least deposition where as high speed steel had best deposition followed by the high carbon steel. Pulse energy was found to be the most significant factor aiding surface deposition as compared to tool material, work material and dielectric fluid. Machining in distilled water high pulse energy resulted in lower surface deposition and depth of diffusion as compared to machining in kerosene.

P.Pecas and E.Henriques [51] carried out the experimental research work and contributes to the generation of knowledge related to EDM technology using a powder-mixed dielectric. The surface quality was assessed through the roughness measurement and the analysis of the craters (diameter and depth) and white-layer dimensions. The application of PMEDM helps in the reduction of surface roughness, crater diameter, crater depth and the white-layer thickness. It was concluded that the electrode area influence in the surface quality. This influence was mathematically described by several linear equations relating the surface roughness, the white-layer thickness, the crater depth and width to the electrode area as the independent variable. Furthermore, it was found that the sensitivity of the surface quality measures to the electrode area is smaller when mixed-power dielectric is used. Also, powder-mixed dielectric significantly reduces surface heterogeneity contributing to increase process robustness. So, it contributes for the performance of the EDM process particularly when large electrode areas are involved and when a high-quality surface is a requirement. In addition, mathematical relations found can be used in the future in a process-planning context.

Gurmail singh [52] In this work, two electrode materials copper and Tungsten-Copper were used to machine High-Carbon High-Chromium (HCHCr), Hot Die Steel (H11) and EN31 using graphite and aluminium powder in kerosene and transformer oil. The effect of input parameters on the MRR, TWR, surface roughness, micro hardness and on the surface properties in PMEDM was studied.

Gurpreet singh [53] In this thesis work, Improvement in surface properties and process optimization of die steels by using powder mixed dielectric in EDM process was studied.

Two electrode materials Graphite and Tungsten-Copper were used to machine High-Carbon High-Chromium (HCHCr), Hot Die Steel (H13) and EN31 using copper and tungsten powder in kerosene and EDM oil. The effect of input parameters on the MRR, TWR, surface roughness, micro hardness and on the surface properties in PMEDM was also studied.

Sanjeev Kumar [54] carried out experimental investigation on the phenomenon of surface modification in three die steels during EDM process using four different tool electrodes and four powders suspended in the dielectric medium.

2.3 SUMMARY OF THE LITERATURE SURVEY

A lot of work has been done in the field of Powder Mixed EDM. Surface modification has been done either with powder mixing in the dielectric medium as well as with electrode material. It is observed that the field of surface modification using EDM process is still at the experimental stage. From the above literature it is observed that the effect of Powder Mixed EDM using different types of powders such as copper, aluminium, silicon and titanium, carbon into the dielectric fluid in EDM on various parameter such as material removal rate(MRR),tool wear rate(TWR) and surface roughness (SR) has been studied. Some researchers [17, 27 and 30] found that by the addition of silicon powder into the dielectric fluid, surface roughness and operating time decrease. Many researchers [15, 22] used silicon metal powder in kerosene dielectric fluid and investigated the various effects on the machining parameters such as surface roughness (SR), material removal rate (MRR) and tool wear rate (TWR). Effect of Silicon carbide powder [30] in kerosene dielectric fluid was studied and found that the Silicon Carbide powder increases the gap distance and hence increases the material removal rate. Some researchers [23, 24] found that addition of Silicon Powder into the dielectric fluid improve the surface roughness of the work piece. It was also found that the stable machining can be achieved without a short circuit between the electrode and the work piece by the addition of silicon and carbon powder [17]. Graphite powder [5] reduced the wear ratio TWR/ MRR about 28%. Material removal rate is increased by 60%. Surface modification by electrode materials also carried out. Some researcher [27, 30] studied the effect on material removal rate and surface roughness value using aluminium powder in the kerosene dielectric fluid. Tungsten copper electrode [47] improves the MRR without increase the TWR. Graphite electrode [48] reduce tool wear rate and increase the material removal rate as compared to copper electrode. It was also found that no work has been done

regarding profile/geometric accuracy. The study related to measurement of overcut is very less.

2.4 GAP IN LITERATURE

A lot of work has been done in surface modification with electrical discharge. From the literature review, it is observed that. It has been found that no work has been done using brass electrode on different types of die steels along with silicon, graphite and tungsten as powder in kerosene oil and EDM oil. No work has been reported on effects of graphite powder, tungsten powder and silicon powder on AISI1045 steel with graphite, brass and tungsten-copper electrode in kerosene oil as well as in EDM oil. Some work has been reported on H13 grade of hot die steel with graphite electrode in EDM oil but no work has been reported on H11 grade of hot die steel with graphite in EDM oil. So in the thesis work it is proposed to study the effect of different input parameters such as current, pulse on time, workpiece material, electrode material, dielectric medium, powder concentration and types of powder on the MRR, TWR, WR, micro hardness and surface roughness. The study on measurement of oversize is almost negligible. Hence measurement of oversize has also been investigated. No studies have been reported on profile/geometric accuracy in PMEDM. So the first time profile/geometric accuracy has been investigated with different proposed front angle of tool (copper) such as 60°, 90° and 120°.The effect of various input parameters on output responses have been analyzed using Analysis of Variance (ANOVA). Deposition of the powder material was also proposed to be studied. XRD and microstructure analysis was done to study the amount of deposition on the surface of the workpiece material.

2.5 OBJECTIVE OF THE PRESENT WORK

The objective of the present work has been discussed below:

1) To study the effect of various input parameters like on MRR, TWR, WR, micro hardness, surface roughness, measurement of overcut size and analyzing the results using Analysis of Variance (ANOVA) and further optimizing the process parameters.
2) To study the XRD and microstructure analysis of selected samples to assess the form and amount of deposition on the surface of the workpiece material.
3) To study the profile/geometric accuracy using copper tool with different front angle such as 60°, 90° and 120° on hot die steel (H11) workpiece.

CHAPTER 3

METHODOLOGY

3.1 METHODOLOGY

The full factorial design is referred to as the technique of defining and investigating all possible conditions in an experiment involving multiple factors while the fractional factorial design investigates only a fraction of all the combinations. Although these approaches are widely used, they have certain limitations: they are inefficient in time and cost when the number of the variables is large; they require strict mathematical treatment in the design of the experiment and in the analysis of results; the same experiment may have different designs thus produce different results; further, determination of contribution of each factors is normally not permitted in this kind of design. The Taguchi method has been proposed to overcome these limitations by simplifying and standardizing the fractional factorial design. The methodology involves identification of controllable and uncontrollable parameters and the establishment of a series of experiments to find out the optimum combination of the parameters which has greatest influence on the performance and the least variation from the target of the design. The effect of various parameters (current , pulse on time, workpiece material, electrode material, dielectric, powder concentration and types of powder) were also be studied using parameterization approach developed by Taguchi[55].

3.2 PROCEDURE OF EXPERIMENTAL DESIGN

The essential steps in the procedure of Taguchi method are as follows. [55]

1. Establishing the objective function.

2. Selection of factors which needs to be evaluated.

3. Identifying the uncontrollable factors as well as test conditions.

4. Selecting the number of levels for the controllable and uncontrollable factors.

5. Calculating the total degree of freedom which are needed

6. Selecting the appropriate Orthogonal Array (OA).

7. Assigning of factors to columns.

8. Executing the experiments according to trial conditions in the array.

9. Analyzing the results.

10. Confirmation of experiments.

3.3 ESTABLISHING THE OBJECTIVE FUNCTION/RESPONSES

The objective of the study is to evaluate the main effects of current, workpiece material, dielectric, electrode material, pulse on time, powder concentration and types of powder on the MRR, TWR, Wear ratio, surface roughness and micro hardness. Profile/geometry accuracy and measurement of overcut is to be investigated. Deposition of the powder material on the workpiece material is also to be studied. XRD and microstructure analysis is to be done to understand the amount of deposition on the surface of the workpiece material. MRR, TWR, Wear ratio and measurement of overcut is calculated using the formula given below:

1) The MRR is given by:

$$\text{MRR} = \frac{W_i - W_f}{\rho t} \times 1000 \text{ mm}^3/\text{min}$$

Where W_i = Initial weight of workpiece material (gms)

W_f = Final weight of workpiece material (gms)

t = Time period of trials in minutes

ρ = Density of workpiece in gms/cc

2) The TWR is given by:

$$\text{TWR} = \frac{A \times L}{t}$$

Where A = front area of electrode (mm^2)

L = Loss in length of electrode (mm)

t = time period of trial (minutes)

TWR = Tool wear rate in mm^3/min

3) The WR is given by:

$$\text{WR} = \frac{\text{TWR}}{\text{MRR}}$$

Where WR = wear ratio, dimensionless quantity

TWR = Tool wear rate in mm^3/min

MRR = Material removal rate in mm^3/min

4) The overcut is given by

$$\text{overcut} = \frac{D - d}{2} \text{ mm}$$

Where D = Diameter of cut made in the workpiece material with the tool (mm)

d = Diameter of tool (mm)

3.4 DEGREE OF FREEDOM (dof)

The total degree of freedom required for the entire experimentation is determined by the number of factors, their interactions and level for factors. The degree of freedom for each factor is given by the number of levels minus one.

dof for each factor = k-1

where k is the number of level for each factor.

3.5 SELECTION OF FACTORS

The determination of factors which needs to be investigated depends on the responses of interest. The factors that affect the responses were identified using several methods such as brainstorming, cause and effect analysis and flowcharting. The lists of factors studied with their levels are given in the Table 3.1. The minimum dof required in the experiment are the sum of all the degrees of freedom of factors. In the present experiment setup, there are six 3-level factors and one is 2-level factor i.e. dielectric fluid. The number of dof for factors B, C, D, E, F and G are two and for factor A is one. The total dof for the experiment is explained in Table 3.2. As the dof required for the experiment is 13; the orthogonal array (OA) to be used should have more than 13 dof. The most suitable orthogonal array which can be used for this experiment is L18, which has 17 dof assigned to its various columns. The additional four dof were used to measure the random error.

Table 3.1: Factors interested and their levels

Factors (units)	Factor designation	Levels		
		Level-1	Level-2	Level-3
Dielectric	A	kerosene	EDM oil	-
Work piece material	B	H11	HCHCr	AISI 1045
Electrode	C	Graphite	W-Cu	Brass
Powder Concentration (g/l)	D	0	5	10
Current(Amp)	E	3	5	7
Pulse On (µs)	F	20	50	100
Types of powder	G	Silicon	Graphite	Tungsten

Table 3.2: Degree of freedom

Factor	A	B	C	D	E	F	G	Total
Degree of Freedom	1	2	2	2	2	2	2	13

3.6 ORTHOGONAL ARRAY

OA is derived from factorial design of experiment by a series of very sophisticated mathematical algorithms including combinatorics, finite fields, geometry and error-correcting codes. OA plays a critical part in achieving the high efficiency of the Taguchi method. The OA is constructed in a statistically independent manner. Within each column, number of occurrences of each level is equal and for each level within one column, each level within any other column will occurs an equal number of times as well. Then, the columns are called orthogonal to each other. OA is available with a variety of factors and levels in the Taguchi method. Since each column is orthogonal to the others, if the results associated with

one level of a specific factor are much different at another level, it is because changing that factor from one level to the next has strong impact on the quality characteristic being measured. Since the levels of the other factors are occurring an equal number of times for each level of the strong factor, any effect by these other factors will be ruled out.

The selection of orthogonal array depends on:

· The number of factors and interactions of interest

· The number of levels for the factors of interest

Taguchi's orthogonal arrays are experimental designs that usually require only a fraction of the full factorial combinations. The columns of arrays are balanced and orthogonal. This means that in each pair of columns, all factor combinations occur same number of times. Orthogonal designs allow estimating the effect of each factor on the response independently of all other factors. Once the degrees of freedom are known, the next step is to select the orthogonal array (OA). The number of treatment conditions is equal to the number of rows in the orthogonal array and it must be equal to or greater than the total degrees of freedom. Once the appropriate orthogonal array has been selected, the factor can be assigned to the various columns [52]. L18 Linear graph is shown in Figure 3.1 and experimental design of L18 is shown in Table 3.2

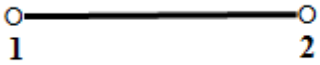

Figure 3.1: L18 Linear Graph

The 18 experimental design represents the set of values of input process parameters with which particular experiment is to be conducted. Machining time during each experiment was 10 minutes. The total 18 experiment were performed with repetition in order to minimize the effect of uncontrollable factors for each combination of all input parameters.

Table 3.3: L18 Experimental design

Trial no	Dielectric	Workpiece	Electrode	Powder Concentration	Current	Pulse On	Types of powder
1	kerosene	HDS	Graphite	0	3	20	Silicon
2	kerosene	HDS	W-Cu	5	5	50	Graphite
3	kerosene	HDS	Brass	10	7	100	Tungsten
4	kerosene	HCHCr	Graphite	0	5	50	Tungsten
5	kerosene	HCHCr	W-Cu	5	7	100	Silicon
6	kerosene	HCHCr	Brass	10	3	20	Graphite
7	kerosene	AISI 1045	Graphite	5	3	100	Graphite
8	kerosene	AISI 1045	W-Cu	10	5	20	Tungsten
9	kerosene	AISI 1045	Brass	0	7	50	Silicon
10	EDM oil	HDS	Graphite	10	7	50	Graphite
11	EDM oil	HDS	W-Cu	0	3	100	Tungsten
12	EDM oil	HDS	Brass	5	5	20	Silicon
13	EDM oil	HCHCr	Graphite	5	7	20	Tungsten
14	EDM oil	HCHCr	W-Cu	10	3	50	Silicon
15	EDM oil	HCHCr	Brass	0	5	100	Graphite
16	EDM oil	AISI 1045	Graphite	10	5	100	Silicon
17	EDM oil	AISI 1045	W-Cu	0	7	20	Graphite
18	EDM oil	AISI 1045	Brass	5	3	50	Tungsten

3.7 EXPERIMENTAL SET UP

The experiments have been conducted on the Electrical Discharge Machine model T-3822 (Figure 3.2) of victory electromech available at Thapar University, Patiala in the Machine Tool lab. Many input parameters like discharge voltage, pulse on time, pulse off time, polarity, peak current, electrode gap and type of flushing can be varied in EDM process. Each factor has its own effect on the output parameters such as tool wear rate (TWR), material removal rate (MRR), surface roughness (SR), hardness of the machined surface, overcut size and profile/geometry accuracy. The ranges of the parameters were varied for the experimental work. The input parameters, which were kept constant during the experimentation, are given in the Table 3.4.

Table 3.4: Constant input parameters

S.No	Parameter	Value set as
1	Open circuit voltage	135±5%
2	Polarity	Positive
3	Machining time	10 minutes
4	Spark energy	Low
5	Pulse off	85µs

Special mild steel tank was designed for the conducting experiments so that the suspended powder particles do not clog the filtering system. This tank of size 330 × 200 × 200 mm was made with 4mm thick mild steel and had capacity of 9 litres. A stirrer rotating at 1400 rpm was used in the tank for proper mixing of the powder in the dielectric. Schematic diagram of set up is shown in Figure 3.3. The tank was installed in EDM machine as shown in Figure 3.4.

Figure 3.2: Electrical Discharge Machine

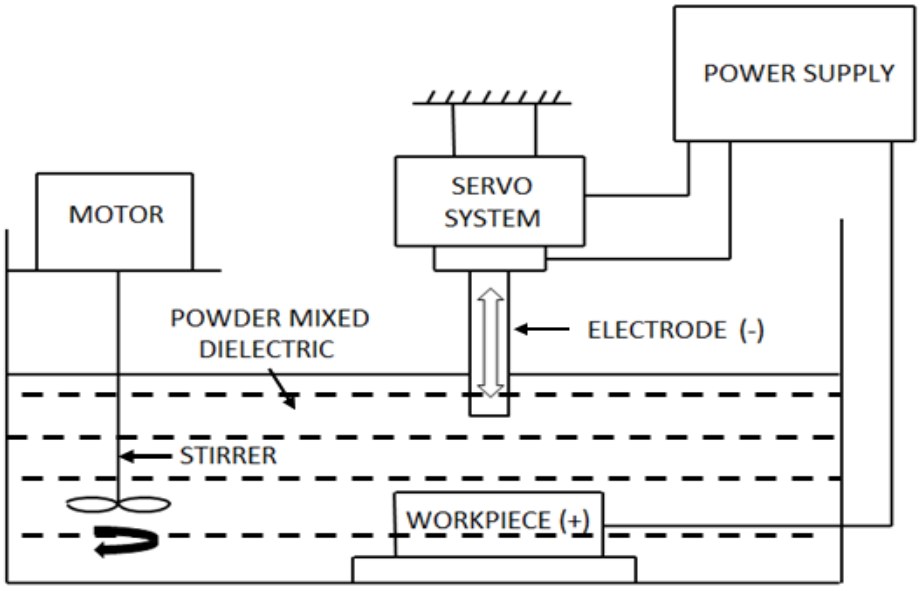

Figure 3.3: Schematic diagram of set up

Figure 3.4: Dielectric Tank with along with stirrer

3.8 MEASURING AND TEST EQUIPMENT USED

Micro hardness and surface roughness tests were conducted on all the 18 samples produced on the EDM machine. MRR was measured using a weighing machine whereas TWR was measured using a Vernier Calliper. The details of important equipment used for the test in the experimental study are given below:

3.8.1 Surface Roughness Tester

Surface roughness was measured using the Perthometer, model M4Pi of Mahr, Germany. The equipment uses the stylus method of measurement, has profile resolution of 12 nm and measure roughness up to 100μm. A tracing length of 4.8 mm was used for analysis. Surface roughness of each sample was measured at three different positions namely, centre, left and right of each machined sample.

3.8.2 Micro Hardness Tester

Micro hardness was measured on a computer interfaced Micro Hardness Tester, (model MVH-2) Metatech industries, Pune, India, available at Thapar University, Patiala. The micro hardness measurement is dependent on the diameter of indentation produced on the samples. The indents formed in the pyramid shaped indenter were measured with Quantimet software using a load of 1 kg for 20 seconds. The micro hardness was measured at deposition as well as non-deposition region.

3.8.3 X-Ray Diffraction Machine

XRD analysis was carried out on X-Ray Diffraction machine, (model ME 210 LA 2) of Rigaku corporation, Japan, available in Material Testing lab of Thapar University, Patiala. The range of 2θ from the 5° to 100° was used at a scan speed of 5°/minute for each test.

3.8.4 Scanning Electron Microscope (SEM) Machine

Microstructure of some selected samples was investigated on Scanning Electron Microscope, (model JSM-840A) of Joel, Japan, available in Material Testing lab of Thapar University, Patiala. The range of magnification from 10× to 3,00,000×. SEM of samples was investigated on three ranges, namely, 200×, 500× and 1000×.

3.8.5 Profile Projector

Measurement of overcut size was investigated on Nikon profile projector (model V-10A) of japan which is available in Material Testing lab of Thapar University, Patiala. The voltage requirement is 220V/230V/240V and current requirement is 0.6 amp.

3.9 ANALYSIS OF RESULTS

Signal-to-noise ratio

The parameters that influence the output can be categorized into two classes, namely controllable (or design) factors and uncontrollable (or noise) factors. Controllable factors are those factors whose values can be set and easily adjusted by the designer. Uncontrollable factors are the sources of variation often associated with operational environment. The best settings of control factors as they influence the output parameters are determined through experiments. From the analysis point of view, there are three possible categories of the response characteristics explained below.

r is the number of tests in a trial (noise of repetitions regardless of noise levels)

$\sum_{i=1}^{r} y^2{}_i$ = summation of all response values under each trial

MSD = Mean square deviation

y_j = Observed value of the response characteristic

y_o = nominal or target value of the results

The three different response characteristics are given by the following.

1) Higher is Better. The S/N for higher the better is given by:

$(S/N)_{HB} = -10 \log (MSD_{HB})$

Where $MSD_{HB} = \frac{1}{r}\sum_{j=1}^{r}\left(\frac{1}{y_j^2}\right)$ equation 3.1.

MSD_{HB} = Mean Square Deviation for higher-the-better response.

2) Nominal is Better. The S/N for nominal is better is:

$(S/N)_{NB} = -10 \log (MSD_{NB})$

Where $MSD_{NB} = \frac{1}{r}\sum_{j=1}^{r}\left(y_j - y_0\right)^2$ equation 3.2.

3) Lower is Better. In this design situation, the heart rate, and oxygen uptake consumed is the type of ‘‘lower is better’’, which is a logarithmic function based on the mean square deviation (MSD), given by

$$S/N_{LB} = -10\log(MSD) = -10\log[(\frac{1}{r}\sum_{i=1}^{r} y^2{}_i)$$

Where $MSD_{LB} = \frac{1}{r}\sum_{j=1}^{r}\left(y_j^2\right)$ equation 3.3.

Signal to noise ratio for response characteristics

The parameters that influence the output can be categorized in two categories, controllable factors and uncontrollable factors. The control factors that may contribute to reduced variation can be quickly identified by looking at the amount of variation present in response. The uncontrollable factors are the sources of variation often associated with operational environment. For this experimental work, response characteristics have given in the Table 3.5.

Measurement of F-value of Fisher’s F ratio

The principle of the *F* test is that the larger the *F* value for a particular parameter, the greater the effect on the performance characteristic due to the change in that process parameter. F value is defined as:

$$F = \frac{\text{MS for the term}}{\text{MS for the error term}}$$

Depending on F-value, percentage contribution is calculated of each factor.

Table 3.5: Response Characteristics

Response name	Response type	Units
Material Removal Rate (MRR)	Higher the better	mm^3/min
Tool Wear Rate (TWR)	Lower the better	mm^3/min
Wear ratio(WR)	Lower the better	-
Micro Hardness	Higher the better	HVN
Surface Roughness	Lower the better	microns
Overcut size	Lower the better	mm

Computation of average performance:

Average performance of a factor at certain level is the influence of the factor at this level on the mean response of the experiments.

Analysis of variance

The knowledge of the contribution of individual factors is critically important for the control of the final response. The analysis of variance (ANOVA) is a common statistical technique to determine the percent contribution of each factor for results of the experiment. It calculates parameters known as sum of squares (*SS*), pure *SS*, degree of freedom (dof), variance, F-ratio and percentage of each factor. Since the procedure of ANOVA is a very complicated and employs a considerable of statistical formula, only a brief description of is given as following.

The Sum of Squares (SS) is a measure of the deviation of the experimental data from the mean value of the data.

Let '*A*' be a factor under investigation

$$SS_T = \sum_{i=1}^{N} (y_i - \overline{T})^2$$

Where N = Number of response observations, $\overline{T}$ is the mean of all observations y_i is the i *th* response

Factor Sum of Squares (SS_A) - Squared deviations of factor (A) averages from overall average

$$SS_A = \left[\sum_{i=1}^{k_A}\left(\frac{A_i^2}{n_{Ai}}\right)\right] - \frac{T^2}{N}$$

equation 3.4.

Where

A_i =Average of all obseravtions under A_i level = A_i / n_{Ai}

T = sum of all observations

$\overline{T}$ = Average of all observations = T / N

n_{Ai} = Number of obsernations under A_i level

Error Sum of Squares (SS_e) - Squared deviations of observations from factor (A) averages

$$SS_e = \sum_{j=1}^{k_A}\sum_{i=1}^{n_{Ai}}\left(y_i - \overline{A}_j\right)^2$$

equation 3.5.

3.10 TEST RESULTS FOR WORKPIECE & ELECTRODE MATERIAL

Three workpiece materials High-Carbon High-Chromium (HCHCr), Hot Die Steel (H11) and AISI 1045 steel and three electrode materials Graphite, Brass and Tungsten-Copper were used. Before the start of experimentation, the chemical composition of workpiece and electrode material was measured on an Optical Emission Spectrometer DV-6. The percentage composition of the workpiece and electrode material is provided in Table 3.6 and 3.7 respectively. The dimension of workpiece selected for High-Carbon High-Chromium and AISI 1045 steel was 100×50×10 mm^3. The dimension of workpiece selected for Hot Die Steel (H11) was 100×80×10 mm^3. The workpieces used before and after machining are shown in the Figure 3.5 and Figure 3.6 respectively. The diameter of each electrode was 20mm and pictorial view of electrodes are shown in the Figure 3.7.The copper tool which was used for measurement of profile/geometric accuracy with different front angle such as 90

and 120 are shown in Figure 3.8(a) and 3.8(b). In order to study profile/geometric accuracy HDS (H11) workpiece after machining with copper tool with different front angle such as 90° and 120° is shown in Figure 3.9.

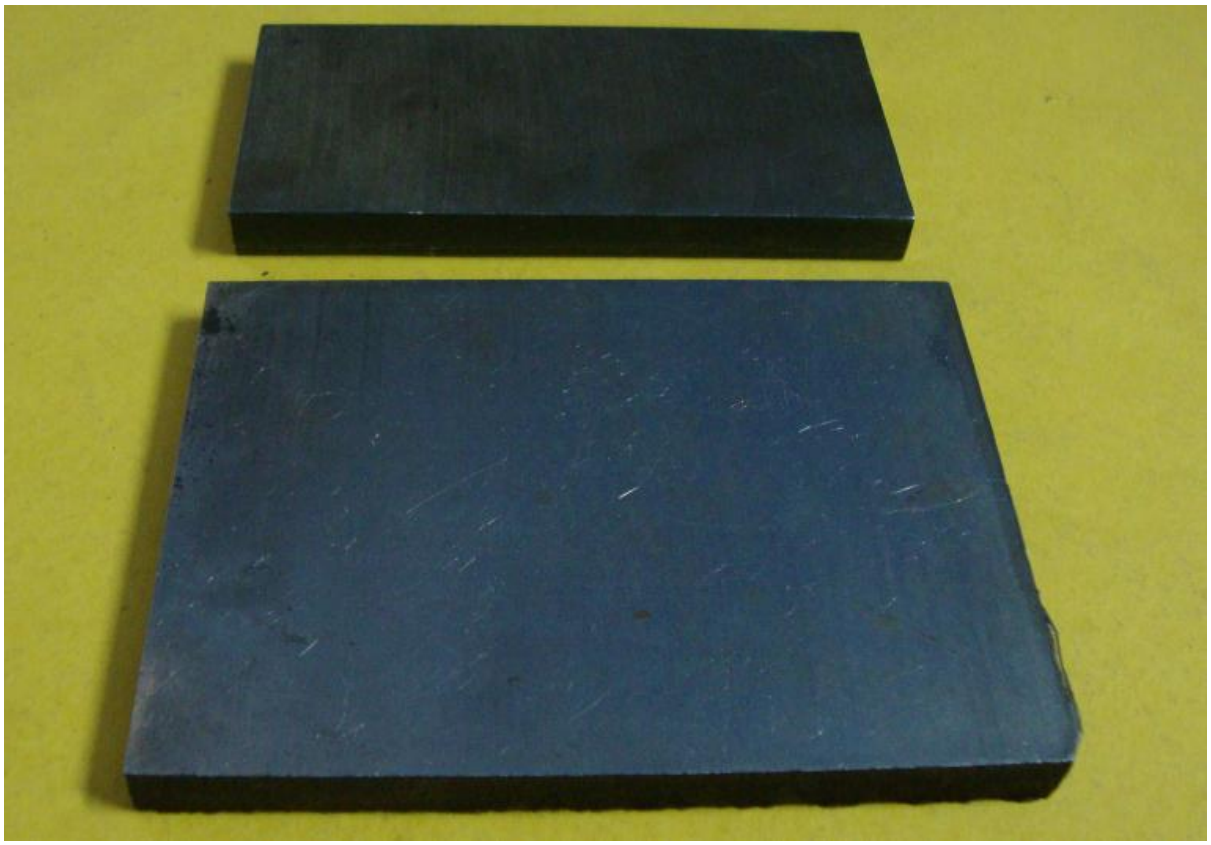

Figure 3.5: Workpiece materials before machining

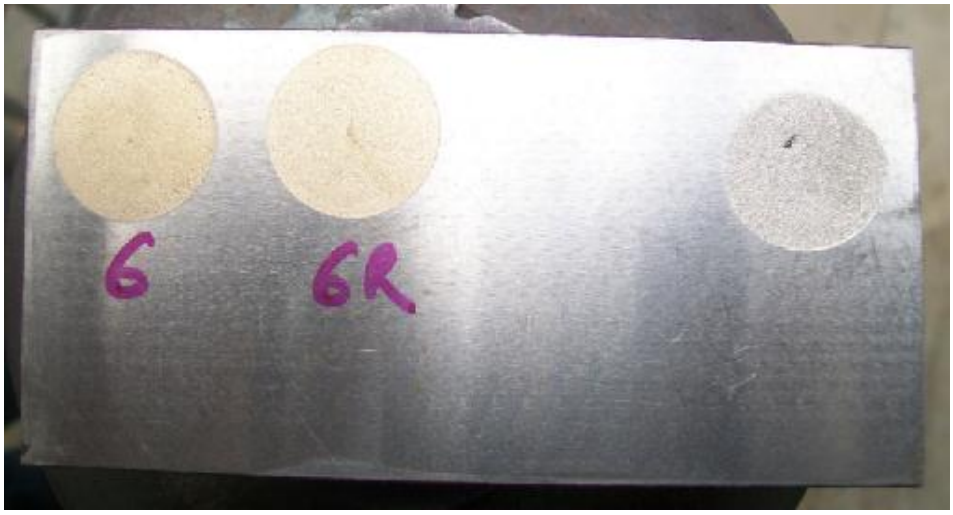

(a)

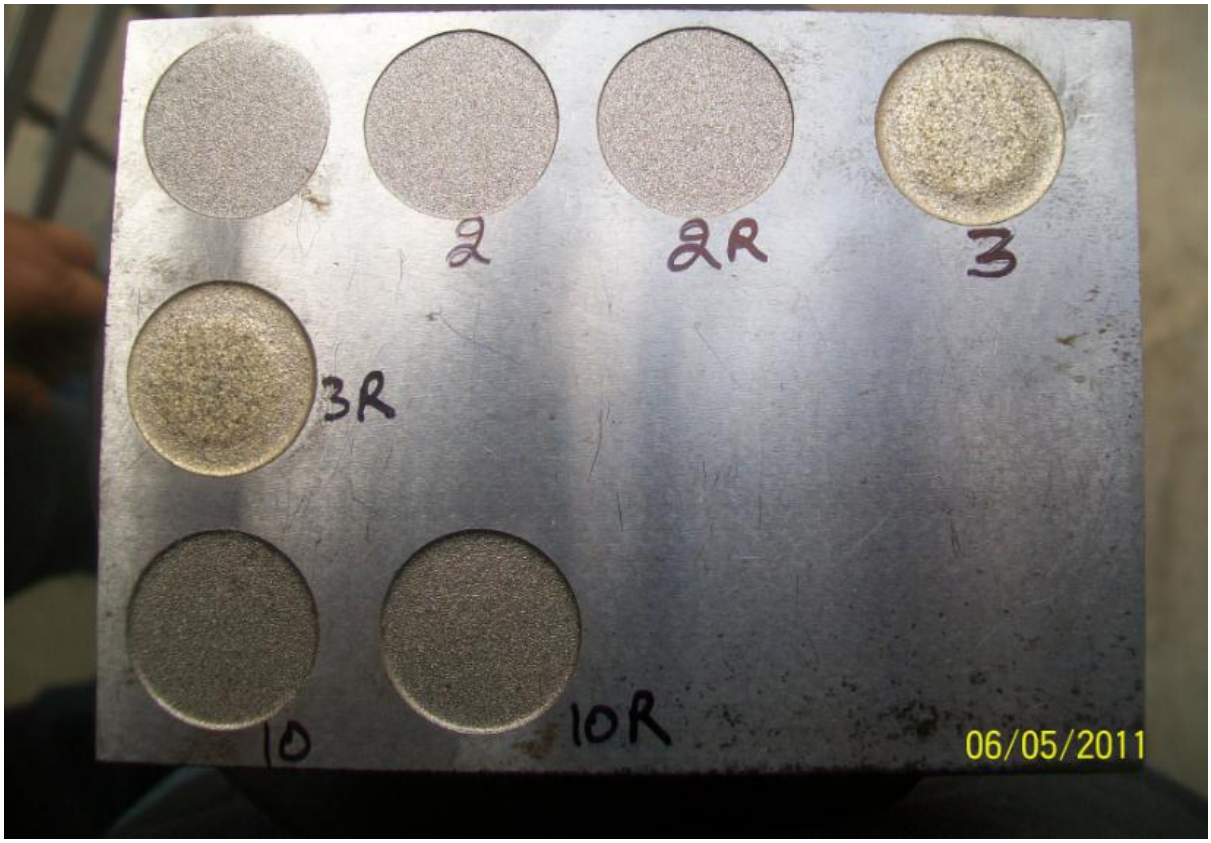

(b)

Figure 3.6: Workpiece materials after machining

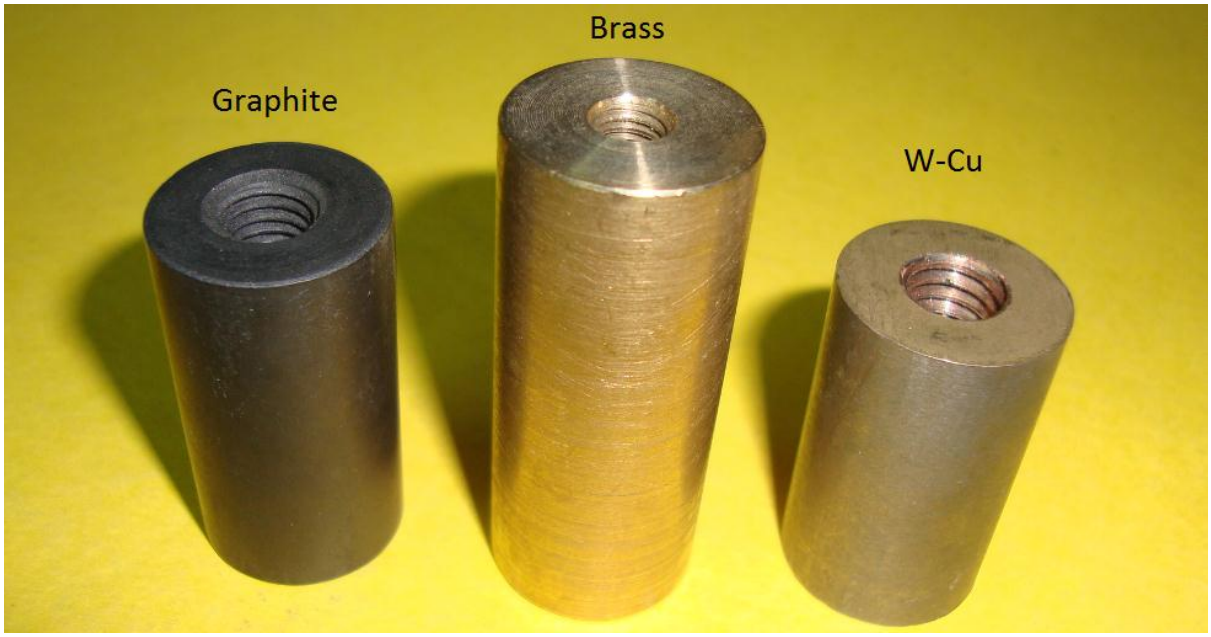

Figure 3.7: Electrodes

Table 3.6: Chemical composition of workpiece materials

workpiece	% composition													
	Fe	C	Si	Mn	P	S	Cr	Mo	Ni	Co	Cu	Ti	V	W
HDS(H11)	91.2	0.364	1.02	0.269	0.0449	0.0417	4.99	1.24	0.171	0.0271	0.112	0.002	0.302	0.0568
HCHCr	85.4	1.59	0.401	0.198	0.0452	0.0942	11.6	0.105	0.240	0.0233	0.0441	0.0210	0.0112	0.0220
AISI 1045	98.0	0.518	0.348	0.749	0.0658	0.0523	0.0605		0.018	0.0065	0.065	0.0020	0.002	0.015

Table 3.7: Chemical composition of electrode materials

Electrode	% composition						
	W	Cu	Ni	Z	Ti	Pb	Zn
Tungsten-copper	79.36	19.462	0.121	0.047	0.014	0.026	
Brass		68.8					30.2
Copper		99.78	0.045	0.09	0.029	0.044	
Graphite	99.99% pure						

Table 3.8: Micro hardness of workpiece materials before machining

Workpiece material	HDS(H11)	HCHCr	AISI 1045
Micro hardness (HVN)	538	576	515

(a) Copper tool with 60°

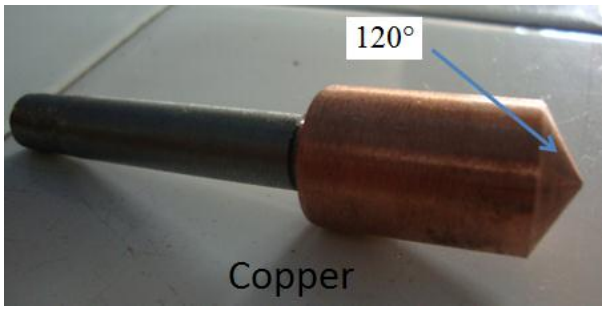

(b) Copper tool with 90° **(c) Copper tool with 120°**

Figure 3.8: Tool geometry with different front angle

CHAPTER 4
RESULTS AND ANALYSIS

4.1 RESULT AND ANALYSIS OF MRR

4.1.1 Introduction

The effect of various parameters such as current, workpiece, dielectric, electrode, pulse on time, powder concentration and types of powder were evaluated using ANOVA and factorial design analysis. A confidence interval of 95% has been used for the analysis. 18 trials were conducted in the experiment using L18 experimental design. One repetition for each of 18 trials was completed so as to measure Signal to Noise ratio (S/N ratio).

4.1.2 Results for MRR

The results of MRR for each of the 18 trials with repetition are given in Table4.1. Weight of workpiece before and after each of the trial was calculated to evaluate the MRR of each sample. The MRR is given by

$$\text{MRR} = \frac{W_i - W_f}{\rho t} \times 1000 \text{ mm}^3/\text{min}$$

Where W_i= Initial weight of workpiece material (gms)

W_f= Final weight of workpiece material (gms)

t = Time period of trials in minutes

ρ = Density of workpiece in gms/cc

Table 4.1: Results for MRR

Trial no.	Dielectric	Workpiece	Electrode	Powder concentration (g/l)	Current (Amp)	Pulse on (μs)	Powder	MRR (mm^3/min)		Mean MRR (mm^3/min)	S/N ratio
								I	II		
1	Kerosene	H11	Gr	0	3	20	Si	4.05	4.119	4.119	12.30
2	Kerosene	H11	W-Cu	5	5	50	Graphite	9.1	9.297	9.195	19.27
3	Kerosene	H11	Brass	10	7	100	W	17	17.50	17.00	24.74
4	Kerosene	HCHCr	Gr	0	5	50	W	4.3	4.506	4.4032	12.88
5	Kerosene	HCHCr	W-Cu	5	7	100	Si	29.9	30.32	30.111	29.57
6	Kerosene	HCHCr	Brass	10	3	20	Graphite	1.0	1.184	1.0918	0.763
7	Kerosene	AISI 1045	Gr	5	3	100	Graphite	8.9	10.64	9.7716	19.80
8	Kerosene	AISI 1045	W-Cu	10	5	20	W	15.65	15.01	15.330	23.71
9	Kerosene	AISI 1045	Brass	0	7	50	Si	9.968	7.9	8.9340	19.02
10	EDM oil	H11	Gr	10	7	50	Graphite	15.03	13.9	14.465	23.21
11	EDM oil	H11	W-Cu	0	3	100	W	11.74	10.89	11.316	21.07
12	EDM oil	H11	Brass	5	5	20	Si	5.553	4.11	4.8315	13.68
13	EDM oil	HCHCr	Gr	5	7	20	W	8.828	7.02	7.9242	17.97
14	EDM oil	HCHCr	W-Cu	10	3	50	Si	12.61	11.95	12.281	21.78
15	EDM oil	HCHCr	Brass	0	5	100	Graphite	13.77	11.55	12.664	22.05
16	EDM oil	AISI 1045	Gr	10	5	100	Si	26.63	24.8	25.716	28.20
17	EDM oil	AISI 1045	W-Cu	0	7	20	Graphite	11.29	9.75	10.5178	20.44
18	EDM oil	AISI 1045	Brass	5	3	50	W	0.977	0.80	0.8883	-1.03

4.1.3 Analysis of variance – MRR

The results were analysed using ANOVA for identifying the significant factors affecting the performance measures. The Analysis of Variance (ANOVA) for the mean MRR at 95% confidence interval is given in Table 4.2. The variation data for each factor were F-tested to find significance of each. The principle of the F-test is that the larger the F value for a particular parameter, the greater the effect on the performance characteristic due to the change in that process parameter. ANOVA table shows that pulse on time (F value 24.08), current (F value 12.78), electrode (F value 9.29), powder concentration (F value 6.11), powder (F value 5.45) are the factors that significantly affect the MRR. All others factors, namely, dielectric and workpiece material were found to be insignificant. Table 4.3 shows the ranks of various factors in the terms of their relative significance. Pulse on has the highest rank, signifying highest contribution to MRR and dielectric has the lowest rank and was observed to be insignificant in affecting MRR. Main effect plot for the mean MRR is shown in the Figure 4.1 which shows the variation of MRR with the input parameters. As it can be seen MRR increases with increase in pulse on time from 20µs to 100µs. MRR increases with increase in current and powder concentration. Higher current means higher spark energy. Higher spark energy cause more material removal from the surface. Hence, MRR increases with increase in current. When pulse on time is high, it means sparking occurs for longer time. So material removal takes place for longer time and thus MRR increases with increase in pulse on time. When powder is added into the insulating dielectric, it becomes conductive and hence improvement in sparking occurs which causes more material removal from the surface. Thus MRR increases with increase in powder concentration. MRR is high with tungsten-copper electrode as compared to graphite and brass electrode and the MRR is high with addition of silicon powder in dielectric fluid as compared to graphite and tungsten powder.

Table 4.2: ANOVA for MRR

Sources	SS	v	V	F	p	SS'	% contribution
Dielectric (A)	0.009	1	0.009	0.00			
Workpiece (B)	8.895	2	4.447	0.53			
Electrode (C)	154.808	2	77.404	9.29	0.031	142.745	14.221
Powder Concentration(D)	101.794	2	50.897	6.11	0.061	89.7308	8.93956
Current(E)	212.899	2	106.450	12.78	0.018	200.836	20.009
Pulse on time(F)	401.220	2	200.610	24.08	0.006	389.157	38.77
Powder (G)	90.808	2	45.404	5.45	0.072	78.745	7.845
Error	33.321	4	8.330				
Total	1003.75	17				1003.75	100
e pooled	42.221	7	6.0316			102.536	10.215

Table 4.3: Response table for means of MRR

Level	Dielectric (A)	Workpiece (B)	Electrode (C)	Powder Concentration(D)	Current€	Pulse on time(F)	Powder (G)
1	11.178	11.860	7.610	8.659	6.578	7.302	9.618
2	11.134	11.413	11.066	10.454	12.023	8.361	14.332
3		10.196	14.792	14.356	14.867	17.805	9.519
Delta	0.044	1.664	7.182	5.697	8.289	10.503	4.813
Rank	7	6	3	4	2	1	5

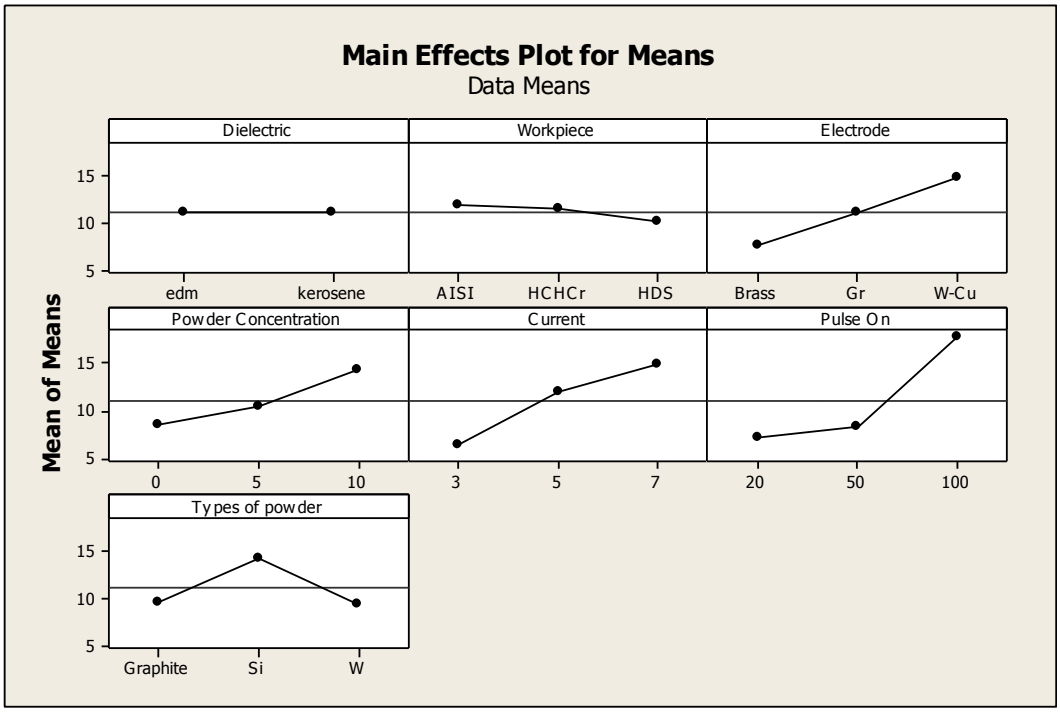

Figure 4.1: Main effect plot for Mean MRR

4.1.4 Results for S/N ratio – MRR

The S/N ratio is an indication of the amount of variation present in the process. The S/N ratios have been calculated to identify the major contributing factors that cause variation in MRR. MRR is a "Higher the better" type response and it is given by a logarithmic function based on the mean square deviation:

$(S/N)_{HB} = -10 \log (MSD_{HB})$

Where $MSD_{HB} = \frac{1}{r}\sum_{j=1}^{r}\left(\frac{1}{y_j^{\,2}}\right)$

MSD_{HB}= Mean Square Deviation for higher-the-better response.

Table 4.4 shows the ANOVA results for S/N ratio of MRR at 95% confidence interval. Current, pulse on and electrode are the factors which are found to be significant. According to F-test current was found to be the most significant factor affecting the MRR, followed by pulse on time and electrode. Main effect plot of S/N ratio for MRR are shown in the Figure 4.2. Table 4.5 shows the ranks of various factors in the terms of their relative significance.

Current has the highest rank which signifies that it provides highest contribution to MRR and dielectric has the lowest rank and was found to be insignificant in affecting MRR.

Table 4.4: ANOVA for S/N ratio of MRR

Sources	SS	v	V	F	p	SS'	% contribution
Dielectric (A)	1.588	1	1.588	0.06			
Workpiece (B)	7.135	2	3.568	0.15			
Electrode (C)	272.403	2	136.202	5.58	0.050	234.362	20.736
Powder Concentration(D)	45.632	2	22.816	0.93			
Current(E)	327.598	2	163.799	6.70	0.05	289.556	25.6192
Pulse on time(F)	320.589	2	160.294	6.56	0.05	282.547	24.999
Powder (G)	57.564	2	28.782	1.18			
Error	97.721	4	24.430				
Total	1130.23	17				1130.23	100
e pooled	209.23	11	19.021			323.765	28.646

Table 4.5: Response table for S/N ratio of MRR

Level	Dielectric (A)	Workpiece (B)	Electrode (C)	Powder Concentration(D)	Current(E)	Pulse on time(F)	Powder (G)
1	18.60	18.36	13.20	17.96	12.45	14.81	17.59
2	18.01	17.50	19.06	16.55	19.97	15.85	20.76
3		19.04	22.64	20.40	22.49	24.24	16.56
Delta	0.59	1.54	9.44	3.85	10.04	9.43	4.2
Rank	7	6	2	5	1	3	4

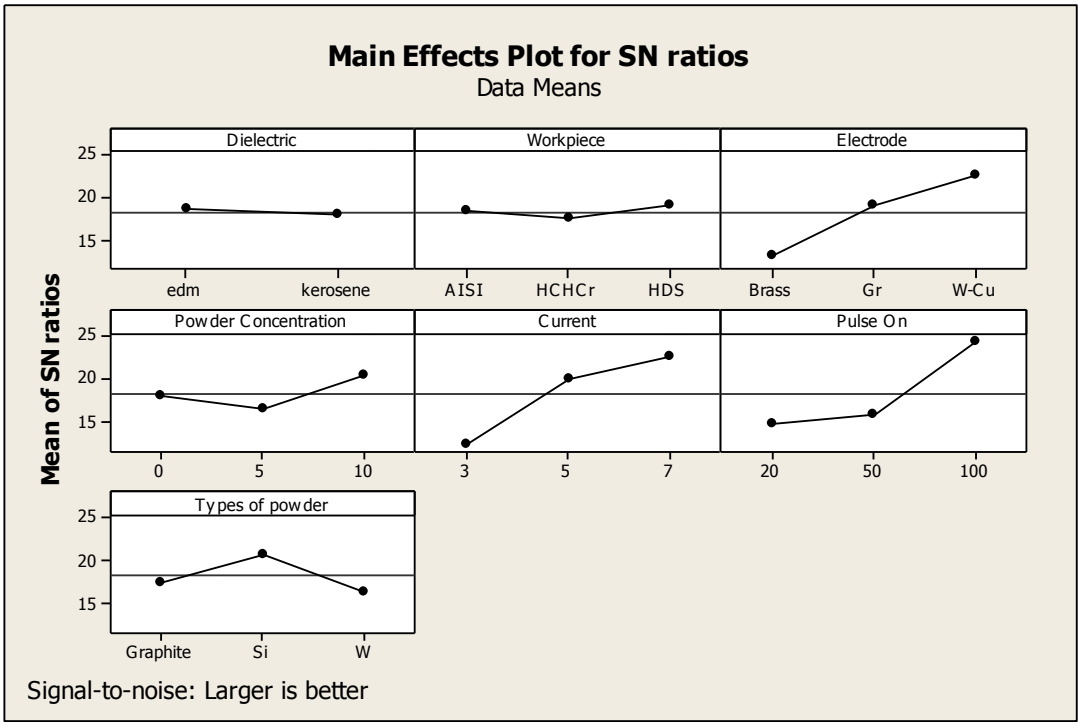

Figure 4.2: Main effects plot of S/N ratio of MRR

4.1.5 Optimal Design

In this experimental analysis, the main effect plot in Figure 4.1 is used to estimate the mean MRR with optimal design conditions. In Table 4.6 it is concluded that highest MRR was achieve when tungsten-copper electrode, silicon powder, powder concentration 10g/l, pulse on time 100 μs and current 7Amp was selected in the experiment trial. In S/N ratio highest MRR was found when tungsten copper electrode, pulse on time 100 μs and current 7Amp was selected in experiment trial. In some case, the same levels of the significant factors provide the higher average and reduced variability; hence nothing has to be compromised. In some case, the levels of factors which improve the average and improve the uniformity may conflict which means compromise may have to be reached. Moreover, a compromise may have to occur when multiple responses are considered and the same level factor may cause one response to improve and another to reduce.

Estimating the mean

MRR is a "Higher the better" type response. In this experiment analysis, different experimental trials have been chosen to obtain satisfactory results. After conducting the experiments the optimum treatment condition within the experiments determined on the basis of prescribed combination of factor levels is determined to one of those in the experiment.

Table 4.6: Significant factors for MRR

Factors	Affecting mean		Affecting variation (S/N ratio)	
	Contribution	Best level	Contribution	Best level
Dielectric (A)	Insignificant	-		-
Workpiece (B)	Insignificant	-		-
Electrode (C)	Significant	Level 3- W-Cu	Significant	Level 3-W-Cu
Powder Concentration(D)	Significant	Level 3-10gm/l		-
Current(E)	Significant	Level 3-7amp	Significant	Level 3-7amp
Pulse on time(F)	Significant	Level 3-100µs	Significant	Level 3-100µs
Powder (G)	Significant	Level 2-Silicon	-	-

Mean value of MRR is given by:

$$\mu_{C_3,D_3,E_3,F_3,G_2} = \overline{C_3} + \overline{D_3} + \overline{E_3} + \overline{F_3} + \overline{G_2} - 4\overline{T}$$

$= 14.792 + 14.356+14.867+17.805+14.332- 4(11.1562)$

$= 31.53 mm^3/min$

Confidence Interval around the Estimated Mean

The confidence interval signifies the maximum and minimum value between which the true average fall at some stated percentage of confidence. The estimate of the mean µ is only a point estimate based on the averages of results obtained from the experiment. Statistically it specifies that there is 50% chance of the true averages being greater than µ and a 50% chance of the true average being less than µ.

Confidence Interval around the estimated MRR

$$CI = \sqrt[2]{\frac{F_{\alpha,\nu_1,\nu_2} V_e}{n_{eff}}}$$ Where F_{α,ν_1,ν_2} = F ratio

α = risk (0.05)

confidence = $1-\alpha$

ν_1 = dof for mean which is always =1

ν_2 = dof for error = ν_e

n_{eff}= Number of tests under that condition using the participating factors

$$n_{eff} = \frac{N}{1 + dof_{C_3, D_3, E_3, F_3, G_2}} = \frac{18}{1+2+2+2+2+2} = 1.64$$

Where N = number of trials in the experiment

$$CI = \sqrt[2]{\frac{F_{\alpha,\nu_1,\nu_2} V_e}{n_{eff}}}$$

$$= \sqrt{\frac{0.07 \text{ X } 6.0316}{1.64}}$$

$= \pm 0.53054$

Thus the confidence interval around the estimated mean of MRR is given by $31.53 \pm 0.5305 mm^3/min$.

4.2 RESULT AND ANALYSIS OF TWR

4.2.1 Introduction

The effect of parameters such as dielectric, electrode, workpiece, pulse on time, current, types of powder and powder concentration on TWR were evaluated using ANOVA and factorial design analysis. A confidence interval of 95% has been used for the analysis. In order to measure Signal to Noise ratio (S/N ratio),one repetition for each of 18 trials was completed.

4.2.2 Results for TWR

The results for TWR for each of the 18 experimental trials with repetition are given in Table 4.7. The TWR is calculated from the loss in length in electrode during performance trial:

$$\text{TWR} = \frac{\text{A} \times \text{L}}{\text{t}}$$

Where A = front area of electrode (mm^2)

L = Loss in length of electrode (mm)

t = time period of trial (minutes)

TWR = Tool wear rate in mm^3/min

4.2.3 Analysis of variance - TWR

The results were analysed using ANOVA for identifying the significant factors affecting the TWR. The ANOVA results for the mean TWR at 95% confidence interval is given in Table 4.8. ANOVA table shows that Powder Concentration (F value10.23), pulse on (8.69), current (7.76), powder (F value 6.44) and electrode (F value 6.39) are the factors that significantly affecting the TWR. Other factors such as workpiece material, dielectric were found to be insignificant. The rank of various factors in the terms of their relative significance is given in the Table 4.9. Powder concentration has the highest rank which signifies that it has highest contribution to TWR and workpiece has the lowest rank and was found that it has insignificant effect on TWR. Main effect plot for mean TWR is shown in the Figure 4.3 which shows the variation of TWR with the various input parameters. TWR decreases with increase in powder concentration. It can be seen that TWR is minimum when W-Cu electrode is used but it is maximum when brass is used. TWR increases with increase in current and pulse on. The reason for this is same as explained in the case of MRR.

Table 4.7: Results for TWR

Trial no. Parameter as per Table 3.3	TWR (mm^3/min)		Mean TWR (mm^3/min)	S/N ratio
	I	II		
1	1.35	1.76	1.5567	-3.84
2	1.09	1.31	1.2016	-1.60
3	1.30	1.79	1.5468	-3.79
4	1.65	2.34	1.9972	-6.01
5	2.28	3.14	2.7080	-8.65
6	.01	.023	0.0164	35.71
7	1.19	1.61	1.3989	-2.92
8	0.02	0.03	0.0202	33.89
9	3.3	4.19	3.7428	-11.46
10	1.15	1.40	1.2756	-2.11
11	0.3	0.8	0.5501	5.19
12	1.25	2.11	1.6806	-4.51
13	0.2	0.42	0.3089	10.20
14	0.01	0.01	0.0100	40.0
15	3.1	3.52	3.3099	-10.40
16	1.21	1.5	1.3567	-2.65
17	0.35	0.79	0.5688	4.900
18	0.51	0.87	0.6906	3.22

Also, TWR decreases with addition of tungsten powder in dielectric as compared to silicon and graphite powder.

Table 4.8: ANOVA for TWR

Sources	SS	v	V	F	p	SS'	% contribution
Dielectric (A)	1.09398	1	1.09398	4.77			
Workpiece (B)	0.03441	2	0.01720	0.08			
Electrode (C)	2.93063	2	1.46531	6.39	0.05	2.3463	11.6415
Powder Concentration(D)	4.68731	2	2.34366	10.23	0.027	4.1030	20.358
Current(E)	3.55777	2	1.77889	7.76	0.042	2.9735	14.753
Pulse on time(F)	3.98170	2	1.99085	8.69	0.035	3.397	16.857
Powder (G)	2.95218	2	1.47609	6.44	0.05	2.3679	11.749
Error	0.91659	4	0.22915				
Total	20.1546	17				20.1546	100
e pooled	2.04501	7	0.2921443			4.9665	24.64

Table 4.9: Response table for means of TWR

Level	Dielectric (A)	Workpiece (B)	Electrode (C)	Powder Concentration(D)	Current(E)	Pulse on time(F)	Powder (G)
1	1.0835	1.2963	1.8312	1.9542	0.7038	0.6919	1.2952
2	1.5765	1.3917	1.3156	1.3314	1.5944	1.4863	1.8425
3		1.3019	0.8431	0.7043	1.6918	1.8117	0.8523
Delta	0.4931	0.0954	0.9881	1.2500	0.9880	1.1198	0.9902
Rank	6	7	4	1	5	2	3

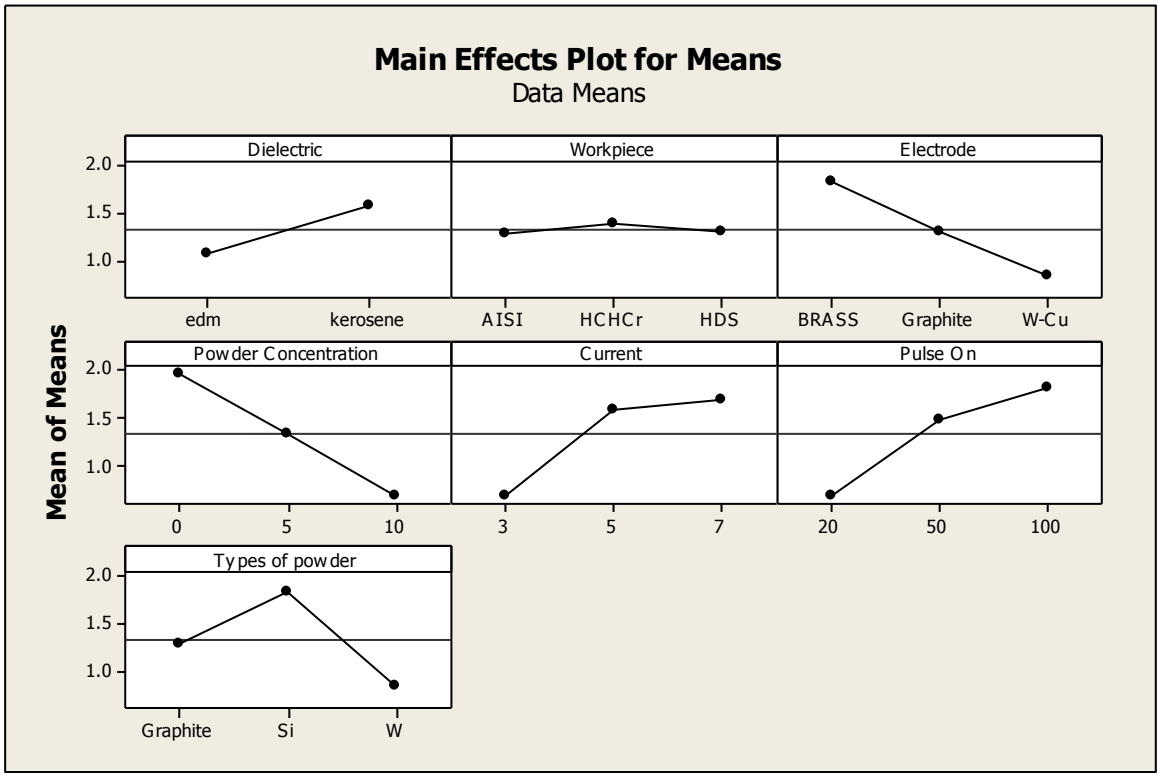

Figure 4.3: Main effects plot for mean TWR

4.2.4 Results for S/N ratio – TWR

The S/N ratios have been calculated to identify the major contributing factors that cause variation in TWR. TWR is a "Lower is better" type response and is given by a logarithmic function based on the mean square deviation (MSD) given by:

$$S/N_{LB} = -10\log(MSD) = -10\log[(\frac{1}{r}\sum_{i=1}^{r} y^2{}_i)$$

Where $MSD_{LB} = \frac{1}{r}\sum_{j=1}^{r}\left(y_j{}^2\right)$

Table 4.10 shows the ANOVA results for S/N ratio of TWR at 95% confidence interval. According to the F test, powder concentration was found to be the most significant factor affecting the TWR, followed by Pulse on time, current and electrode. The rank of various factors in the terms of their relative significance is given in the Table 4.11. The Pulse on time has the highest rank which signifies that it has highest contribution in affecting TWR and dielectric has the lowest rank and was found to be insignificant in affecting TWR. Main effect plot of S/N ratio for TWR are shown in the Figure 4.4.

Table 4.10: ANOVA for S/N of TWR

Sources	SS	v	V	F	p	SS'	% contribution
Dielectric (A)	8.70	1	8.696	0.25			
Workpiece (B)	426.12	2	213.062	6.09			
Electrode (C)	613.92	2	306.959	8.78	0.034	464.896	10.818
Powder Concentration(D)	1468.59	2	734.295	21.00	0.008	1319.566	30.7071
Current(E)	715.83	2	357.917	10.23	0.027	566.806	13.19
Pulse on time(F)	828.31	2	414.154	11.84	0.021	679.286	15.807
Powder (G)	95.90	2	47.952	1.37			
Error	139.89	4	34.972				
Total	4297.26	17				4297.26	100
e pooled	670.61	9	74.512			1266.446	29.471

Table 4.11: Response table for S/N ratio of TWR

Level	Dielectric (A)	Workpiece (B)	Electrode (C)	Powder Concentration(D)	Current(E)	Pulse on time(F)	Powder (G)
1	4.8711	4.1632	1.4605	-2.5980	12.8916	12.7247	3.9309
2	4.1512	11.1468	-0.2158	-0.7089	2.4609	4.6773	1.4795
3		-1.7767	12.2887	16.8402	-1.8192	-3.8686	8.1230
Delta	0.7199	12.9235	12.5045	19.4382	14.7108	16.5934	6.6435
Rank	7	4	5	1	3	2	6

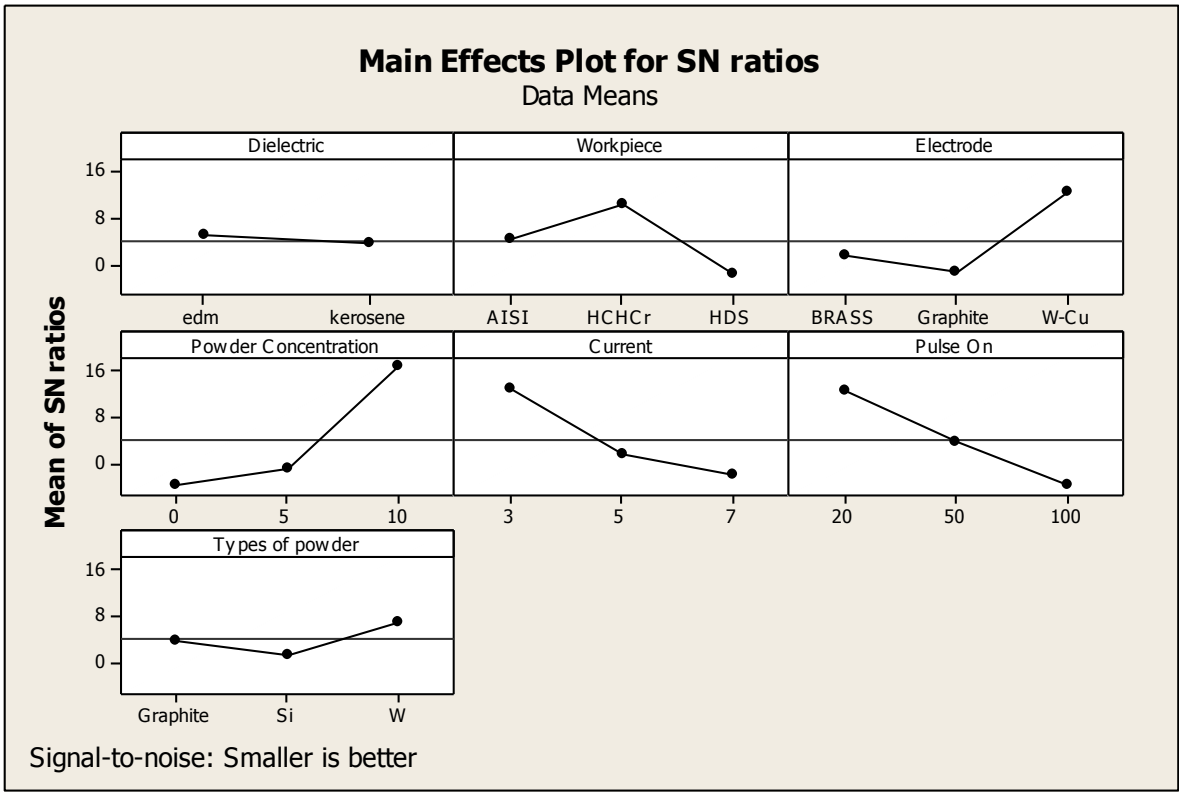

Figure 4.4: Main effects plot for S/N ratio of TWR

4.2.5 Optimal Design

In this experiment, the main effect plot in Figure 4.3 is used to evaluate the mean TWR with optimal design conditions. From the, Table 4.12 it is concluded that least TWR was achieve when tungsten-copper electrode, current 3Amp, pulse on time 20µs and tungsten powder with powder concentration 10g/l was selected in the experimental trial. In S/N ratio minimum TWR was found when tungsten-copper electrode, pulse on time 20µs, current 7Amp and powder concentration of 10g/l was selected in experimental trials. In this case, there are same levels of the significant factors which provide the higher average and reduced variability, thus nothing has to be compromised. In some cases, the levels of factors which improve the average and improve the uniformity may conflict and hence a compromise may have to be reached. Also, a compromise may have to occur when multiple responses are considered and the same factor level may cause one response to improve and another to reduce.

Estimating the mean for TWR

TWR is a "Lower the better" type response. In this experiment analysis, different experimental trials have been chosen to obtain satisfactory results.

Mean value of TWR is given by:

$\mu_{C_3,D_3,E_1,F_1,G_3} = \overline{C_3} + \overline{D_3} + \overline{E_1} + \overline{F_1} + \overline{G_3} - 4\overline{T}$

= 0.8431 + 0.7043 + 0.7038 + 0.6919 + 0.8523- 4(0.92)

= 0.92mm^3/min

Table 4.12: Significant factors for TWR

Factors	Affecting mean		Affecting variation (S/N ratio)	
	Contribution	Best level	Contribution	Best level
Dielectric (A)	Insignificant	-	Insignificant	-
Workpiece (B)	Insignificant	-	Insignificant	-
Electrode (C)	Significant	Level 3- W-Cu	Significant	Level 3- W-Cu
Powder Concentration(D)	Significant	Level 3-10gm/l	Significant	Level 3-10gm/l
Current(E)	Significant	Level 1-3amp	Significant	Level 1- 3amp
Pulse on time(F)	Significant	Level 1-20µs	Significant	Level 1- 20µs
Powder (G)	Significant	Level 3- Tungsten	Insignificant	-

Confidence Interval around the Estimated Mean

The confidence interval is a maximum and minimum value between which the true average should fall at some stated percentage of confidence.

Confidence Interval around the estimated TWR is given by:

$CI = \sqrt[2]{\frac{F_{\alpha,\nu_1,\nu_2} V_e}{n_{eff}}}$ Where F_{α,ν_1,ν_2} = F ratio

α =0.05, risk

Confidence = 1−α

ν_1 = dof for mean which is always =1

ν_2 =dof for error, ν_e

n_{eff}= Number of tests under that condition using the participating factors

$$n_{eff} = \frac{N}{1 + dof_{C_3, D_3, E_1, F_1, G_3}} = \frac{18}{1+2+2+2+2+2} = 1.64$$

Where N = number of trials in the experiment

$$CI = \sqrt[2]{\frac{F_{\alpha,\nu_1,\nu_2} V_e}{n_{eff}}}$$

$$= \sqrt{\frac{0.07 \text{ X } .292144}{1.64}}$$

=0.112

Hence the confidence interval around the TWR is given by 0.92 ± 0.112mm^3/min.

4.3 RESULT AND ANALYSIS OF WEAR RATIO (WR)

4.3.1 Introduction

The effect of parameters such as dielectric, electrode, workpiece, pulse on time, current, types of powder and powder concentration on WR were evaluated using ANOVA and factorial design analysis. A confidence interval of 95% has been used for the analysis. In order to measure Signal to Noise ratio (S/N ratio), one repetition for each of 18 trials was completed.

4.3.2 Results for WR

The results for WR for each of the 18experimental trials with repetition are given in Table 4.13. The WR is calculated for each of the experimental trials. The WR is given by:

$$\mathrm{WR} = \frac{\mathrm{TWR}}{\mathrm{MRR}}$$

Where WR = wear ratio, dimensionless quantity

TWR = Tool wear rate in mm^3/min

MRR = Material removal rate in mm^3/min

Table 4.13: Results for WR

Trial no. as per Table 3.3	MRR (mm^3/min)		Mean MRR (mm^3/min)	TWR (mm^3/min)		Mean TWR (mm^3/min)	Mean WR, No units	S/N ratio
	I	II		I	II			
1	4.05	4.119	4.119	1.35	1.76	1.5567	0.377970	-8.4509
2	9.1	9.297	9.195	1.09	1.31	1.2016	0.130680	-17.6758
3	17	17.50	17.00	1.30	1.79	1.5468	0.089670	-20.9471
4	4.3	4.506	4.4032	1.65	2.34	1.9972	0.453594	-6.86665
5	29.9	30.32	30.111	2.28	3.14	2.7080	0.089933	-20.9216
6	1.0	1.184	1.0918	0.01	0.023	0.0164	0.015020	-36.4666
7	8.9	10.64	9.7716	1.19	1.61	1.3989	0.143160	-16.8836
8	15.65	15.01	15.330	0.02	0.03	0.0202	0.0013177	-57.6037
9	9.968	7.9	8.9340	3.3	4.19	3.7428	0.418940	-7.55696
10	15.03	13.9	14.465	1.15	1.40	1.2756	0.088180	-21.0926
11	11.74	10.89	11.316	0.3	0.8	0.5501	0.048612	-26.2651
12	5.553	4.11	4.8315	1.25	2.11	1.6806	0.347848	-9.17221
13	8.828	7.02	7.9242	0.2	0.42	0.3089	0.0389805	-28.1831
14	12.61	11.95	12.281	0.01	0.01	0.0100	0.0008143	-61.7846
15	13.77	11.55	12.664	3.1	3.52	3.3099	0.261352	-11.6555
16	26.63	24.8	25.716	1.21	1.5	1.3567	0.052760	-25.5539
17	11.29	9.75	10.5178	0.35	0.79	0.5688	0.054080	-25.3393
18	0.977	0.80	0.8883	0.51	0.87	0.6906	0.777390	-2.18722

4.3.3 Analysis of variance - WR

The results were analysed using ANOVA for identifying the significant factors affecting the WR. The ANOVA results for the mean WR at 95% confidence interval is given in Table 4.14. ANOVA table shows that all the factors were found to be insignificant.

Table 4.14: ANOVA for wear ratio

Sources	SS	v	V	F	p
Dielectric (A)	0.000140	1	0.000140	0.01	0.943
Workpiece (B)	0.029363	2	0.014682	0.61	0.589
Electrode (C)	0.209446	2	0.104723	4.33	0.100
Powder Concentration(D)	0.195255	2	0.097627	4.03	0.110
Current(E)	0.031791	2	0.015895	0.66	0.567
Pulse on time(F)	0.138582	2	0.069291	2.86	0.169
Powder (G)	0.049106	2	0.024553	1.01	0.440
Error	0.096807	4	0.024202		
Total	0.750490	17			

Table 4.15: Response table for means of wear ratio

Level	Dielectric (A)	Workpiece (B)	Electrode (C)	Powder Concentration(D)	Current(E)	Pulse on time(F)	Powder (G)
1	0.18556	0.24127	0.31837	0.26909	0.22716	0.13920	0.11541
2	0.19114	0.14328	0.19244	0.25467	0.20793	0.31160	0.21471
3		0.18049	0.4424	0.3129	0.12996	0.11425	0.23493
Delta	0.00559	0.09799	0.26413	0.22780	0.09720	0.19735	0.11952
Rank	7	5	1	2	6	3	4

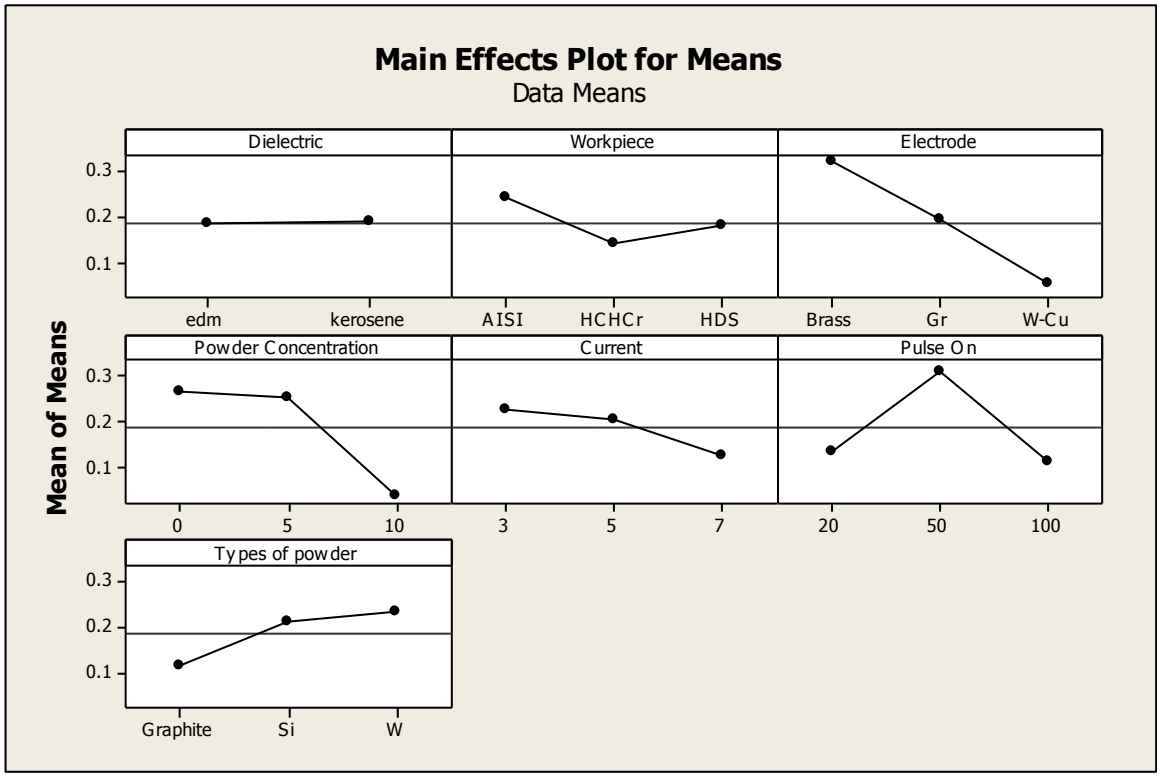

Figure 4.5: Main effects plot for mean wear ratio

4.3.4 Results for S/N ratio of WR

The S/N ratios have been calculated to identify the major contributing factors that cause variation in WR. WR is a "Lower is better" type response and is given by a logarithmic function based on the mean square deviation (MSD) given by:

$$S/N_{LB} = -10\log(MSD) = -10\log[(\frac{1}{r}\sum_{i=1}^{r} y^2{}_i)$$

Where $MSD_{LB} = \frac{1}{r}\sum_{j=1}^{r}\left(y_j{}^2\right)$

Table 4.16 shows the ANOVA results for S/N ratio of WR at 95% confidence interval. According to the F test, powder concentration was found to be the most significant factor affecting the WR, followed by electrode. The rank of various factors in the terms of their relative significance is given in the Table 4.17. Powder concentration has the highest rank which signifies that it has highest contribution in affecting WR and powder has the lowest rank and was found to be insignificant in affecting WR. Main effect plot of S/N ratio for WR are shown in the Figure 4.5.

Table 4.16: ANOVA for S/N ratio of wear ratio

Sources	SS	v	V	F	p	SS'	% contribution
Dielectric (A)	17.72	1	17.722	0.17			
Workpiece (B)	323.19	2	161.595	1.57			
Electrode (C)	1426.05	2	713.024	6.93	0.05	1260.686	28.21
Powder Concentration(D)	1968.18	2	984.088	9.56	0.030	1802.816	37.18
Current(E)	75.37	2	37.687	0.37			
Pulse on time(F)	232.37	2	116.185	1.13			
Powder (G)	14.46	2	7.231	0.07			
Error	411.74	4	102.936				
Total	4469.09	17				4469.09	100
e pooled	1074.86	13	82.682			1405.588	9.08

Table 4.17: Response table for S/N ratio of wear ratio

Level	Dielectric (A)	Workpiece (B)	Electrode (C)	Powder Concentration(D)	Current(E)	Pulse on time(F)	Powder (G)
1	23.47	22.52	14.66	14.36	25.34	27.54	21.52
2	21.49	27.65	17.84	15.84	21.42	19.53	22.24
3		17.27	34.93	37.24	20.67	20.37	23.68
Delta	1.98	10.38	20.27	22.89	4.67	8.01	2.16
Rank	7	3	2	1	5	4	6

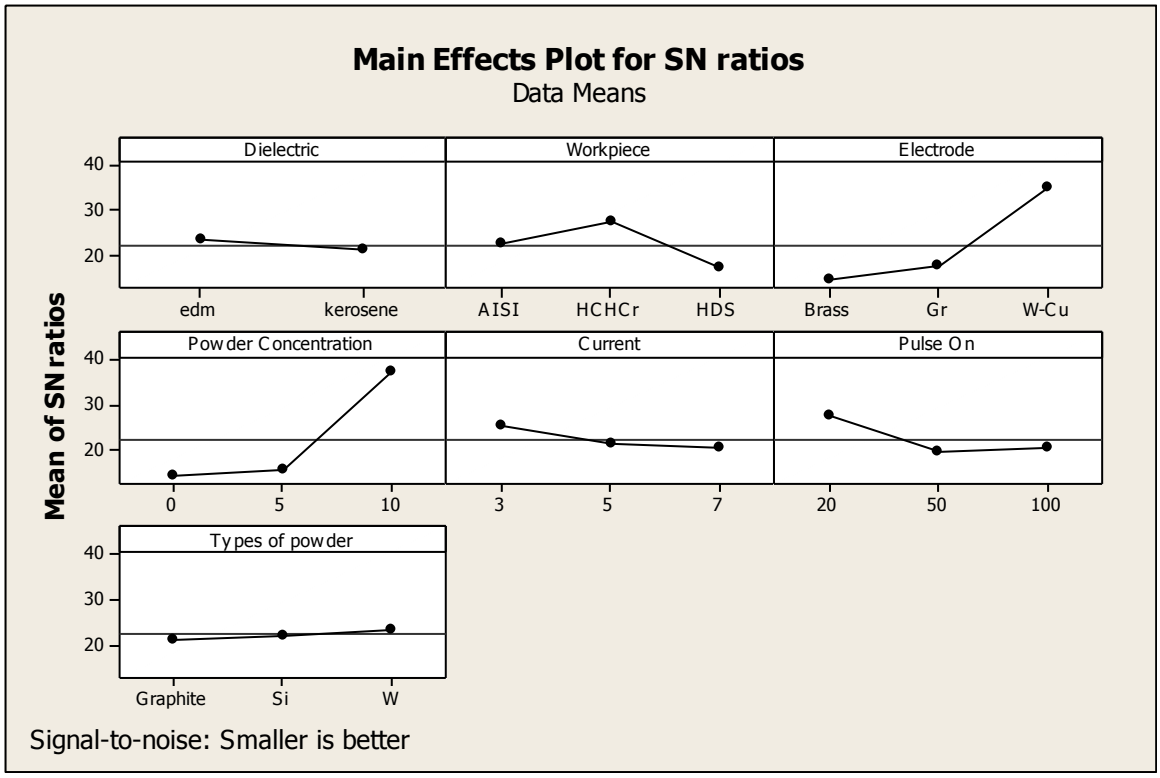

Figure 4.6: Main effects plot for S/N ratio of wear ratio

4.3.5 Optimal Design

In this experiment, the main effect plot for S/N ratio of wear ratio in Figure 4.6 is used to evaluate the mean WR with optimal design conditions. In S/N ratio least WR was found when Brass electrode and powder concentration of 10g/l was selected in the experimental trials. Table 4.18 shows the significant factors for WR.

Estimating the mean for WR

WR is a "Lower the better" type response. In this experiment analysis, different experimental trials have been chosen to obtain satisfactory results.

Mean value of WR is given by:

$$\mu_{C_3,D_3} = \overline{C_3} + \overline{D_3} - \overline{T}$$

$$= 0.4424 + 0.3129 - (0.39911)$$

$$= 0.35619$$

Table 4.18: Significant factors for WR

Factors	Affecting mean		Affecting variation (S/N ratio)	
	Contribution	Best level	Contribution	Best level
Dielectric (A)	Insignificant	-	Insignificant	-
Workpiece (B)	Insignificant	-	Insignificant	-
Electrode (C)	Insignificant	-	Significant	Level 3- W-Cu
Powder Concentration(D)	Insignificant	-	Significant	Level 3-10g/l
Current(E)	Insignificant	-	Insignificant	-
Pulse on time(F)	Insignificant	-	Insignificant	-
Powder (G)	Insignificant	-	Insignificant	-

Confidence Interval around the Estimated Mean

The confidence interval is a maximum and minimum value between which the true average should fall at some stated percentage of confidence.

Confidence Interval around the estimated WR is given by:

$$CI = \sqrt[2]{\frac{F_{\alpha,\nu_1,\nu_2} V_e}{n_{eff}}}$$ Where F_{α,ν_1,ν_2} = F ratio

α =0.05, risk

Confidence = $1-\alpha$

ν_1 = dof for mean which is always =1

ν_2 =dof for error, ν_e

n_{eff}= Number of tests under that condition using the participating factors

$$n_{eff} = \frac{N}{1 + dof_{C_3,D_3}} = \frac{18}{1+2+2} = 3.6$$

Where N = number of trials in the experiment

$$CI = \sqrt[2]{\frac{F_{\alpha,\nu_1,\nu_2} V_e}{n_{eff}}}$$

$$= \sqrt{\frac{0.13 \text{ X } 0.750490}{3.6}}$$

= 0 .0271

Hence the confidence interval around the WR is given by 0.35619± 0.0271.

4.4 RESULTS AND ANALYSIS OF SURFACE ROUGHNESS

4.4.1 Introduction

The effect of various parameters such as current, workpiece, dielectric, electrode, pulse on time, powder concentration and types of powder were evaluated using ANOVA and factorial design analysis. A confidence interval of 95% has been used for the analysis. 18 trials were conducted in the experiment using L18 experimental design. One repetition for each of 18 trials was conducted to measure Signal to Noise ratio (S/N ratio).

4.4.2 Results for surface roughness (Ra)

In this experiment surface roughness of 18 experimental trials with repetition are measured at different three positions, namely, centre, left and right of each sample. The left and right positions were taken 5 mm on each side of centre. The results for surface roughness at centre for each of the 18experimental trials with repetition are given in Table 4.19.

4.4.3 Analysis of variance- surface roughness at centre position

The results were analysed using ANOVA for identifying the significant factors affecting the performance measures. The Analysis of Variance (ANOVA) for the mean surface roughness at centre position at 95% confidence interval is given in Table 4.20. The factors such as powder concentration (F value 23.34), current (F value 12.15), pulse on time (F value 9.52), powder (F value 7.82) and electrode (F value 7.10) were found to be significant in surface roughness at centre position. All other factors such as workpiece and dielectric were found to be insignificant for surface roughness. Table 4.21 shows the ranks of various factors in terms of their relative significance. Powder concentration has the highest rank, signifying the highest contribution to surface roughness and workpiece material has the lowest rank and was observed to be insignificant in affecting surface roughness. Main effect plot are shown in Figure 4.7. It can be seen in Figure 4.7, as the powder concentration increases, surface roughness decreases. When no powder is added into the dielectric fluid then sparking strikes the surface with an impulsive force which creates rough surface but when powder is added into the dielectric fluid, the impulsive force is dispersed among the powder and thus strike the surface with less impulsive force. Hence smooth surface is created. When current and pulse on time increases, surface roughness is increased. High current means more heat input and high pulse on time means spark energy is available for longer time. When high input is available for longer time then high spark energy creates rough surface. Surface roughness is found to be maximum when tungsten copper electrode is used and it is minimum when brass

electrode is used. With tungsten powder, Surface roughness of machined surface decreases and with silicon powder, surface roughness increases.

Table 4.19: Results for surface roughness at centre, left and right position

Trial No	Surface roughness at centre position (microns)		Mean	S/N ratio	Surface roughness at left position (microns)		Mean	S/N ratio	Surface roughness at right position (microns)		Mean	S/N ratio
	I	II			I	II			I	II		
1	5.01	5.69	5.35	-14.57	4.95	5.35	5.15	-14.236	5.22	5.88	5.550	-14.567
2	6.51	7.09	6.8	-16.65	6.25	6.95	6.60	-16.391	7.11	6.89	7.00	-16.650
3	3.18	3.64	3.41	-10.65	3.15	3.268	3.21	-10.127	3.33	3.89	3.609	-10.653
4	6.65	7.34	7.00	-16.90	6.19	7.4	6.8	-16.644	7.06	7.33	7.195	-16.896
5	11.52	12.03	11.78	-21.42	11.12	12.03	11.58	-21.27	12.38	11.569	11.975	-21.419
6	2.08	2.12	2.1	-6.444	2.0	2	2	-6.021	2.39	2.21	2.300	-6.444
7	4.95	5.43	5.19	-14.30	4.53	5.45	4.99	-13.96	5.36	5.16	5.39	-14.30
8	2.65	3.25	2.95	-9.396	2.55	2.95	2.75	-8.787	3.15	3.02	3.150	-9.396
9	8.72	9.1	8.91	-18.998	8.36	9.06	8.71	-18.80	8.85	9.37	9.110	-18.998
10	4.59	5.01	4.8	-13.625	4.21	4.99	4.60	-13.255	4.89	5.11	5.00	-13.625
11	6.79	7.21	7	-16.90	6.59	7.01	6.8	-16.65	6.8	7.6	7.2	-16.90
12	3.73	4.13	3.93	-11.89	3.19	3.87	3.53	-10.955	3.87	4.39	4.130	-11.888
13	3.95	4.45	4.2	-12.47	4.24	4.76	4.50	-13.064	4.01	4.39	4.2	-13.255
14	3.42	3.96	3.69	-11.341	3.33	3.6	3.49	-10.857	3.28	4.1	3.69	-11.341
15	7.95	8.45	8.2	-18.276	7.75	8.25	8	-18.062	7.8	8.5	8.2	-18.276
16	5.46	6.24	5.69	-15.095	5.15	5.82	5.49	-14.784	5.38	5.99	5.685	-15.095
17	8.15	8.85	8.5	-18.589	8.1	8.5	8.30	-18.382	8.29	8.71	8.5	-18.588
18	2.18	2.22	2.2	-6.849	2	2	2	-6.021	2.15	2.25	2.2	-6.849

Table 4.20: ANOVA for surface roughness at centre position

Sources	SS	v	V	F	p	SS'	% contribution
Dielectric (A)	1.545	1	1.5453	1.74			
Workpiece (B)	2.733	2	1.3664	1.54			
Electrode (C)	12.633	2	6.3166	7.10	0.048	10.3938	9.08
Powder Concentration(D)	41.529	2	20.7645	23.34	0.006	39.2898	34.32413
Current(E)	21.615	2	10.8075	12.15	0.020	19.3758	16.927
Pulse on time(F)	16.934	2	8.4672	9.52	0.030	14.6948	12.838
Powder (G)	13.919	2	6.9596	7.82	0.041	11.6798	10.2036
Error	3.558	4	0.8896				
Total	114.467	17				114.467	100
e pooled	7.837	7	1.1196			19.033	16.6273

Table 4.21: Response table for means of surface roughness at centre position

Level	Dielectric (A)	Workpiece (B)	Electrode (C)	Powder Concentration(D)	Current(E)	Pulse on time(F)	Powder (G)
1	5.356	5.572	4.792	7.492	4.255	4.505	5.932
2	5.942	6.160	5.370	5.683	5.760	5.566	6.557
3		5.215	6.786	3.772	6.932	6.877	4.459
Delta	0.586	0.945	1.994	3.720	2.677	2.372	2.098
Rank	7	6	5	1	2	3	4

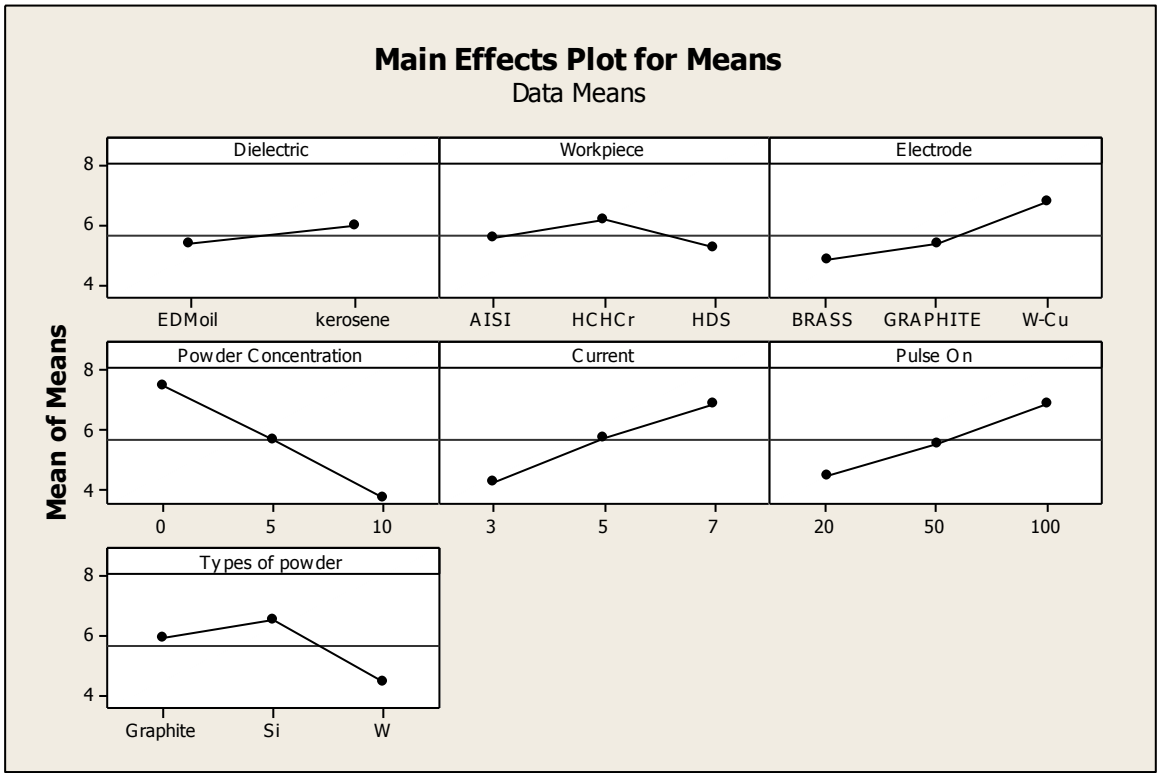

Figure 4.7: Main effect plot for mean surface roughness at centre position

4.4.4 Results for S/N ratio - surface roughness at centre position

The S/N ratios have been calculated to identify the significant factors that cause variation in surface roughness. Surface roughness is a "Lower is better" type of response and is given by a logarithmic function based on the mean square deviation (MSD) given by:

$$S/N_{LB} = -10\log(MSD) = -10\log[(\frac{1}{r}\sum_{i=1}^{r} y^2{}_i)$$

Where $MSD_{LB} = \frac{1}{r}\sum_{j=1}^{r}\left(y_j{}^2\right)$

Table 4.22 shows the ANOVA for S/N ratio for roughness at 95% confidence interval. Mean effect plot for S/N ratio of surface roughness is shown in Figure 4.8. The factors such as powder concentration (F value 131.84), current (F value 62.71), pulse on time (F value 50.32), electrode (F value 42.88)and powder (F value 40.26) were found to be significant in surface roughness at centre position. The factors such as dielectric and workpiece were found to be insignificant in surface roughness. Table 4.23 shows the ranks of various factors in terms of their relative significance. Powder Concentration has the highest rank, signifying the highest contribution to surface roughness and workpiece has the lowest rank and was observed to be insignificant in affecting surface roughness.

Table 4.22: ANOVA for S/N ratio of surface roughness at centre position

Sources	SS	v	V	F	p	SS'	% contribution
Dielectric (A)	1.027	1	1.0266	2.28	0.205		
Workpiece (B)	1.150	2	0.5750	1.28	0.372		
Electrode (C)	38.589	2	19.2947	42.88	0.002	37.4528	12.52
Powder Concentration(D)	118.642	2	59.3210	131.84	0.000	117.506	39.28
Current(E)	56.435	2	28.2174	62.71	0.001	55.2988	18.485
Pulse on time(F)	45.282	2	22.6410	50.32	0.001	44.1458	14.76
Powder (G)	36.231	2	18.1153	40.26	0.002	35.0948	11.73
Error	1.800	4	0.450				
Total	299.155	17				299.155	100
e pooled	3.977	7	0.5681				

Table 4.23: Response table for S/N ratio of roughness at centre position

Level	Dielectric (A)	Workpiece (B)	Electrode (C)	Powder Concentration(D)	Current(E)	Pulse on time(F)	Powder (G)
1	-13.89	-13.87	-12.18	-17.37	-11.73	-12.22	-14.65
2	-14.37	-14.47	-14.49	-13.93	-14.70	-14.06	-15.55
3		-14.05	-15.72	-11.09	-15.96	-16.11	-12.19
Delta	0.48	0.60	3.53	6.28	4.22	3.88	3.36
Rank	7	6	4	1	2	3	5

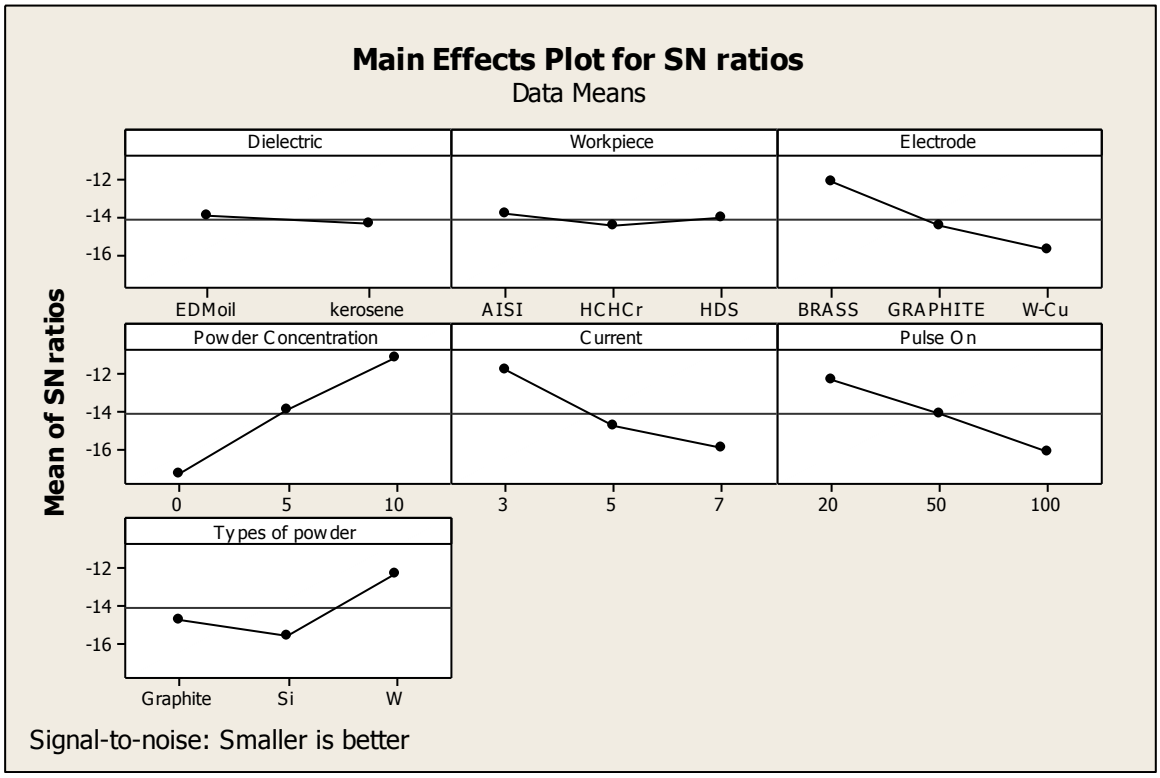

Figure 4.8: Main effect plot for S/N ratio of surface roughness at centre position

4.4.5 Optimal Design

In this experimental analysis, the main effect plot in Figure 4.7 is used to estimate the mean value of surface roughness. From the Table 4.24, it is concluded that least surface roughness was found when current 3amp, pulse on time 20µs, brass electrode, powder concentration 10g/l of tungsten powder were chosen in the experimental trials. In some cases, the levels of factors which improve the average and improve the uniformity may conflict and hence a compromise may have to be reached. Also, a compromise may have to occur when multiple responses are considered and the same factor level may cause one response to improve and another to reduce.

Estimating the mean

Surface roughness is a "Lower the better" type response. In this experiment analysis, different experimental trials have been chosen to obtain satisfactory results.

Mean value of surface roughness at centre position is given by:

$$\mu_{C_1,D_3,E_1,F_1,G_3} = \overline{C_1} + \overline{D_3} + \overline{E_1} + \overline{F_1} + \overline{G_3} - 4\overline{T}$$

$$= 4.792 + 3.772 + 4.255 + 4.505 + 6.557 - 4(4.80175) = 4.67$$

Table 4.24: Significant factors for surface roughness at centre position

Factors	Affecting mean		Affecting variation (S/N ratio)	
	Contribution	Best level	Contribution	Best level
Dielectric (A)	Insignificant	-	Insignificant	-
Workpiece (B)	Insignificant	-	Insignificant	-
Electrode (C)	Significant	Level 1- Brass	Significant	Level 1- Brass
Powder Concentration(D)	Significant	Level 3- 10g/l	Significant	Level 3- 10g/l
Current(E)	Significant	Level 1-3Amp	Significant	Level 1- 3Amp
Pulse on time(F)	Significant	Level 1-20µs	Significant	Level 1- 20µs
Powder (G)	Significant	Level 3-Tungsten	Significant	Level 3-Tungsten

Confidence Interval around the Estimated Mean

The confidence interval is a maximum and minimum value between which the true average should fall at some stated percentage of confidence. The estimate of the mean µ is only a point estimate based on the averages of results obtained from the experiment. It provides a 50% chance of the true averages being greater than µ and a 50% chance of the true average being less than µ.

Confidence Interval around the estimated mean of surface roughness at centre position

$CI = \sqrt[2]{\frac{F_{\alpha,\nu_1,\nu_2} V_e}{n_{eff}}}$ Where F_{α,ν_1,ν_2} = F ratio

α =0.05, risk

Confidence = 1−α

ν_1 = dof for mean which is always =1

ν_2 =dof for error, ν_e

n_{eff}= Number of tests under that condition using the participating factors

$$n_{eff} = \frac{N}{1 + dof_{C_1, D_3, E_1, F_1, G_2}} = \frac{18}{1 + 2 + 2 + 2 + 2 + 2} = 1.64$$

Where N = number of trials in the experiment

$$CI = \sqrt[2]{\frac{F_{\alpha,\nu_1,\nu_2} V_e}{n_{eff}}}$$

$$= \sqrt{\frac{0.17 \text{ X } 1.1196}{1.64}}$$

$= \pm 0.34$

So the confidence interval around the surface roughness at centre position is given by 4.67 ± 0.34 microns.

4.4.6 Analysis of variance- surface roughness at left position

The results were analysed using ANOVA for identifying the significant factors affecting the performance measures. The Analysis of Variance (ANOVA) for the mean surface roughness at left position at 95% confidence interval is given in Table 4.25. The factors such as powder concentration (F value 24.08), current (F value 13.22), pulse on time (F value 9.38),electrode (F value 7.34) and powder (F value 7.29) were found to be significant in surface roughness at left position. All other factors such as workpiece and dielectric were found to be insignificant for surface roughness. Table 4.26 shows the ranks of various factors in terms of their relative significance. Powder concentration has the highest rank, signifying the highest contribution to surface roughness and dielectric has the lowest rank and was observed to be insignificant in affecting surface roughness. Main effect plot surface roughness at left position is shown in Figure 4.9. It can be seen in Figure 4.9, as the powder concentration increases, surface roughness decreases. When current and pulse on time increases, surface roughness is increased. Surface roughness is found to be maximum when tungsten copper electrode is used and it is minimum when brass electrode is used. With tungsten powder, Surface roughness of machined surface decreases and with silicon powder, surface roughness increases.

Table 4.25: ANOVA for surface roughness at left position

Sources	SS	v	V	F	p	SS'	% contribution
Dielectric (A)	1.430	1	1.4303	1.67			
Workpiece (B)	3.577	2	1.7887	2.09			
Electrode (C)	12.560	2	6.2800	7.34	0.046	10.152	8.96
Powder Concentration(D)	41.181	2	20.5907	24.08	0.006	38.773	34.23
Current(E)	22.616	2	11.3081	13.22	0.017	20.208	17.838
Pulse on time(F)	16.037	2	8.0185	9.38	0.031	13.629	12.03
Powder (G)	12.464	2	6.2318	7.29	0.046	10.056	8.877
Error	3.421	4	0.8553				
Total	113.287	17				113.287	100
e pooled	8.428	7	1.204			20.469	18.07

Table 4.26: Response table for means of surface roughness at left position

Level	Dielectric (A)	Workpiece (B)	Electrode (C)	Powder Concentration(D)	Current(E)	Pulse on time(F)	Powder (G)
1	5.189	5.373	4.575	7.293	4.072	4.372	5.748
2	5.753	6.060	5.253	5.532	5.527	5.366	6.323
3		4.981	6.586	3.589	6.816	6.676	4.342
Delta	0.564	1.079	2.011	3.704	2.744	2.305	1.981
Rank	7	6	4	1	2	3	5

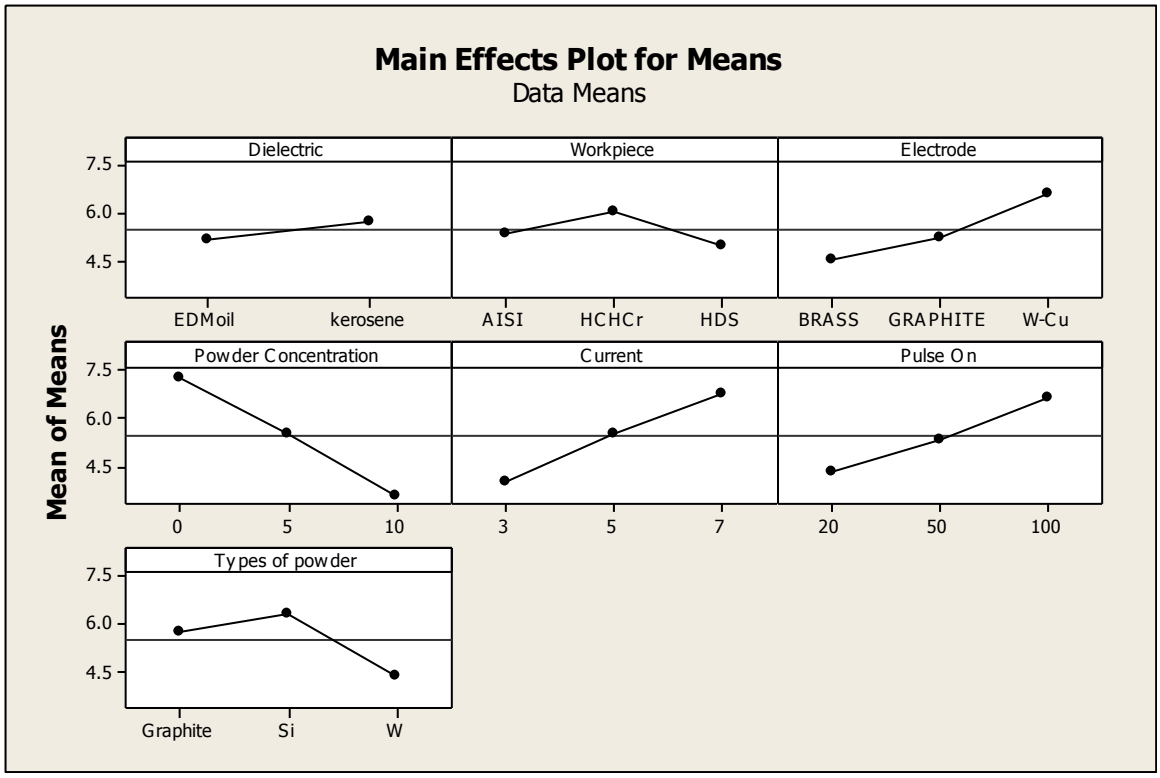

Figure 4.9: Main effect plot for surface roughness at left position

4.4.7 Results for S/N ratio - surface roughness at left position

The S/N ratios have been calculated to identify the significant factors that cause variation in surface roughness. Surface roughness is a "Lower is better" type of response and is given by a logarithmic function based on the mean square deviation (MSD) given by:

$$S/N_{LB} = -10\log(MSD) = -10\log[(\frac{1}{r}\sum_{i=1}^{r} y^2{}_i)$$

Where $MSD_{LB} = \frac{1}{r}\sum_{j=1}^{r}\left(y_j{}^2\right)$

Table 4.27 shows the ANOVA for S/N ratio for surface roughness at 95% confidence interval. Mean effect plot for S/N ratio of surface roughness at left position is shown in Figure 4.10. The factors such as powder concentration (F value 90.28), current (F value 45.25), pulse on time (F value 32.66), electrode (F value31.48)and powder (F value 24.79) were found to be significant in surface roughness at left position. The factors such as dielectric and workpiece were found to be insignificant in surface roughness at left position. Table 4.28 shows the ranks of various factors in terms of their relative significance. Powder Concentration has the highest rank, signifying the highest contribution to surface roughness

and dielectric has the lowest rank and was found to be insignificant in affecting surface roughness.

Table 4.27: ANOVA for S/N ratio of surface roughness at left position

Sources	SS	v	V	F	p	SS'	% contribution
Dielectric (A)	0.984	1	0.9843	1.4			
Workpiece (B)	2.564	2	1.2818	1.83			
Electrode (C)	44.169	2	22.0846	31.48	0.004	42.3532	13.846
Powder Concentration(D)	126.684	2	63.3422	90.28	0.000	124.8682	40.82
Current(E)	63.495	2	31.7475	45.25	0.002	61.679	20.164
Pulse on time(F)	45.827	2	22.9134	32.66	0.003	44.011	14.388
Powder (G)	34.794	2	17.3970	24.79	0.006	32.978	10.78
Error	2.807	4	0.7016				
Total	321.324	17				321.324	100
e pooled	6.355	7	0.9079			15.435	4.8

Table 4.28: Response table for S/N ratio of surface roughness at left position

Level	Dielectric (A)	Workpiece (B)	Electrode (C)	Powder Concentration(D)	Current(E)	Pulse on time(F)	Powder (G)
1	-13.56	-13.46	-11.66	-17.13	-11.29	-11.91	-14.35
2	-14.03	-14.32	-14.32	-13.61	-14.27	-13.66	-15.15
3		-13.60	-15.39	-10.64	-15.82	-15.81	-11.88
Delta	0.47	0.86	3.72	6.49	2.744	3.90	3.27
Rank	7	6	4	1	2	3	5

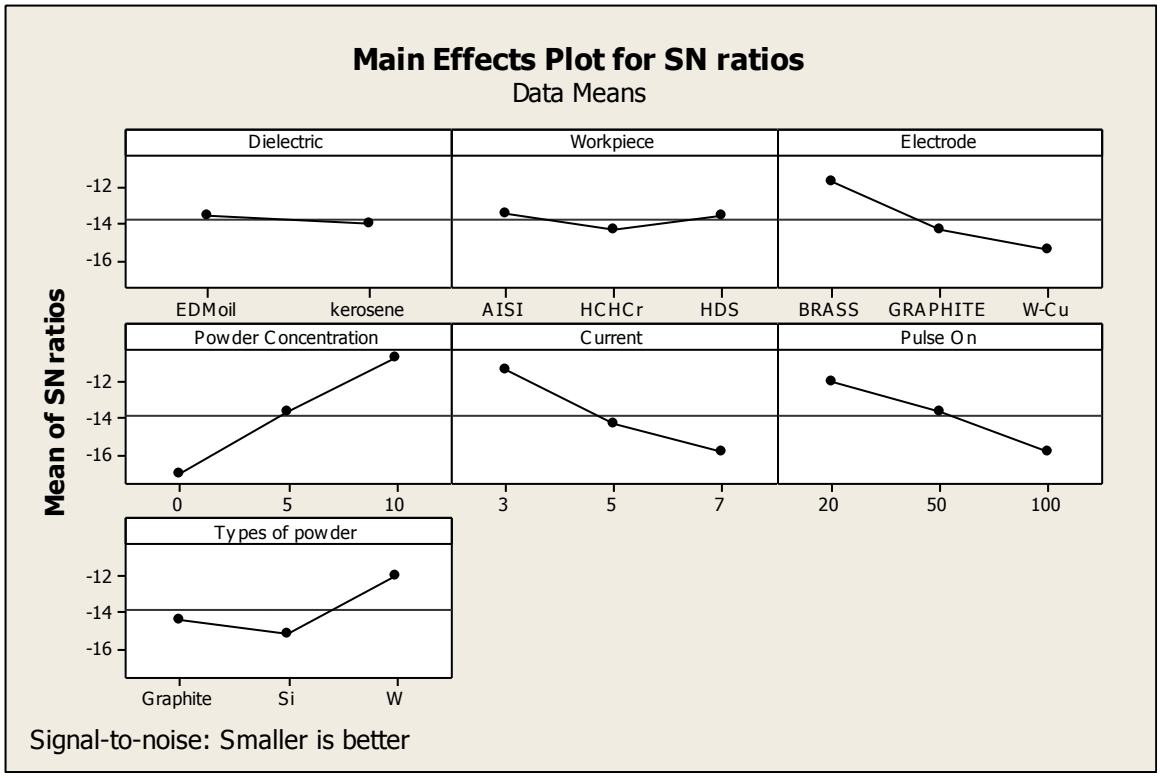

Figure 4.10: Main effect plot for S/N ratio of surface roughness at left position

4.4.8 Optimal Design

In this experimental analysis, the main effect plot for surface roughness at left position in Figure 4.9 is used to estimate the mean value of surface roughness. From the Table 4.29, it is concluded that least surface roughness was found when current 3amp, pulse on time 20µs, brass electrode, powder concentration 10g/l of tungsten powder were chosen in the experimental trials. In some cases, the levels of factors which improve the average and improve the uniformity may conflict and hence a compromise may have to be reached. Also, a compromise may have to occur when multiple responses are considered and the same factor level may cause one response to improve and another to reduce.

Estimating the mean

Surface roughness is a "Lower the better" type response. In this experiment analysis, different experimental trials have been chosen to obtain satisfactory results.

Mean value of surface roughness at left position is given by:

$$\mu_{C_1,D_3,E_3,F_3,G_3} = \overline{C_1} + \overline{D_3} + \overline{E_3} + \overline{F_3} + \overline{G_3} - 4\overline{T}$$

$$= 4.1128$$

Table 4.29: Significant factors for surface roughness at left position

Factors	Affecting mean		Affecting variation (S/N ratio)	
	Contribution	Best level	Contribution	Best level
Dielectric (A)	Insignificant	-	Insignificant	-
Workpiece (B)	Insignificant	-	Insignificant	-
Electrode (C)	Significant	Level 1- Brass	Significant	Level 1- Brass
Powder Concentration(D)	Significant	Level 3- 10g/l	Significant	Level 3- 10g/l
Current(E)	Significant	Level 1-3Amp	Significant	Level 1-3Amp
Pulse on time(F)	Significant	Level 1-20µs	Significant	Level 1- 20µs
Powder (G)	Significant	Level 3-Tungsten	Significant	Level 3-Tungsten

Confidence Interval around the Estimated Mean

The confidence interval is a maximum and minimum value between which the true average should fall at some stated percentage of confidence. The estimate of the mean µ is only a point estimate based on the averages of results obtained from the experiment. It provides a 50% chance of the true averages being greater than µ and a 50% chance of the true average being less than µ.

Confidence Interval around the estimated mean of surface roughness at left position

$$CI = \sqrt[2]{\frac{F_{\alpha,\nu_1,\nu_2} V_e}{n_{eff}}}$$ Where F_{α,ν_1,ν_2} = F ratio

α =0.05, risk

Confidence = 1−α

ν_1 = dof for mean which is always =1

ν_2 =dof for error, ν_e

n_{eff}= Number of tests under that condition using the participating factors

$$n_{eff} = \frac{N}{1 + dof_{C_1, D_3, E_1, F_1, G_3}} = \frac{18}{1+2+2+2+2+2} = 1.64$$

Where N = Number of trials in the experiment

$$CI = \sqrt[2]{\frac{F_{\alpha,\nu_1,\nu_2} V_e}{n_{eff}}}$$

$$= \sqrt{\frac{0.07 \text{ X } 1.204}{1.64}}$$

$= \pm 0.23$

So the confidence interval around the surface roughness at left position is given by 4.1128 ±0. 23microns.

4.4.9 Analysis of variance- surface roughness at right position

The results were analysed using ANOVA for identifying the significant factors affecting the performance measures. The Analysis of Variance (ANOVA) for the mean surface roughness at right position at 95% confidence interval is given in Table 4.30. The factors such as powder concentration (F value 23.34), current (F value 12.15), pulse on time (F value 9.52), powder (F value 7.82) and electrode (F value 7.10) were found to be significant in surface roughness at right position. All other factors such as workpiece and dielectric were found to be insignificant for surface roughness. Table 4.31 shows the ranks of various factors in terms of their relative significance. Powder concentration has the highest rank, signifying the highest contribution to surface roughness and workpiece material has the lowest rank and was found to be insignificant in affecting surface roughness. Main effect plot for surface roughness at right position is shown in Figure 4.11. It can be seen in Figure 4.11, as the powder concentration increases, surface roughness decreases. When current and pulse on time increases, surface roughness is increased. Surface roughness is found to be maximum when tungsten copper electrode is used and it is minimum when brass electrode is used. With tungsten powder, Surface roughness of machined surface decreases and with silicon powder, surface roughness increases.

Table 4.30: ANOVA for surface roughness at right position

Sources	SS	v	V	F	p	SS'	% contribution
Dielectric (A)	1.545	1	1.5453	1.74			
Workpiece (B)	2.733	2	1.3664	1.54			
Electrode (C)	12.633	2	6.3166	7.10	0.048	10.394	9.08
Powder Concentration(D)	41.529	2	20.7645	23.34	0.006	39.29	34.32
Current(E)	21.615	2	10.8075	12.15	0.020	19.376	16.927
Pulse on time(F)	16.934	2	8.4672	9.52	0.030	14.695	12.838
Powder (G)	13.919	2	6.9596	7.82	0.041	11.68	10.204
Error	3.558	4	0.8896				
Total	114.467	17				114.467	100
e pooled	7.836	7	1.1194			19.435	16.98

Table 4.31: Response table for means of surface roughness at right position

Level	Dielectric (A)	Workpiece (B)	Electrode (C)	Powder Concentration(D)	Current(E)	Pulse on time(F)	Powder (G)
1	5.556	5.772	4.992	7.692	4.455	4.705	6.132
2	6.142	6.360	5.570	5.882	5.96	5.766	6.757
3		5.415	6.986	3.972	7.132	7.077	4.659
Delta	0.586	0.945	1.994	3.72	2.677	2.372	2.098
Rank	7	6	5	1	2	3	4

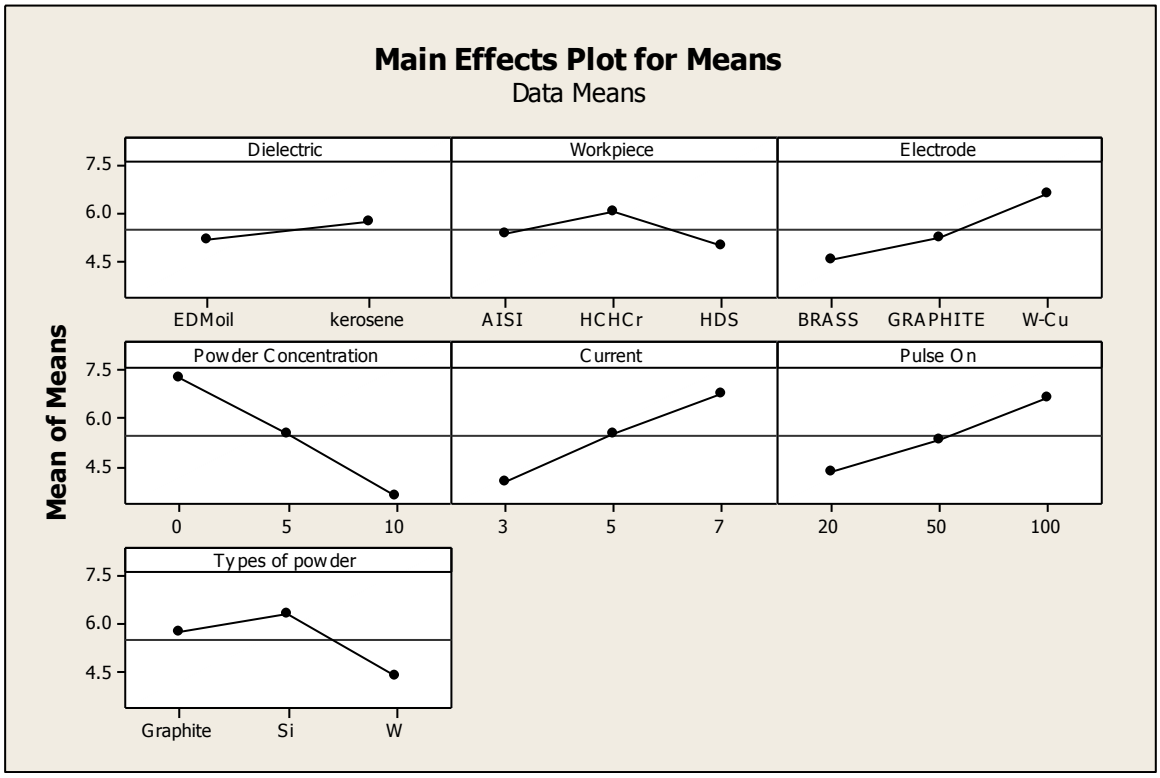

Figure 4.11: Main effect plot for of surface roughness at right position

4.4.10 Results for S/N ratio - surface roughness at right position

The S/N ratios have been calculated to identify the significant factors that cause variation in surface roughness. Surface roughness is a "Lower is better" type of response and is given by a logarithmic function based on the mean square deviation (MSD) given by:

$$S/N_{LB} = -10\log(MSD) = -10\log[(\frac{1}{r}\sum_{i=1}^{r} y^2{}_i)$$

Where $MSD_{LB} = \frac{1}{r}\sum_{j=1}^{r}\left(y_j{}^2\right)$

Table 4.32 shows the ANOVA for S/N ratio for roughness at 95% confidence interval. Mean effect plot for S/N ratio of surface roughness at right position is shown in Figure 4.12. The factors such as powder concentration (F value 123.65), current (F value 58.42), pulse on time (F value 47.08), electrode (F value 39.53)and powder (F value 37.70) were found to be significant in surface roughness at right position. The factors such as dielectric and workpiece were found to be insignificant in affecting surface roughness. Table 4.33 shows the ranks of various factors in terms of their relative significance. Powder Concentration has the highest rank, signifying the highest contribution to surface roughness and workpiece has the lowest rank and was found to be insignificant in affecting surface roughness.

Table 4.32: ANOVA for S/N ratio of surface roughness at right position

Sources	SS	v	V	F	p	SS'	% contribution
Dielectric (A)	1.016	1	1.016	2.30			
Workpiece (B)	1.132	2	0.5659	1.28			
Electrode (C)	34.851	2	17.4256	39.53	0.002	33.734	12.3098
Powder Concentration(D)	109.024	2	54.5120	123.65	0.000	107.9066	39.376
Current(E)	51.512	2	25.7558	58.42	0.001	50.395	18.390
Pulse on time(F)	41.508	2	20.7539	47.08	0.002	40.3906	14.739
Powder (G)	33.236	2	16.6181	37.70	0.003	32.1186	11.72
Error	1.763	4	0.4409				
Total	274.042	17				274.042	100
e pooled	3.911	7	0.5587			9.4972	0.03466

Table 4.33: Response table for S/N ratio of surface roughness at right position

Level	Dielectric (A)	Workpiece (B)	Electrode (C)	Powder Concentration(D)	Current(E)	Pulse on time(F)	Powder (G)
1	-14.27	-14.26	-12.66	-17.61	-12.22	-12.68	-15.00
2	-14.74	-14.85	-14.82	-14.32	-15.03	-14.44	-15.86
3		-14.40	-16.03	-11.59	-16.26	-16.40	-12.65
Delta	0.48	0.59	3.36	6.02	4.04	3.72	3.21
Rank	7	6	4	1	2	3	5

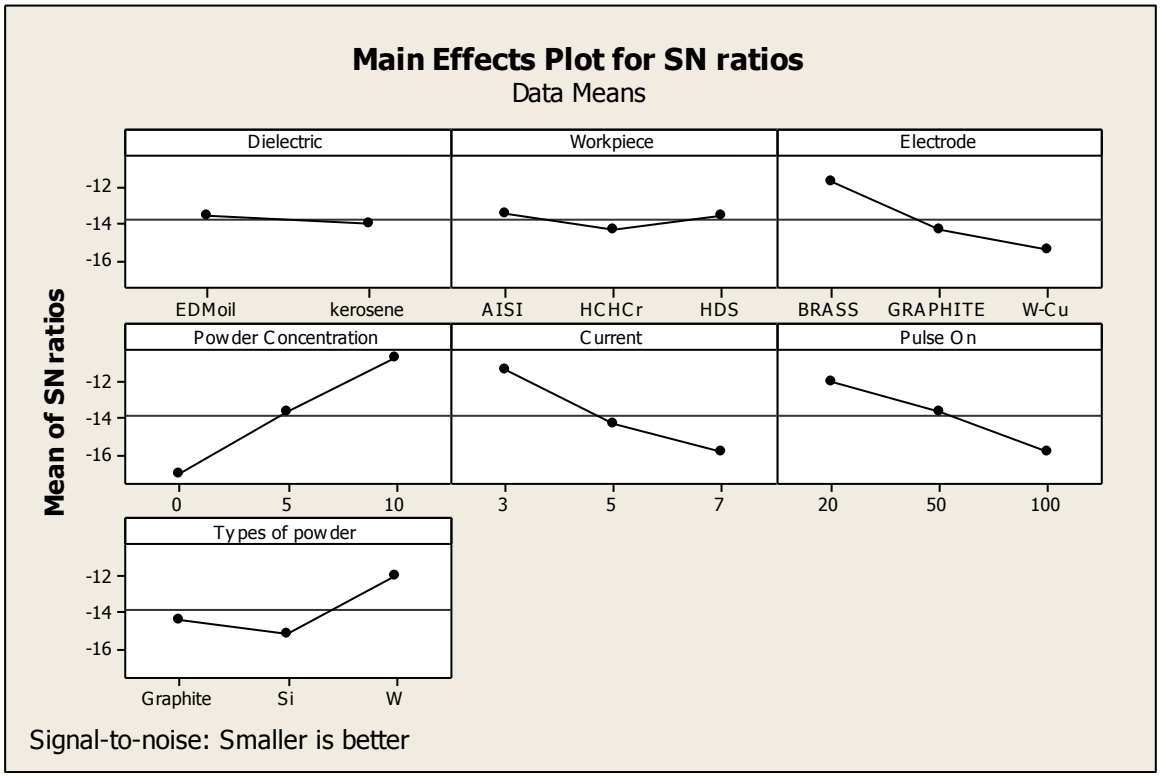

Figure 4.12: Main effect plot for S/N ratio of surface roughness at right position

4.4.11 Optimal Design

In this experimental analysis, the main effect plot for surface roughness at right position in Figure 4.11 is used to estimate the mean value of surface roughness. From the Table 4.34, it is concluded that least surface roughness was found when pulse on time 10μs, current 2Amp were chosen in the experimental trials. In this case, there are same levels of the significant factors which provide the higher average and reduced variability, thus nothing has to be compromised. In some cases, the levels of factors which improve the average and improve the uniformity may conflict and hence a compromise may have to be reached. Also, a compromise may have to occur when multiple responses are considered and the same factor level may cause one response to improve and another to reduce.

Estimating the mean

Surface roughness is a "Lower the better" type response. In this experiment analysis, different experimental trials have been chosen to obtain satisfactory results.

Mean value of surface roughness at right position is given by:

$$\mu_{C_1,D_3,E_1,F_1,G_3} = \overline{C_1} + \overline{D_3} + \overline{E_1} + \overline{F_1} + \overline{G_3} - 4\overline{T}$$

$$= 4.435$$

Table 4.34: Significant factors for surface roughness at right position

Factors	Affecting mean		Affecting variation (S/N ratio)	
	Contribution	Best level	Contribution	Best level
Dielectric (A)	Insignificant	-	Insignificant	-
Workpiece (B)	Insignificant	-	Insignificant	-
Electrode (C)	Significant	Level 1- Brass	Significant	Level 1- Brass
Powder Concentration(D)	Significant	Level 3- 10g/l	Significant	Level 3- 10g/l
Current(E)	Significant	Level 1-3amp	Significant	Level 1-3amp
Pulse on time(F)	Significant	Level 1-20µs	Significant	Level 1-20µs
Powder (G)	Significant	Level 3-Tungsten	Significant	Level 3-Tungsten

Confidence Interval around the Estimated Mean

The confidence interval is a maximum and minimum value between which the true average should fall at some stated percentage of confidence.

Confidence Interval around the estimated mean of surface roughness at right position is given by:

$$CI = \sqrt[2]{\frac{F_{\alpha,\nu_1,\nu_2} V_e}{n_{eff}}}$$ Where F_{α,ν_1,ν_2} = F ratio

α =0.05, risk

Confidence = 1−α

ν_1 = dof for mean which is always =1

ν_2 =dof for error, ν_e

n_{eff}= Number of tests under that condition using the participating factors

$$n_{eff} = \frac{N}{1 + dof_{C_1,D_3,E_1,F_1,G_3}} = \frac{18}{1+2+2+2+2+2} = 1.64$$

Where N = Number of trials in the experiment

$$CI = \sqrt[2]{\frac{F_{\alpha,\nu_1,\nu_2} V_e}{n_{eff}}}$$

$$= \sqrt{\frac{0.07 \text{ X } 1.1194}{1.64}}$$

$= \pm 0.2186$

So the confidence interval around the surface roughness at right position is given by 4.435 ±0. 2186microns.

4.5 RESULTS AND ANALYSIS OF MICRO HARDNESS

4.5.1 Introduction

The effect of various parameters such as current, workpiece, dielectric, electrode, pulse on time, powder concentration and types of powder were evaluated using ANOVA and factorial design analysis. A confidence interval of 95% has been used for the analysis. 18 trials were conducted in the experiment using L18 experimental design. One repetition for each of 18 trials was completed so as to measure Signal to Noise ratio (S/N ratio).

4.5.2 Results for Micro Hardness

The results for micro hardness at deposited region and non-deposited region for each of the experimental with repetition are given in Table 4.35. The measurement in micro hardness is dependent on the diameter of indentation on the samples. The indents formed in the pyramid shaped on the machined workpiece by the indenter were measured with Quantimet software using a load of 1 kg for 20 seconds.

4.5.3 Analysis of variance- Micro Hardness at non-deposited region

The results for micro hardness at non deposited region for each of the 18 experimental trials with repetition are given in Table 4.35. The results were analysed using ANOVA for identifying the significant factors affecting the performance at 95% confidence interval. ANOVA Table 4.36 shows that factors such as powder concentration (F value 36.48), current (F value 24.94), pulse on time (F value 16.46), electrode (F value 10.62) and powder (F value 7.15) are the factors that significantly affect the micro hardness. Table 4.37 shows ranks of various factors in terms of their relative significance. Powder concentration has the highest rank, signifying the highest contribution in micro hardness and workpiece has the lowest rank and was found to be insignificant in micro hardness at non-deposited region. Main effect plots for micro hardness at non deposited region are shown in the Figure 4.13 which shows that micro hardness increases with addition of powder in dielectric medium. The tungsten powder increased the micro hardness more as compared to silicon and graphite powder. The micro hardness increases with increase in current, pulse on time and powder concentration. The micro hardness was found to be high when machined with tungsten copper electrode as compared to graphite and brass electrode.

Table 4.35: Results for micro hardness at non-deposited and deposited region

Trial no.	Micro hardness at non deposited region (HVN)		Mean Micro hardness	S/N ratio	Micro hardness at deposited region (HVN)		Mean Micro hardness	S/N ratio
	I	II			I	II		
1	608	612	610	55.7066	818	822	820	58.2763
2	755	759	757	57.5819	958	962	960	59.6454
3	816	822	819	58.2657	1021	1019	1020	60.1720
4	711	817	714	57.0740	913	919	916	59.2379
5	830	830	830	58.3816	1034	1028	1031	60.2652
6	664	656	660	56.3909	851	861	856	58.6495
7	719	715	717	57.1104	912	918	915	59.2284
8	790	798	794	57.9964	997	991	994	59.9477
9	694	706	700	56.9020	914	926	920	59.2758
10	830	820	825	58.3291	1022	1030	1026	60.2229
11	739	731	735	57.3257	936	936	936	59.4255
12	700	700	700	56.9020	889	891	890	58.9878
13	767	753	760	57.6163	959	963	961	59.6545
14	745	749	747	57.4664	941	949	945	59.5086
15	668	672	670	56.5215	867	871	869	58.7804
16	802	808	805	58.1159	1005	1007	1006	60.0520
17	716	704	710	57.0252	908	910	909	59.1713
18	746	734	740	57.3846	934	944	939	59.4533

Table 4.36: ANOVA for micro hardness at non-deposited region

Sources	SS	v	V	F	p	SS'	% contribution
Dielectric (A)	460.1	1	460.1	1.45			
Workpiece (B)	658.3	2	329.2	1.04			
Electrode (C)	6721.3	2	3360.7	10.62	0.025	6040.01	9.5973
Powder Concentration(D)	23092.3	2	11546.2	36.48	0.003	22411.01	35.61
Current(E)	15789.0	2	7894.5	24.94	0.006	15107.71	24.008
Pulse on time(F)	10423.0	2	5211.5	16.46	0.012	9741.714	15.48
Powder (G)	4524.3	2	2262.2	7.15	0.048	3843.014	6.11
Error	1266.1	4	316.5				
Total	62934.5	17				62934.5	100
e pooled	2384.5	7	340.643			5791.04	9.2

Table 4.37: Response table for means of micro hardness at non-deposited region

Level	Dielectric (A)	Workpiece (B)	Electrode (C)	Powder Concentration(D)	Current(E)	Pulse on time(F)	Powder (G)
1	743.6	744.3	714.8	689.8	701.5	705.7	723.2
2	733.4	730.2	738.5	750.7	740.0	747.2	732.0
3		741	762.2	775.0	774.0	762.7	760.3
Delta	10.1	14.2	47.3	85.2	72.5	57.0	37.2
Rank	7	6	4	1	2	3	5

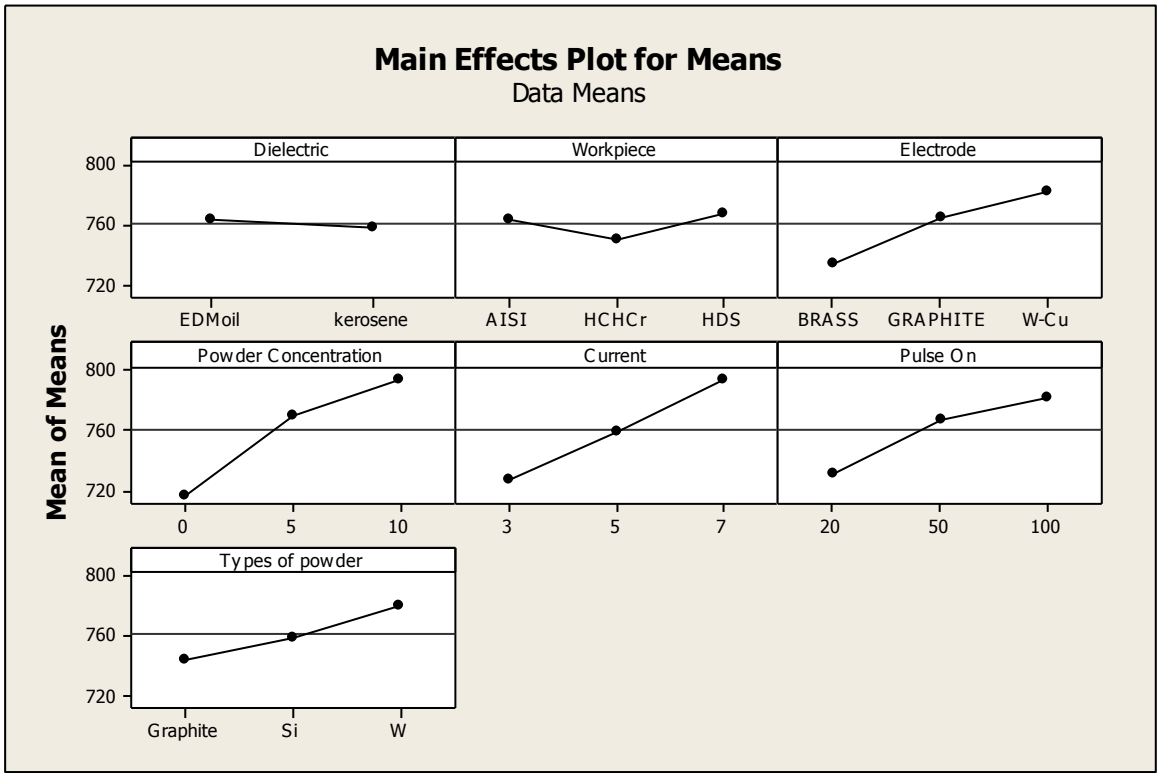

Figure 4.13: Main effect plots for mean micro hardness at non-deposited region

4.5.4 Results for S/N ratio – Micro Hardness at non-deposited region

The S/N ratio is an indication of the amount of variation present in the process. The S/N ratios have been calculated to identify the major contributing factors that cause variation in non-deposited region. Micro hardness is a "Higher the better" type response and it is given by a logarithmic function based on the mean square deviation:

$(S/N)_{HB} = -10 \log (MSD_{HB})$

Where $MSD_{HB} = \frac{1}{r}\sum_{j=1}^{r}\left(\frac{1}{y_j^{\,2}}\right)$

MSD_{HB}= Mean Square Deviation for higher-the-better response.

Table 4.38 shows the ANOVA results for S/N ratio of micro hardness at non-deposited region at 95% confidence interval. The factors such as powder concentration (F value 42.37), current (F value 28.89), pulse on time (F value 19.85), electrode (F value 12.73) and powder (F value 9) were found to be significant for micro hardness at non-deposited region. Table 4.39shows ranks of various factors in terms of their relative significance. Powder concentration has the highest rank signifying the highest contribution to micro hardness and workpiece has the lowest rank and was found to be insignificant for micro hardness. Main

effect plots for S/N ratio for micro hardness at non-deposited region are shown in the Figure 4.14.

Table 4.38: ANOVA for S/N ratio of micro hardness at non-deposited region

Sources	SS	v	V	F	p	SS'	% contribution
Dielectric (A)	0.09064	1	0.09064	2.38			
Workpiece (B)	0.09946	2	0.04973	1.30			
Electrode (C)	0.97095	2	0.48547	12.73	0.018	0.87305	9.754
Powder Concentration(D)	3.23257	2	1.61629	42.37	0.002	3.13467	35.02
Current(E)	2.20378	2	1.10189	28.89	0.004	2.10588	23.527
Pulse on time(F)	1.51417	2	0.34347	19.85	0.008	1.41627	15.822
Powder (G)	0.68693	2	0.03814	9	0.033	0.58903	6.58
Error	0.15257	4	316.5				
Total	8.95109	17				8.95109	100
e pooled	0.34267	7	0.04895			0.83219	9.297

Table 4.39: Response table for S/N ratio of micro hardness at non-deposited region

Level	Dielectric (A)	Workpiece (B)	Electrode (C)	Powder Concentration(D)	Current(E)	Pulse on time(F)	Powder (G)
1	57.41	57.42	57.06	56.76	56.90	56.94	57.16
2	57.27	57.24	57.33	57.50	57.37	57.46	57.25
3		57.35	57.63	57.76	57.75	57.62	57.61
Delta	0.14	0.18	0.57	1.00	0.86	0.68	0.45
Rank	7	6	4	1	2	3	5

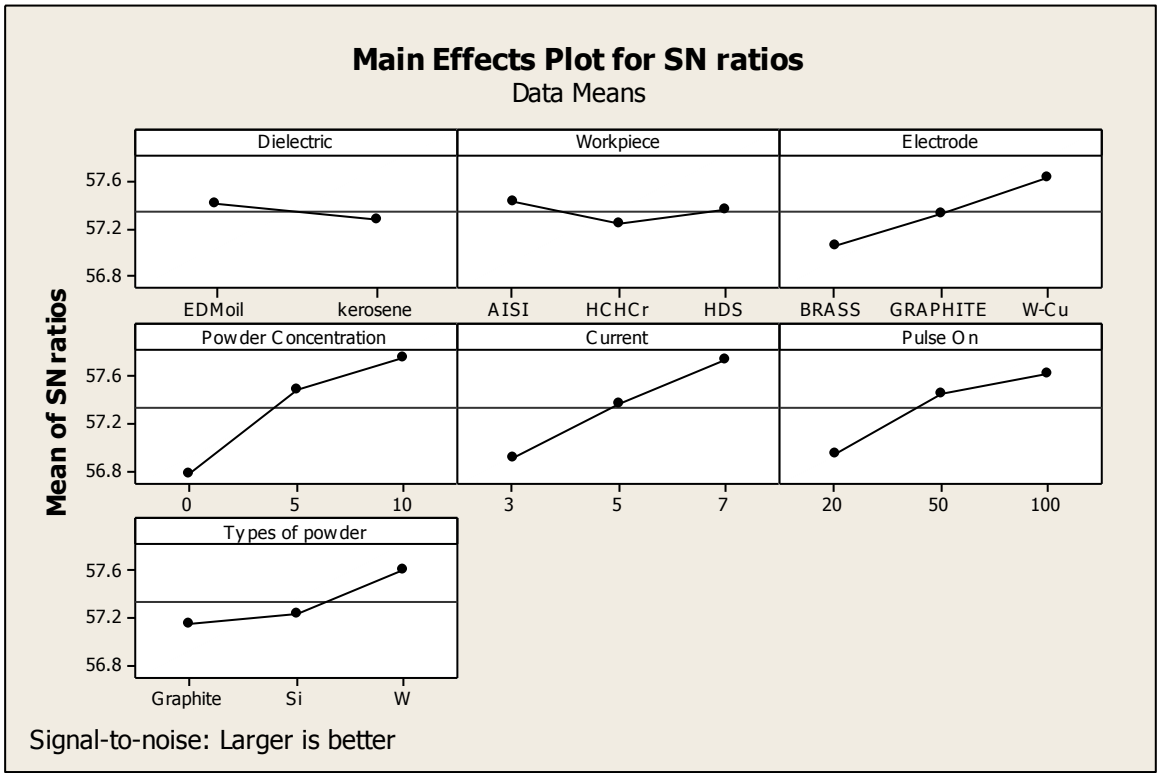

Figure 4.14: Main effect plot for S/N ratio of micro hardness at non-deposited region

4.5.5 Optimal Design

In this experimental analysis, the main effect plot for mean micro hardness in Figure 4.13 is used to estimate the mean micro hardness at non-deposited region with optimal design conditions. From the Table 4.40, it is concluded that the highest micro hardness at non-deposited was found when current 7amp, pulse on time 100µs, W-Cu electrode and powder concentration10g/l of tungsten powder was selected in the experimental trials. In S/N ratio the highest micro hardness was found at same experimental trials.

Estimating the mean

Micro Hardness is a "Higher the better" type response. In this experiment analysis, different experimental trials have been chosen to obtain satisfactory results. After conducting the experiments the optimum treatment condition within the experiments determined on the basis of prescribed combination of factor levels is determined to one of those in the experiment.

Mean value of micro hardness at non-deposited region:

$$\mu_{C_3,D_3,E_3,F_3,G_3} = \overline{C_3} + \overline{D_3} + \overline{E_3} + \overline{F_3} + \overline{G_3} - 4\overline{T}$$

$$=762.2+ 775 + 774 + 762.7+ 760.3 - 4(738.505) = 880.18$$

Table 4.40 Significant factors for micro hardness at non-deposited region

Factors	Affecting mean		Affecting variation (S/N ratio)	
	Contribution	Best level	Contribution	Best level
Dielectric (A)	Insignificant	-		-
Workpiece (B)	Insignificant	-		-
Electrode (C)	Significant	Level 3- W-Cu	Significant	Level 3-W-Cu
Powder Concentration(D)	Significant	Level 3-10g/l	Significant	Level 3-10g/l
Current(E)	Significant	Level 3-7amp	Significant	Level 3-7amp
Pulse on time(F)	Significant	Level 3-100µs	Significant	Level 3-100µs
Powder (G)	Significant	Level 3-Tungsten	Significant	Level 3-Tungsten

Confidence Interval around the Estimated Mean

The confidence interval is a maximum and minimum value between which the true average should fall at some stated percentage of confidence

Confidence Interval around the estimated micro hardness at non-deposited region

$$CI = \sqrt[2]{\frac{F_{\alpha,\nu_1,\nu_2} V_e}{n_{eff}}}$$ Where F_{α,ν_1,ν_2} = F ratio

α =0.05, risk

Confidence = 1−α

ν_1 = dof for mean which is always =1

ν_2 =dof for error, ν_e

n_{eff}= Number of tests under that condition using the participating factors

$$n_{eff} = \frac{N}{1 + dof_{C_3,D_3,E_3,F_3,G_3}} = \frac{18}{1+2+2+2+2+2} = 1.64$$

Where N = Number of trials in the experiment

$$CI = \sqrt[2]{\frac{F_{\alpha,\nu_1,\nu_2} V_e}{n_{eff}}}$$

$$= \sqrt{\frac{0.07 \text{ X } 316.5}{1.64}}$$

$= \pm 3.813$

So the confidence interval around the mean micro hardness at non-deposited region is given by 880.18 ± 3.813HVN.

4.5.6 Analysis of variance - Micro Hardness at deposited region

The results were analysed using ANOVA for identifying the significant factors affecting the performance measures. The Analysis of Variance (ANOVA) for the mean micro hardness at 95% confidence interval is given in Table 4.41. ANOVA table shows that factors such as powder concentration (F value 34.74), current (F value 30.39), pulse on time (F value 19.64), electrode (F value 11.56) and powder (F value 8.09) were found to be significant for micro hardness at deposited region. Table 4.42 shows rank of various factors in the terms their relative significance. The powder concentration has the highest rank, signifying highest contribution in micro hardness and dielectric has the lowest rank and was found to be insignificant in affecting micro hardness at deposited region. Main effect plots for mean micro hardness at deposited region are shown in the Figure 4.15 which shows that micro hardness has increased with addition of powder in dielectric medium. It was found that with tungsten powder micro hardness increased as compared to graphite and silicon powder. The micro hardness increased with increase in current and pulse on time. The micro hardness was found to be more when machined with tungsten electrode as compared to graphite and brass electrode.

Table 4.41: ANOVA for micro hardness at deposited region

Sources	SS	v	V	F	p	SS'	% contribution
Dielectric (A)	133.4	1	133.4	0.47			
Workpiece (B)	970.1	2	485.1	1.70			
Electrode (C)	6590.1	2	3295.1	11.56	0.022	5948.93	9.63
Powder Concentration(D)	19811.4	2	9905.7	34.74	0.003	19170.23	31.03
Current(E)	17329.8	2	8664.9	30.39	0.004	16688.63	27.01
Pulse on time(F)	11201.4	2	5600.7	19.64	0.009	10560.23	17.1
Powder (G)	4611.4	2	2305.7	8.09	0.039	3970.23	6.426
Error	1140.6	4	285.1				
Total	61788.3	17				61788.3	100
e pooled	2244.1	7	320.586			5450.05	8.82

Table 4.42: Response table for means of micro hardness at deposited region

Level	Dielectric (A)	Workpiece (B)	Electrode (C)	Powder Concentration(D)	Current(E)	Pulse on time(F)	Powder (G)
1	942.3	947.2	915.7	895	901.8	905.0	922.5
2	936.9	929.7	940.7	949.3	939.2	951.0	935.3
3		942	962.5	974.5	977.8	962.8	961
Delta	5.4	17.5	46.8	79.5	76	57.8	38.5
Rank	7	6	4	1	2	3	5

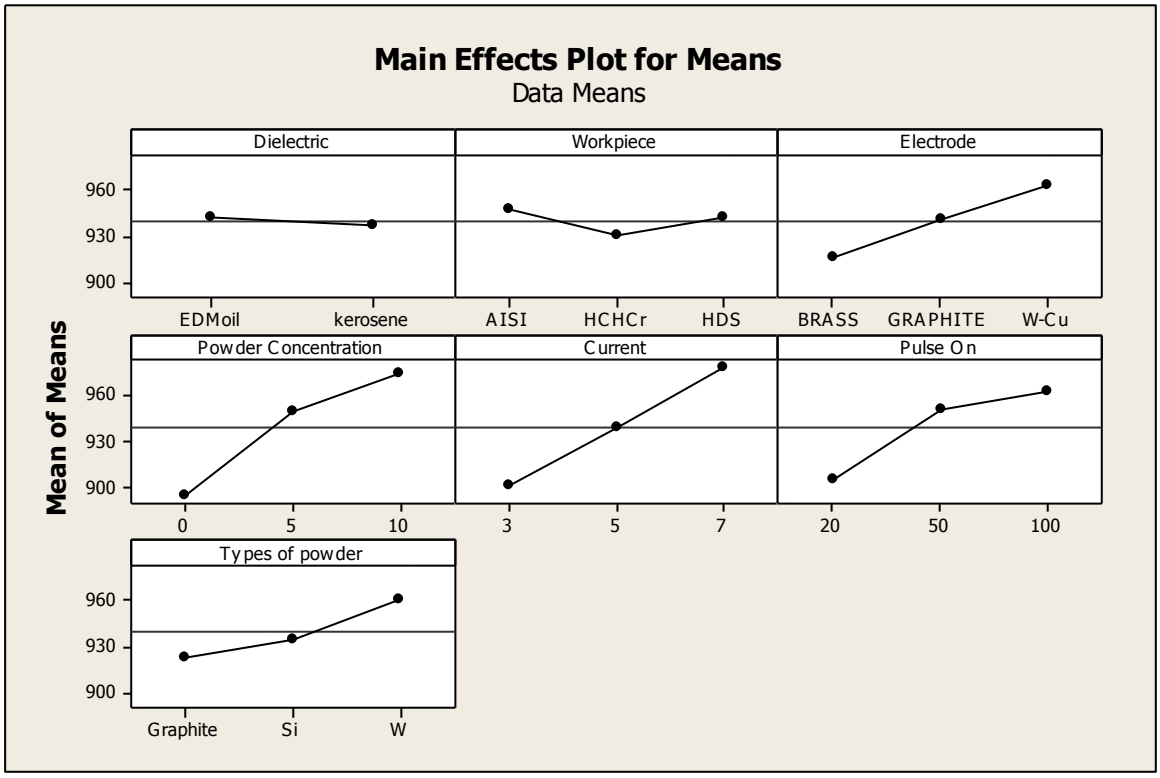

Figure 4.15: Main effect plot for means of micro hardness at deposited region

4.5.7 Results for S/N ratio – Micro Hardness at deposited region

The S/N ratio is an indication of the amount of variation present in the process. The S/N ratios have been calculated to identify the major contributing factors that cause variation in micro hardness at deposited region. Micro hardness is a "Higher the better" type response is given by a logarithmic function based on the mean square deviation:

$(S/N)_{HB} = -10 \log (MSD_{HB})$

Where $MSD_{HB} = \frac{1}{r}\sum_{j=1}^{r}\left(\frac{1}{y_j^{\,2}}\right)$

MSD_{HB}= Mean Square Deviation for higher-the-better response.

Table 4.43 shows the ANOVA for S/N ratio for micro hardness at 95% confidence interval. The factors such as powder concentration (F value 41.06), current (F value 36.10), pulse on time (F value 24.15), electrode (F value 14.19) and powder (F value 10.25) were found to be significant for micro hardness at deposited region. According to F-test powder concentration is the most significant factor whereas dielectric is the least insignificant factor which is affecting the micro hardness at deposited region. Main effect plots for S/N ratio of micro hardness at deposited region are shown in the Figure 4.16.

Table 4.43: ANOVA for S/N ratio of micro hardness at deposited region

Sources	SS	v	V	F	p	SS'	% contribution
Dielectric (A)	0.01731	1	0.01731	0.84			
Workpiece (B)	0.09036	2	0.04518	2.20			
Electrode (C)	0.58311	2	0.29156	14.19	0.015	0.5289	9.87
Powder Concentration(D)	1.68781	2	0.84390	41.06	0.002	1.6336	30.484
Current(E)	1.48402	2	0.74201	36.10	0.003	1.42976	26.681
Pulse on time(F)	0.99277	2	0.49638	24.15	0.006	0.93851	17.513
Powder (G)	0.42120	2	0.21060	10.25	0.027	0.36694	6.85
Error	0.08221	4	0.02055				
Total	5.35879	17				5.35879	100
e pooled	0.18988	7	0.02713			0.46108	8.604

Table 4.44: Response table for S/N ratio of micro hardness at deposited region

Level	Dielectric (A)	Workpiece (B)	Electrode (C)	Powder Concentration(D)	Current(E)	Pulse on time(F)	Powder (G)
1	59.47	59.52	59.22	59.03	59.09	59.11	59.28
2	59.41	59.35	59.45	59.54	59.44	59.56	59.39
3		59.45	59.66	59.76	59.79	59.65	59.65
Delta	0.06	0.17	0.44	0.73	0.70	0.54	0.37
Rank	7	6	4	1	2	3	5

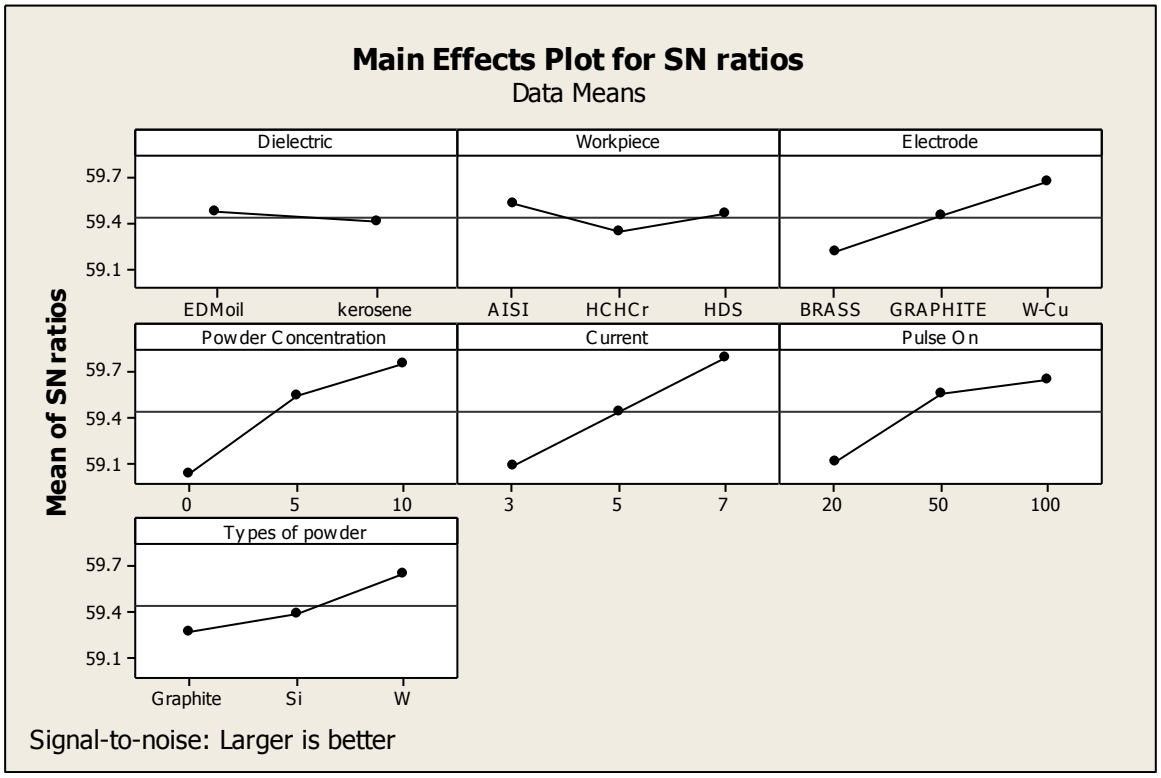

Figure 4.16: Main effect plot for S/N ratio of micro hardness at deposited region

4.5.8 Optimal Design

In this experimental analysis, the main effect plot in Figure 4.15 is used to estimate the mean micro hardness at deposited region. From the Table 4.46 it is concluded that the highest micro hardness at deposited was found when current 7amp, pulse on time 100µs, W-Cu electrode and powder concentration10g/l of tungsten powder was selected in the experimental trials. In S/N ratio the highest micro hardness was found at same experimental trials.

$(S/N)_{HB} = -10 \log (MSD_{HB})$

Where $MSD_{HB} = \frac{1}{r}\sum_{j=1}^{r}\left(\frac{1}{y_j^{\,2}}\right)$

MSD_{HB}= Mean Square Deviation for higher-the-better response.

Estimating the mean

In experimental analysis, the micro hardness is a higher average response is better (HB) characteristic. Depending on the characteristic, different treatment combinations has chosen to obtain satisfactory results. In some case, the same levels of the significant factors provide the higher average and reduced variability; hence nothing has to be compromised. After conducting the experiments the optimum treatment condition within the experiments

determined on the basis of prescribed combination of factor levels is determined to one of those in the experiment.

Table 4.45 Significant factors for micro hardness at deposited region

Factors	Affecting mean		Affecting variation (S/N ratio)	
	Contribution	Best level	Contribution	Best level
Dielectric (A)	Insignificant	-	Insignificant	-
Workpiece (B)	Insignificant	-	Insignificant	-
Electrode (C)	Significant	Level 3- W-Cu	Significant	Level 3-W-Cu
Powder Concentration(D)	Significant	Level 3-10g/l	Significant	Level 3-10g/l
Current(E)	Significant	Level 3-7amp	Significant	Level 3-7amp
Pulse on time(F)	Significant	Level 3-100µs	Significant	Level 3-100µs
Powder (G)	Significant	Level 3-Tungsten	Significant	Level 3-Tungsten

Mean value of micro hardness at deposited region:

$$\mu_{C_3,D_3,E_3,F_3,G_3} = \overline{C_3} + \overline{D_3} + \overline{E_3} + \overline{F_3} + \overline{G_3} - 4\overline{T}$$

$$=962.5 + 974.5 + 977.8 + 962.8 + 961 - 4(939.61) = 1080.16$$

Confidence Interval around the Estimated Mean

The confidence interval is a maximum and minimum value between which the true average should fall at some stated percentage of confidence. The estimate of the mean µ is only a point estimate based on the averages of results obtained from the experiment. Statistically this provides a 50% chance of the true averages being greater than µ and a 50% chance of the true average being less than µ.

Confidence Interval around the estimated micro hardness at deposited region

$$CI = \sqrt[2]{\frac{F_{\alpha,\nu_1,\nu_2} V_e}{n_{eff}}}$$ Where F_{α,ν_1,ν_2} = F ratio

α =0.05, risk

Confidence = 1−α

ν_1 = dof for mean which is always =1

ν_2 =dof for error, ν_e

n_{eff}= Number of tests under that condition using the participating factors

$$n_{eff} = \frac{N}{1 + dof_{C_3, D_3, E_3, F_3, G_3}} = \frac{18}{1+2+2+2+2+2} = 1.64$$

Where N = Number of trials in the experiment

$$CI = \sqrt[2]{\frac{F_{\alpha,\nu_1,\nu_2} V_e}{n_{eff}}}$$

$$= \sqrt{\frac{0.07 \text{ X } 320.586}{1.64}}$$

$= \pm 3.6991$

So the confidence interval around the mean micro hardness at deposited region is given by 1080.16 ±3.6991HVN.

4.6 RESULT AND ANALYSIS OF OVERCUT

4.6.1 Introduction

The effect of various parameters such as current, workpiece, dielectric, electrode, pulse on time, powder concentration and types of powder were evaluated using ANOVA and factorial design analysis. A confidence interval of 95% has been used for the analysis. 18 trials were conducted in the experiment using L18 experimental design. One repetition for each of 18 trials was completed so as to measure Signal to Noise ratio (S/N ratio).

4.6.2 Results for overcut (OC)

It is the discharge by which the machined hole in the work piece exceeds the electrode size and is determined by both the initiating voltage and the discharge energy. During the process of machining EDM or PMEDM, cavity produced are always larger than the electrode this difference (size of electrode and cavity) is called Over Cut (OC). The results of overcut for each of the 18 trials are given in Table 4.47. Diameter of tool and diameter of cut made in the workpiece material with the tool for each of the trial was calculated to evaluate the overcut of each sample. The overcut is given by

$$\text{overcut} = \frac{\mathrm{D} - \mathrm{d}}{2} \text{ mm}$$

Where D= Diameter of cut made in the workpiece material with the tool (mm)

d= Diameter of tool (mm)

The diameter of each tool material (d) is 20mm.The diameter of cut made in the workpiece material with the tool is calculated at four places for each trial with the help of profile projector and then the average of these four values is considered as diameter of cut (D) for that trial.

4.6.3 Analysis of variance - overcut (OC)

The results were analysed using ANOVA for identifying the significant factors affecting the performance measures. The Analysis of Variance (ANOVA) for the mean of overcut (OC) at 95% confidence interval is given in Table 4.48. The variation data for each factor were F-tested to find significance of each. The principle of the F-test is that the larger the F value for a particular parameter, the greater the effect on the performance characteristic due to the change in that process parameter.

Table 4.46: Results for overcut

Trial no. Parameter as per Table 3.3	Diameter of cut, D(mm)	Diameter of tool, d (mm)	overcut (mm)	S/N ratio
1	20.02	20	0.01000	40.0000
2	20.331	20	0.165275	15.6359
3	20.481	20	0.240625	12.3732
4	20.134	20	0.066875	23.4947
5	20.456	20	0.227813	12.8484
6	20.14	20	0.069788	23.1244
7	20.341	20	0.170250	15.3783
8	20.313	20	0.156250	16.1236
9	20.147	20	0.073688	22.6521
10	20.449	20	0.224387	12.9800
11	20.306	20	0.152875	16.3133
12	20.135	20	0.067312	23.4381
13	20.2	20	0.100000	20.0000
14	20.279	20	0.139462	17.1109
15	20.329	20	0.164412	15.6813
16	20.355	20	0.177563	15.0130
17	20.218	20	0.109188	19.2365
18	20.2	20	0.100000	20.0000

ANOVA table shows that pulse on time (F value 32.23), powder concentration (F value 15.54) and current (F value 9.21) are the factors that significantly affect the overcut. All others factors such as dielectric, workpiece material electrode and powder were found to be insignificant. Table 4.49 shows the ranks of various factors in the terms of their relative significance. Pulse on time has the highest rank, signifying highest contribution to overcut and dielectric has the lowest rank and was found to be insignificant in affecting overcut. Main effect plot for the mean of overcut is shown in the Figure 4.18 which shows the variation of overcut with the input parameters. As it can be seen overcut increases with increase in pulse on time from 20µs to 100µs. Increase in pulse on time means sparking occurs for more duration. When heat input is high and pulse on time is more then overcut is more. Also, when heat input is less and pulse on time is more even then overcut increases. Overcut increases with increase in current and powder concentration. When powder is added into the dielectric then the dielectric which is an insulating material becomes conductive due to presence of conductive powder and hence sparking between the tool and workpiece is concentrated where powder is present and thus overcut increases with increases in powder concentration. It is quite clear in the Figure 4.17 shown below. When current is high, it means more heat energy is supplied and thus high heat input causes increase in overcut.

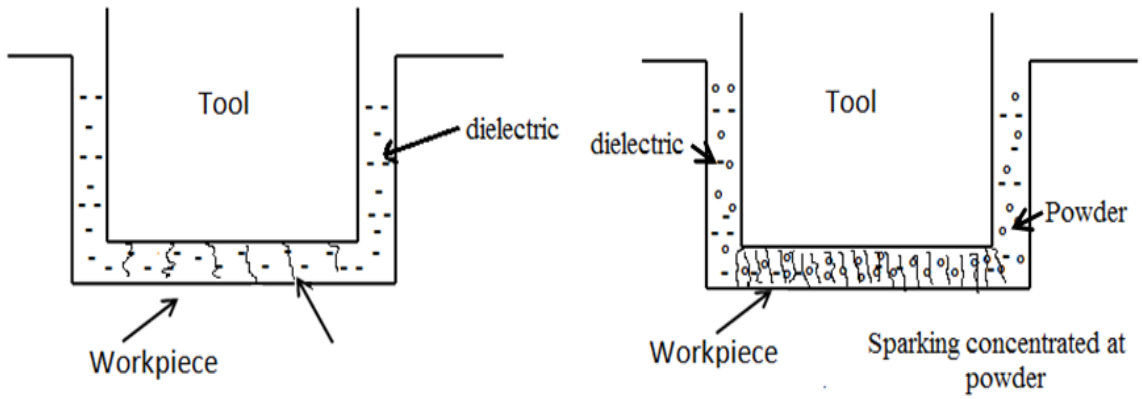

(a) **(b)**

Figure 4.17: Schematic diagram showing sparking between tool and workpiece with powder and without powder in EDM

Table 4.47: ANOVA for means of overcut

Sources	SS	v	V	F	P (critical)	SS'	% contribution
Dielectric (A)	0.000166	1	0.000166	0.33			
Workpiece (B)	0.000791	2	0.000396	0.79			
Electrode (C)	0.005393	2	0.002696	5.36			
Powder Concentration(D)	0.015644	2	0.007822	15.54	0.013	0.0134654	19.416
Current(E)	0.009273	2	0.004637	9.21	0.032	0.0070944	10.23
Pulse on time(F)	0.032453	2	0.016226	32.23	0.003	0.0302744	43.65
Powder (G)	0.003619	2	0.001810	3.59			
Error	0.002014	4	0.000503				
Total	0.069352	17				0.069352	100
e pooled	0.011982	11	.0010893			0.0185178	26.7

Table 4.48: Response table for means of overcut

Level	Dielectric (A)	Workpiece (B)	Electrode (C)	Powder Concentration(D)	Current(E)	Pulse on time(F)	Powder (G)
1	0.13724	0.13116	0.11930	0.09617	0.10706	0.08542	0.15055
2	0.13117	0.12806	0.12485	0.13844	0.13295	0.12828	0.11597
3		0.14341	0.15848	0.16801	0.16262	0.18892	0.13610
Delta	0.00607	0.01535	0.03917	0.07184	0.05555	0.10350	0.03458
Rank	7	6	4	2	3	1	5

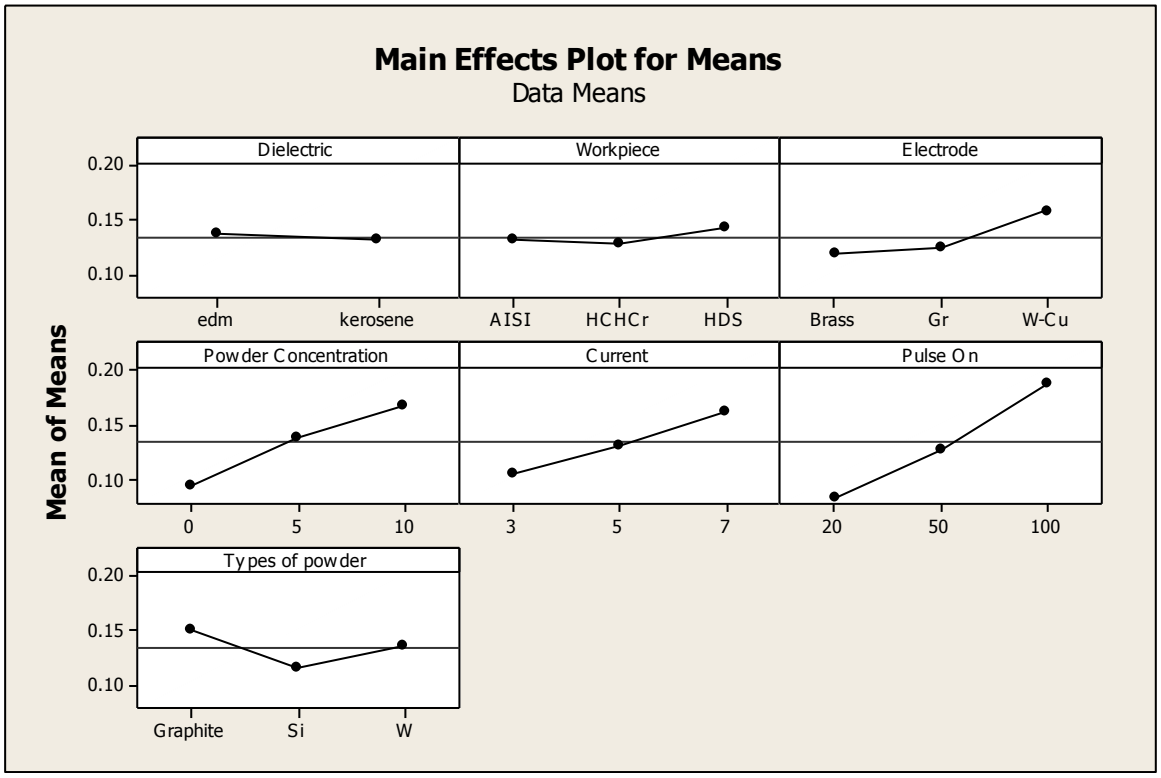

Figure 4.18: Main effect plot for the mean overcut

4.6.4 Results for S/N ratio – overcut

The S/N ratio is an indication of the amount of variation present in the process. The S/N ratios have been calculated to identify the major contributing factors that cause variation in overcut. Overcut is a "Lower the better" type response and it is given by a logarithmic function based on the mean square deviation:

$$S/N_{LB} = -10\log(MSD) = -10\log[(\frac{1}{r}\sum_{i=1}^{r} y^2{}_i)$$

Where $MSD_{LB} = \frac{1}{r}\sum_{j=1}^{r}\left(y_j{}^2\right)$

MSD_{LB}= Mean Square Deviation for lower-the-better response.

Table 4.50 shows the ANOVA results for S/N ratio of overcut at 95% confidence interval. Pulse on time (F value 20.82), powder concentration (F value 12.51) and current (F value 7.54) are the factors which are found to be significant. According to F-test pulse on time was found to be the most significant factor affecting the overcut, followed by powder concentration and current. Main effect plot for S/N ratio of overcut is shown in the Figure 4.19. Table 4.51 shows the ranks of various factors in the terms of their relative significance.

Pulse on time has the highest rank which signifies that it provides highest contribution to overcut and workpiece has the lowest rank and was found to be insignificant in affecting overcut.

Table 4.49: ANOVA for S/N ratio of overcut

Sources	SS	V	V	F	P (critical)	SS'	% contribution
Dielectric (A)	26.54	1	26.542	4.48			
Workpiece (B)	13.28	2	6.639	1.12			
Electrode (C)	76.01	2	38.004	6.41			
Powder Concentration(D)	148.29	2	74.143	12.51	0.019	108.783	15.503
Current(E)	89.34	2	44.668	7.54	0.044	49.8328	7.10
Pulse on time(F)	246.77	2	123.387	20.82	0.008	207.263	29.538
Powder (G)	77.76	2	38.881	3.59			
Error	23.70	4	5.925				
Total	701.69	17				701.69	100
e pooled	217.29	11	19.7536				

Table 4.50: Response table for S/N ratio of overcut

Level	Dielectric (A)	Workpiece (B)	Electrode (C)	Powder Concentration(D)	Current(E)	Pulse on time(F)	Powder (G)
1	17.75	18.07	19.54	22.90	21.99	23.65	17.01
2	20.18	18.71	21.14	17.88	18.23	18.65	21.84
3		20.12	16.21	16.12	16.68	14.60	18.05
Delta	2.43	2.06	4.93	6.78	5.31	9.05	4.84
Rank	6	7	4	2	3	1	5

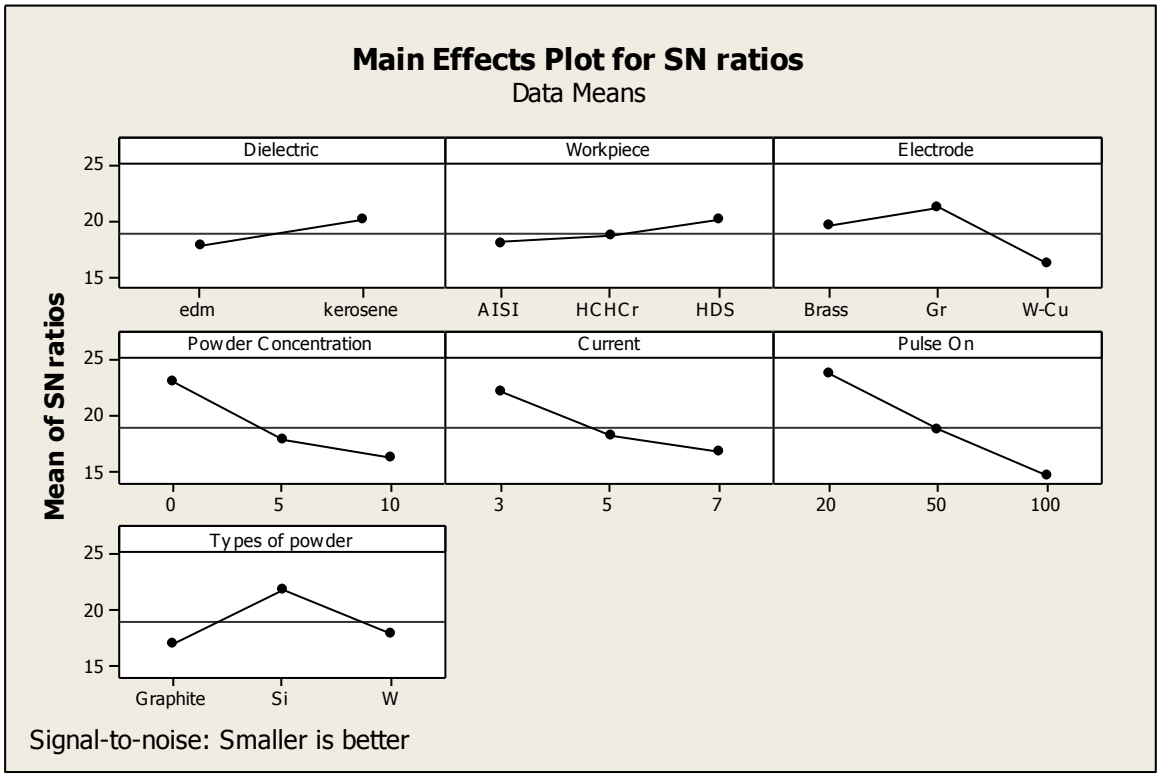

Figure 4.19: Main effect plot for S/N ratio of overcut

4.6.5 Optimal Design

In this experimental analysis, the main effect plot for mean of overcut in Figure 4.18 is used to estimate the mean overcut with optimal design conditions. In Table 4.52, it is concluded that least overcut was achieved when powder concentration 0g/l, pulse on time 20 μs and current 3amp was selected in the experiment trial. In S/N ratio least overcut was found when pulse on time 100 μs, powder concentration 10g/land current 7amp was selected in the experiment trial. In some case, the levels of factors which improve the average and improve the uniformity may conflict which means compromise may have to be reached. Moreover, a compromise may have to occur when multiple responses are considered and the same level factor may cause one response to improve and another to reduce.

Estimating the mean

Overcut is a "Lower the better" type response. In this experiment analysis, different experimental trials have been chosen to obtain satisfactory results.

Mean value of overcut is given by:

$$\mu_{D_1,E_1,F_1} = \overline{D_1} + \overline{E_1} + \overline{F_1} - 2\overline{T}$$

$$= 0.02$$

Table 4.51: Significant factors for overcut

Factors	Affecting mean		Affecting variation (S/N ratio)	
	Contribution	Best level	Contribution	Best level
Dielectric (A)	Insignificant	-	Insignificant	-
Workpiece (B)	Insignificant	-	Insignificant	-
Electrode (C)	Insignificant	-	Insignificant	-
Powder Concentration(D)	Significant	Level 1-0gm/l	Significant	Level 1-0g/l
Current(E)	Significant	Level 1-3Amp	Significant	Level 1-3Amp
Pulse on time(F)	Significant	Level 1-20µs	Significant	Level 1-20µs
Powder (G)	Insignificant	-	Insignificant	-

Confidence Interval around the Estimated Mean

The confidence interval is a maximum and minimum value between which the true average should fall at some stated percentage of confidence.

Confidence Interval around the estimated mean of overcut is given by:

$$CI = \sqrt[2]{\frac{F_{\alpha,\nu_1,\nu_2} V_e}{n_{eff}}}$$ Where F_{α,ν_1,ν_2} = F ratio

α =0.05, risk

Confidence = 1−α

ν_1 = dof for mean which is always =1

ν_2 =dof for error, ν_e

n_{eff}= Number of tests under that condition using the participating factors

$$n_{eff} = \frac{N}{1 + dof_{D_1,E_1,F_1}} = \frac{18}{1+2+2+2} = 2.5714$$

Where N = Number of trials in the experiment

$$CI = \sqrt[2]{\frac{F_{\alpha,\nu_1,\nu_2} V_e}{n_{eff}}}$$

$$= \sqrt{\frac{0.11 \text{ X } 0.0010893}{2.5714}}$$

$$= \pm 0.0068398$$

So the confidence interval around the mean of overcut is given by 0.02 ± 0.0068398mm.

4.7 RESULT AND ANALYSIS OF GEOMETRIC ACCURACY

4.7.1 Introduction

In this experiment, the profile or geometric accuracy has been studied using a tool with different front angle such as 60°, 90° and 120° under various parameters such as current, pulse on time, powder concentration, tool front angle. The angle generated on the workpiece is measured to evaluate the accuracy of the profile produced.

4.7.2 Materials used:

The profile or geometric accuracy has been studied using a copper tool with different front angle such as 60°, 90° and 120°and material of the workpiece used is hot die steel. The dielectric fluid used is kerosene. Powder added into the dielectric is silicon powder.

4.7.3 Equipment's used:

The equipment's used to measure the angle generated on the workpiece with different tool front angle are profile projector and dial indicator.

4.7.4 Parameters used:

Copper tool is used with different front angle such as 60°, 90° and 120° to machine hot die steel (workpiece).The various parameters for each of the trials are shown in table 4.53. The experimental trials with copper tool with front angle 60° is not shown in the Table 4.53 because the tool with 60° could not machine the workpiece.

Table 4.52: The various parameters in the experimental trials

Trial no.	Workpiece	Current (Amp)	Pulse on Time (µs)	Pulse off Time (µs)	Powder Concentration(µs) (g/l)	Tool front angle(Ɵ)
1	H11	7	50	57	5	120°
2	H11	5	100	57	10	120°
3	H11	7	100	57	10	120°
4	H11	7	50	57	5	90°
5	H11	5	100	57	10	90°
6	H11	7	100	57	10	90°

4.7.5 Result of Profile accuracy or Geometric accuracy

The experimental trials as shown in Table 4.53 were carried out and the corresponding angle generated on the workpiece was calculated by using profile projector and dial indicator. Profile projector and dial indicator were used to measure the diameter (d) and the depth of cut (h) respectively. The diameter (d) and the depth of cut (h) were used to evaluate the angle generated on the workpiece(Φ) by using the formula given below.

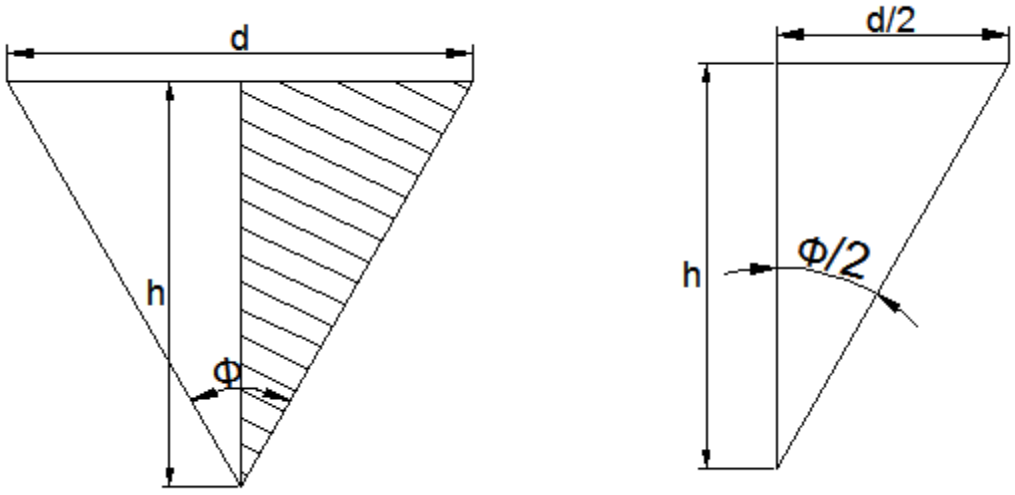

Figure 4.20: Diagram showing the calculation of the angle generated on the workpiece(Φ)

$$Tan\frac{\Phi}{2} = \frac{d}{2h}$$

Where d = diameter of cut on the workpiece

h = depth of cut in the workpiece

The copper tool geometry with different front angle such as 60°, 90° and 120° is shown in Figure 4.21. Figure 4.22 shows the HDS (H11) workpiece after machining with copper tool with different front angle such as 90° and 120°.

(a) Copper tool with 60°

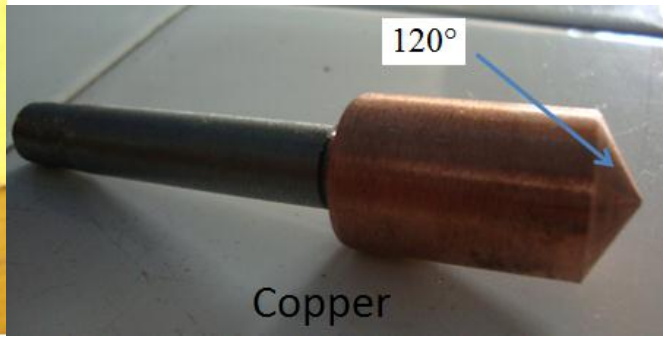

(b) Copper tool with 90° **(c) Copper tool with 120°**

Figure 4.21: Tool geometry with different front angle

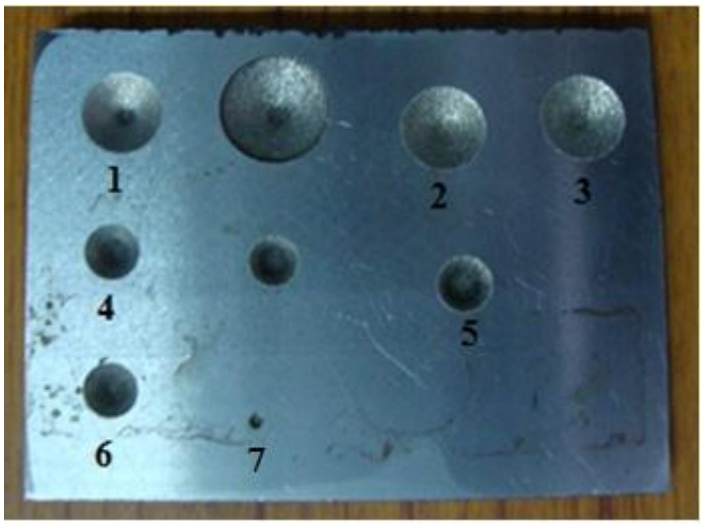

Figure 4.22: HDS (H11) workpiece after machining with copper tool with different front angle such as 90° and 120°

The angle generated on the workpiece(Φ) in each of the experimental trials are shown in Table 4.54.

Table 4.53: Angle generated on the workpiece(Φ) in each of the experimental trials

Trial no.	Workpiece	Current (Amp)	Pulse on Time (µs)	Pulse off Time (µs)	Powder Concentration(µs) (g/l)	Tool front angle(Θ)	Angle generated on Workpiece(Φ)
1	H11	7	50	57	5	120°	123.229°
2	H11	5	100	57	10	120°	121.531°
3	H11	7	100	57	10	120°	122.8°
4	H11	7	50	57	5	90°	94.86°
5	H11	5	100	57	10	90°	92.91°
6	H11	7	100	57	10	90°	94.35°

The Profile of the angle generated on the workpiece by the tool for each of the experimental trial is shown in the Figure 4.23.

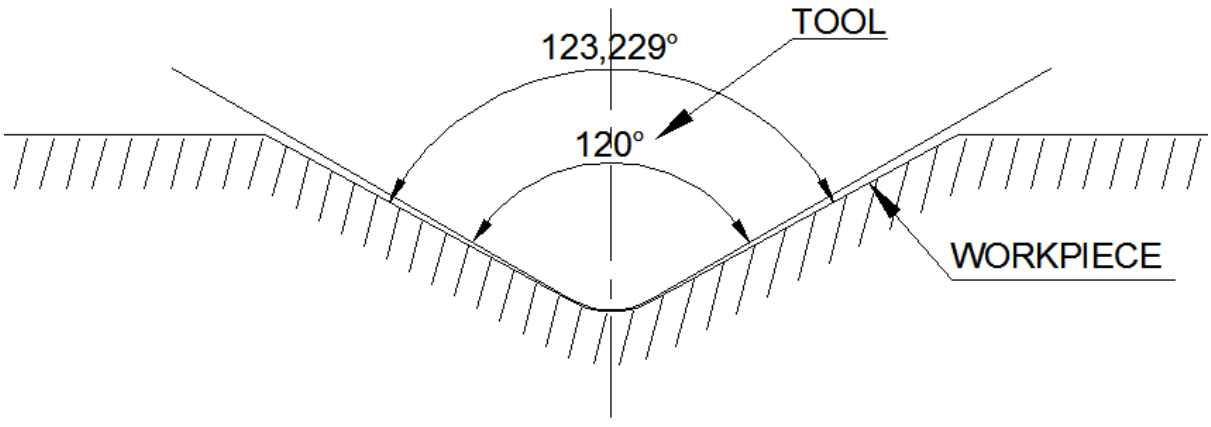

(1)

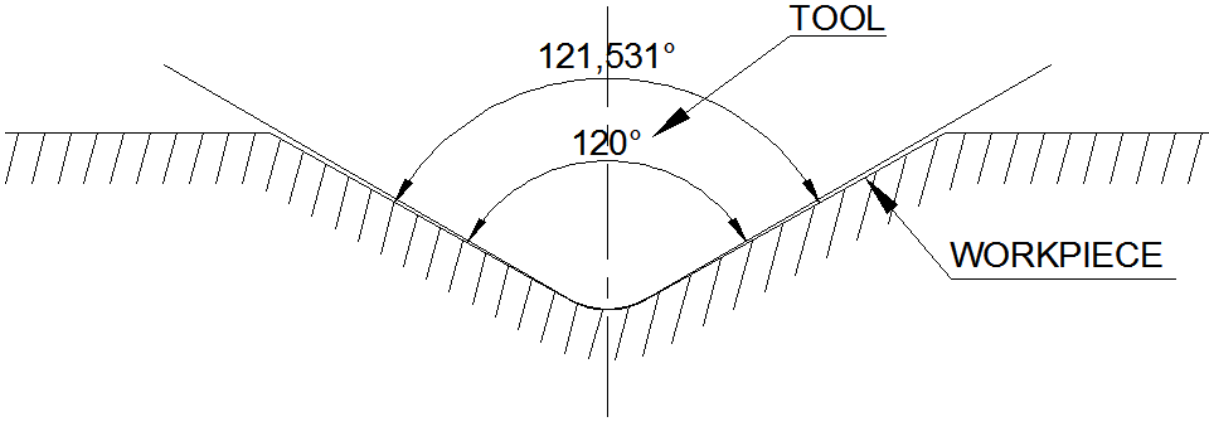
TOOL
121,531°
120°
WORKPIECE

(2)

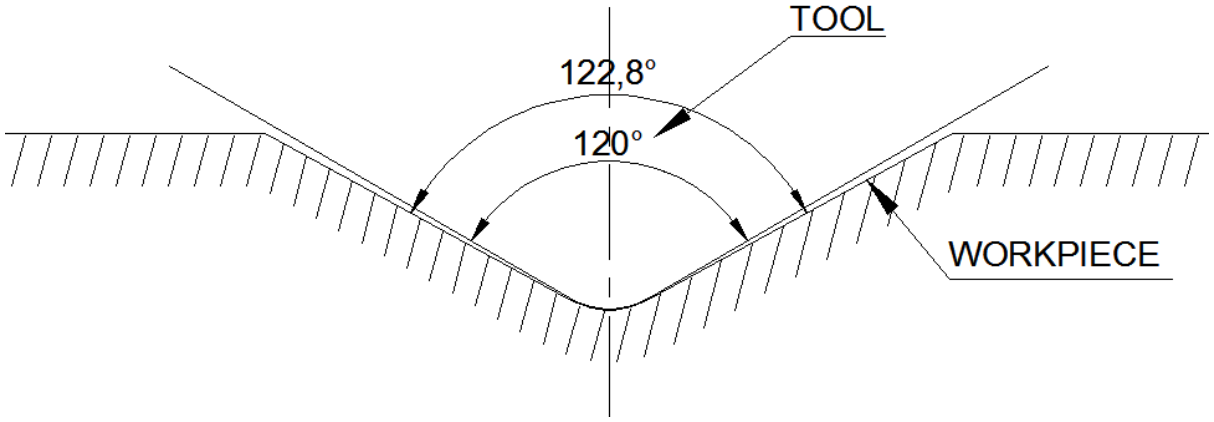
TOOL
122,8°
120°
WORKPIECE

(3)

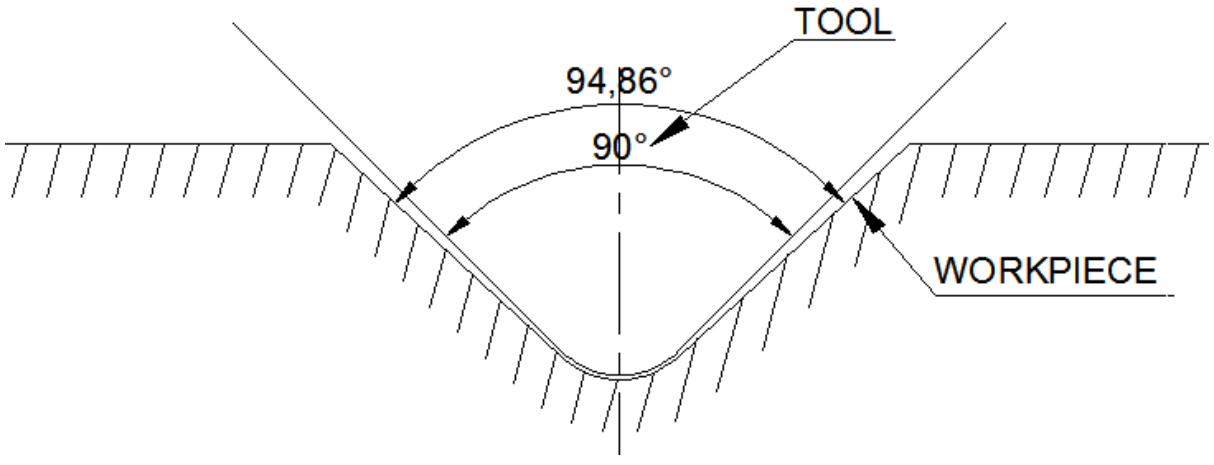
TOOL
94,86°
90°
WORKPIECE

(4)

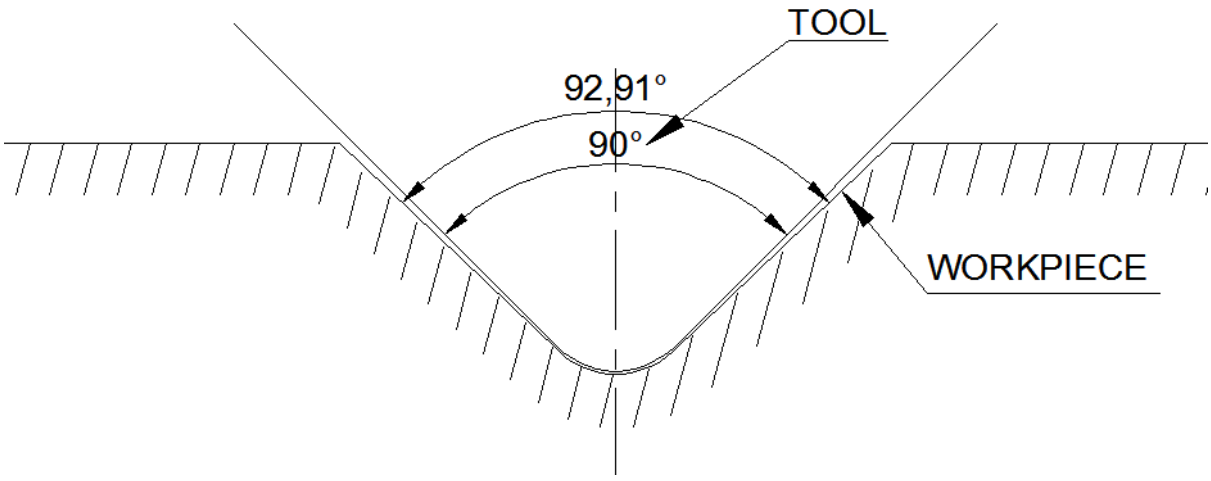

(5)

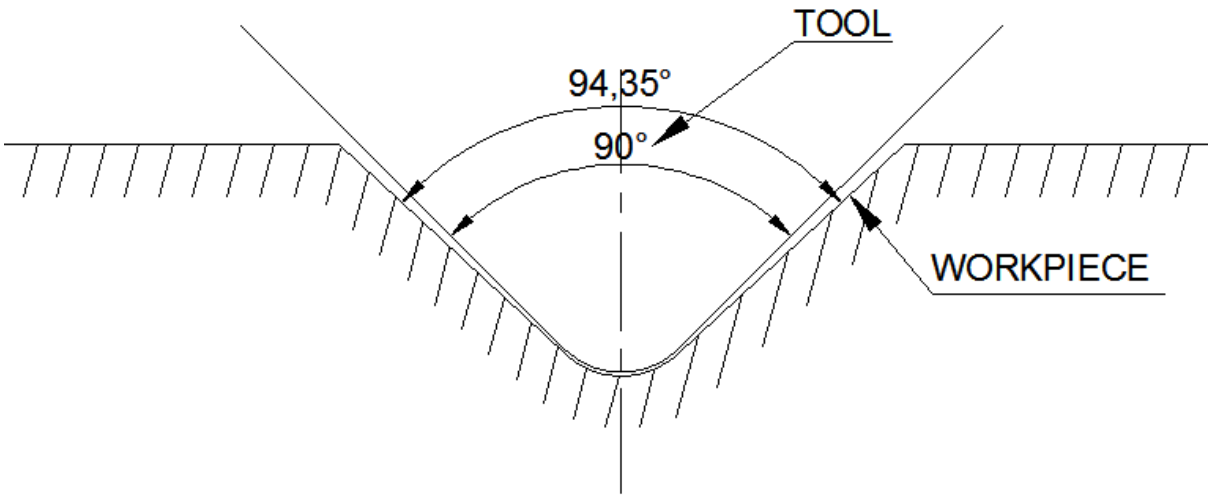

(6)

Figure 4.23: Different angle generated on the workpiece in the experimental trials 1 - 6

From the Figure 4.23, it can be seen that the angle generated on the workpiece by the 90° tool front angle is more as compared to 120°.For example let us take the trial number 1 and 4 into consideration. All the parameters except the tool front angle (Θ) are same. In trial number 1, the angle generated on the workpiece(Φ) is 123.229° when tool front angle is 120° whereas in trial number 4, the angle generated on the workpiece(Φ) is 94.86° when tool front angle is 90°. Hence it is quite clear that the angle generated on the workpiece(Φ) is high when the tool front angle is small and vice versa. The same result can be observed in trials 2 and 5 as well as in 3 and 6. The reason for this might be that when tool front angle is large then the distance between the tool and workpiece would remain less uneven and thus the spark energy remains more uniform at different places between the tool and workpiece whereas when the tool front angle is small then the distance between the tool and workpiece would remain more

uneven because when the tool moves from up to down into the workpiece ,the sparking between the tool and workpiece starts at region 1 as shown in the Figure 4.24 as compared to region 2 which is at the tip of the tool and thus the sparking at region 1 occurs for more time as compared to the region 2 as shown in Figure 4.24 and thus more machining takes place at region 1. Hence it can be concluded that when the tool front angle is small then more variation occurs in sparking at different places between the tool and workpiece and thus the angle generated on the workpiece is less accurate. Similarly when the tool front angle is large, the angle generated between the tool and workpiece is more accurate.

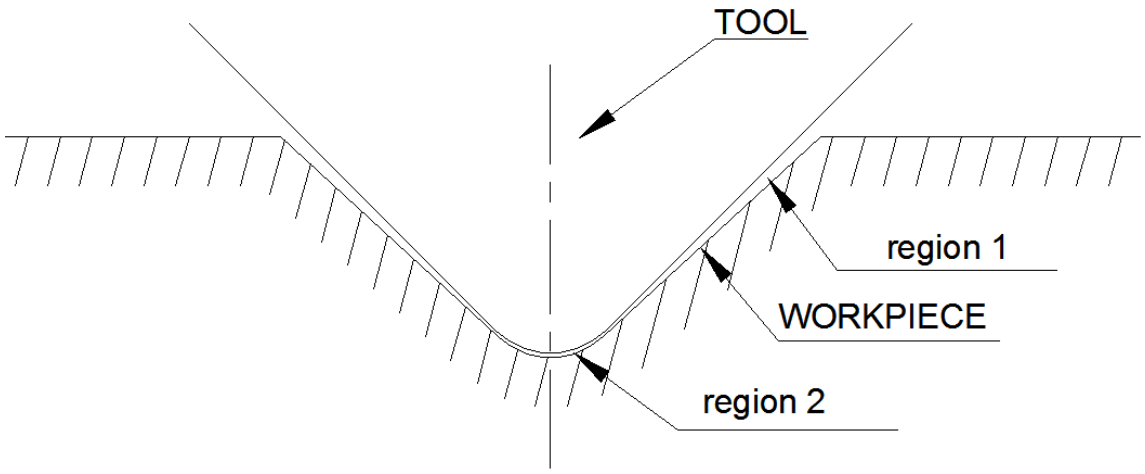

Figure 4.24: Diagram showing variation in the distance between the tool and workpiece

4.8 XRD AND SEM ANALYSIS

4.8.1 Introduction

Further analysis of the machined surfaces after confirmation experiments was performed to find out surface composition and microstructure and it has been presented in this part. Surface composition was determined with the help of X-ray diffraction (XRD) analysis and microstructural studies were carried out on a Scanning Electron Microscope (SEM). In this work, the effect of various input parameters i.e. current, pulse on time, electrode material, powder concentration and types of powder on the surface properties of the workpiece material was evaluated. During machining, sparking between the tool and workpiece takes place and causes very high rise in temperature and this high temperature causes vaporization of the molten metal at the point of discharge. Due to very high temperature the workpiece material is subjected to recrystallization of the metal grains and subsequent cooling of the heated metal causes change in the micro structure. The heating and cooling rate decides the shape, size of grains and properties of machined surface. Moreover transfer of material takes place from the powder suspended in the dielectric fluid and also from the electrode to the machined surface. The chemical composition of the machined surface was determined with the help of X-Ray Diffraction (XRD) analysis. Micro structural analysis was carried using Scanning Electron Microscope (SEM) and Lieca Metallurgical Microscope. During this analysis chemical composition of machined surface and micro structure of machined surface was evaluated.

4.8.2 XRD analysis

The material is transferred to the workpiece from the powder mixed in the dielectric fluid or from the electrode. It forms various compound on the surface of workpiece. To analyze this, the workpiece was tested for XRD on selected samples. The range of 2θ from 5° to 100° was used at a scan speed of 5°/minute at wavelength 1.54 angstrom for each test.

4.8.2.1. XRD Analysis of H11 (HDS)

The XRD pattern of H11 (hot die steel) machined with tungsten-copper electrode in kerosene with 5g/l powder concentration of graphite powder mixed in dielectric medium is shown in the Figure 4.22. The pattern shows the presence of cohenite synthetic (Fe_3C), chromium carbide ($Cr_{23}C_6$) and chromium (Cr). The cohenite is rich iron meteorites which contain carbon content not more than 0.4-0.6% less than α-γ eutectoid composition. The presence of cohenite (Fe_3C compound) increases the hardness of the surface. Cohenite is iron carbide

with an orthorhombic crystal structure. The thermal expansion coefficient of chromium carbide is almost equal to that of steel, reducing the mechanical stress build-up at the layer boundary. After the spectrometer analysis, it was observed that carbon percentage increased intensely from 0.364% to 7.25%.The bulk increase of carbon content is possible due to significant transfer of carbon from graphite powder. The increase in carbon content improves the hardness and strength of the surface. All steels containing more than 0.8 % carbon will have some amount of cementite present in the microstructure along with pearlite. The iron atoms in cementite can be substituted by atoms of chromium. The chromium percentage also increased from 4.99% to 5.58% whereas sulphur increased from 0.0417% to 0.47%. This might be due to rejection of chromium and sulphur from grains during rapid solidification due to the phenomenon of segregation (coring) and thus the percentage increased at the grain boundaries. The chromium reduces the stresses and improves the corrosion resistance. When chromium is more than 5%, the high temperature properties and corrosion resistance of steels is improves and also the, hardenability. The presence of silicon can also be seen with a percentage of 0.76%.

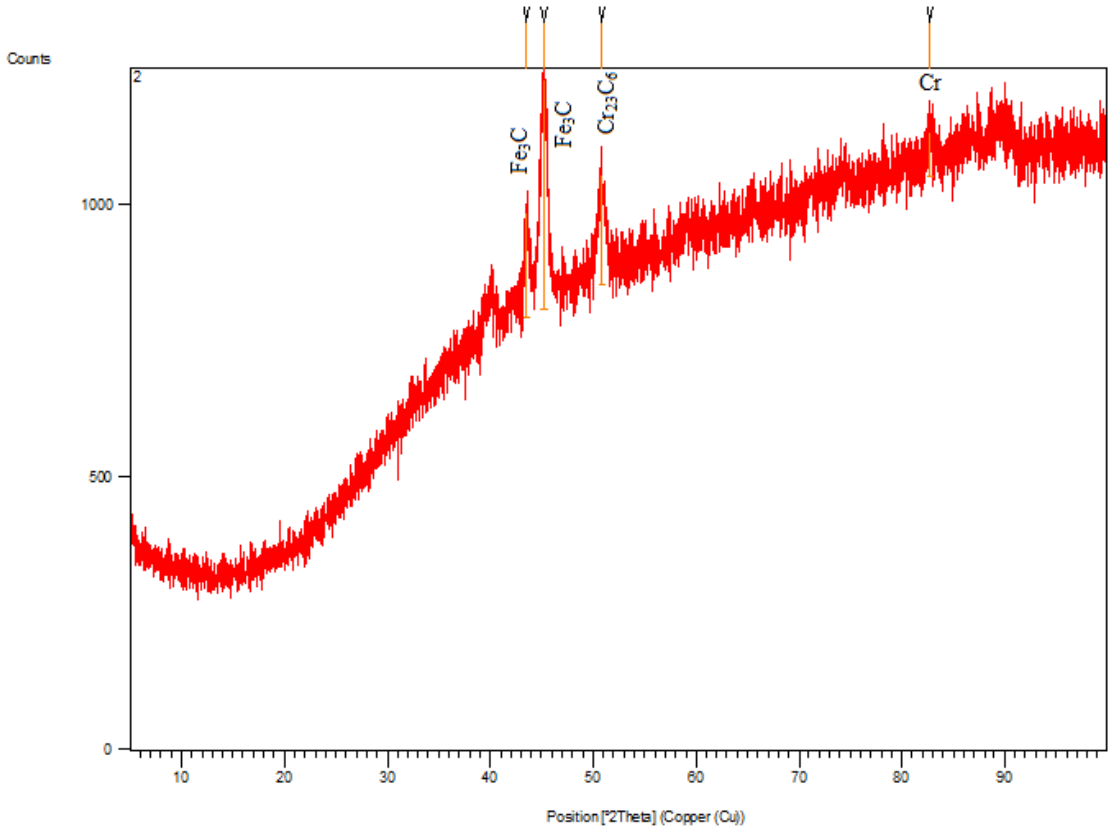

Figure 4.25: XRD pattern of HDS machined with W-Cu electrode in kerosene with Graphite powder mixing. (I 5Amp, Pulse on time 50µs, Powder concentration 5g/l)

The XRD pattern of H11 (hot die steel) machined with brass electrode in EDM oil with 5g/l powder concentration of silicon powder mixed in dielectric medium is shown in the Figure 4.23. The pattern shows the traces of cohenite synthetic (iron carbide, Fe_3C), copper and synthetic carbon. As it is already explained that cohenite is rich iron meteorites which contain carbon content not more than 0.4-0.6% less than α-γ eutectoid composition. Cohenite is iron carbide with an orthorhombic crystal structure. The presence of cohenite (Fe_3C compound) increases the hardness of the surface. The copper has not formed any compound. The increase in carbon content improves the hardness and strength of the surface. After the spectrometer analysis, it was observed that percentage of copper increased significantly from 0.112% to 7.71% and carbon increased significantly from 0.364% to 9.04%. The percentage of various elements on the surface before and after machining is shown in Table 4.53. The transfer of copper and zinc occurs from the brass electrode on the surface as well as silicon has transferred from powder which was suspended in the edm oil. Silicon improves the oxidation resistance and strengthens the surface. The increase in copper improves the resistance to corrosion. However copper has not formed compound with other elements.

Table 4.54: Chemical composition of HDS machined with Brass electrode in edm oil with silicon powder mixing. (I=5 Amp, Pulse on= 20µs, Powder concentration 5g/l)

Composition	Before machining (%)	After machining (%)
Carbon	0.364	9.04
Copper	0.112	7.71
Zinc	-	1.75
Vanadium	0.302	0.47
Silicon	-	0.84
Chromium	4.99	4.21

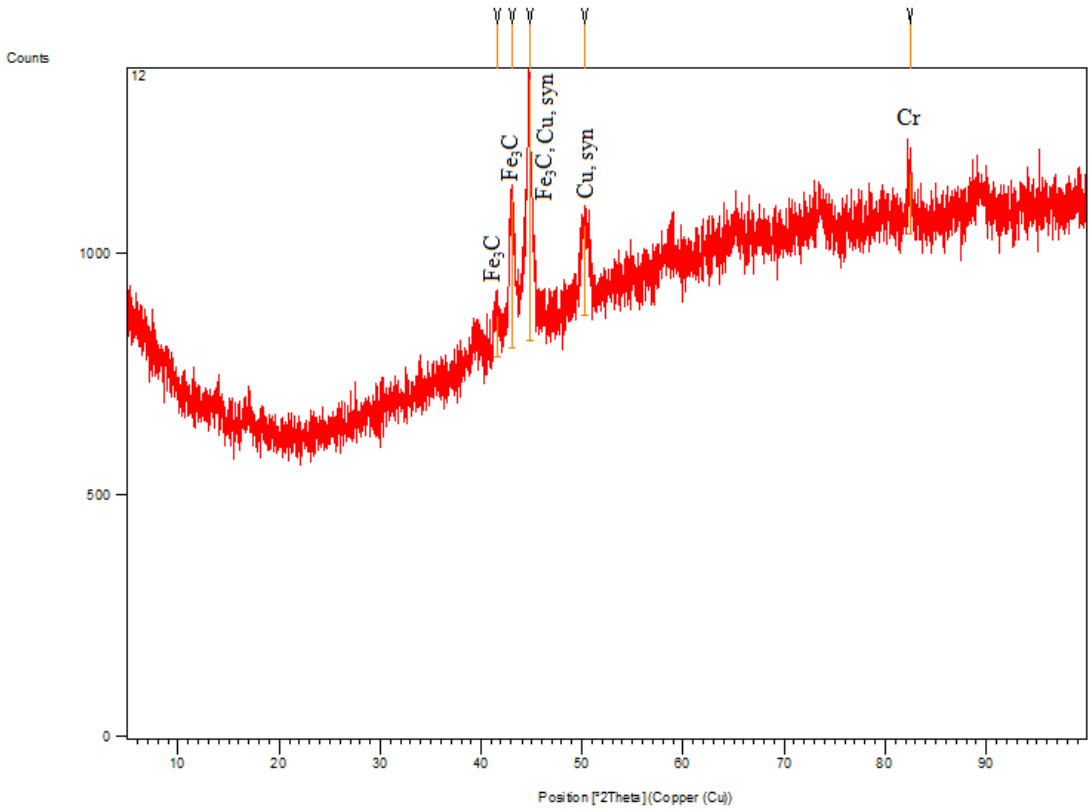

Figure 4.26: XRD pattern of HDS machined with Brass electrode in edm oil with silicon powder mixing. (I=5 Amp, Pulse on= 20µs, Powder concentration 5g/l)

4.8.2.2. XRD Analysis of High Carbon High Chromium (HCHCr)

The XRD pattern of HCHCr machined with tungsten –copper electrode in kerosene with 5g/l powder concentration of silicon powder mixed in dielectric medium is shown in the Figure4.24. The pattern shows the traces of cohenite synthetic (iron carbide, Fe_3C) and chromium carbide ($Cr_{23}C_6$). Cohenite is iron carbide with an orthorhombic crystal structure whereas chromium carbide has a cubic crystal structure. The presence of cohenite (Fe_3C compound) increases the hardness of the surface. Corrosion resistance of steels improved and hardenability improved with chromium carbide. The composition of the machined surface before and after machining is shown in Table 4.54.It can be seen that carbon increases in bulk amount. The transfer of carbon takes place from kerosene to the machined surface. After the spectrometer analysis, it was found that silicon increased from 0.401% to 0.85% and chromium decreased from 11.6% to 10.2%. It might be because some replacement of chromium with silicon on surface occurred. Increase in silicon improves the oxidation resistance.

Table 4.55: Chemical composition of HCHCr machined with W-Cu electrode in kerosene with silicon powder mixing. (I 7Amp, Pulse on time 100µs, Powder concentration 5g/l)

Composition	Before machining (%)	After machining (%)
Carbon	1.59	9.38
Chromium	11.6	10.20
Silicon	0.401	0.85

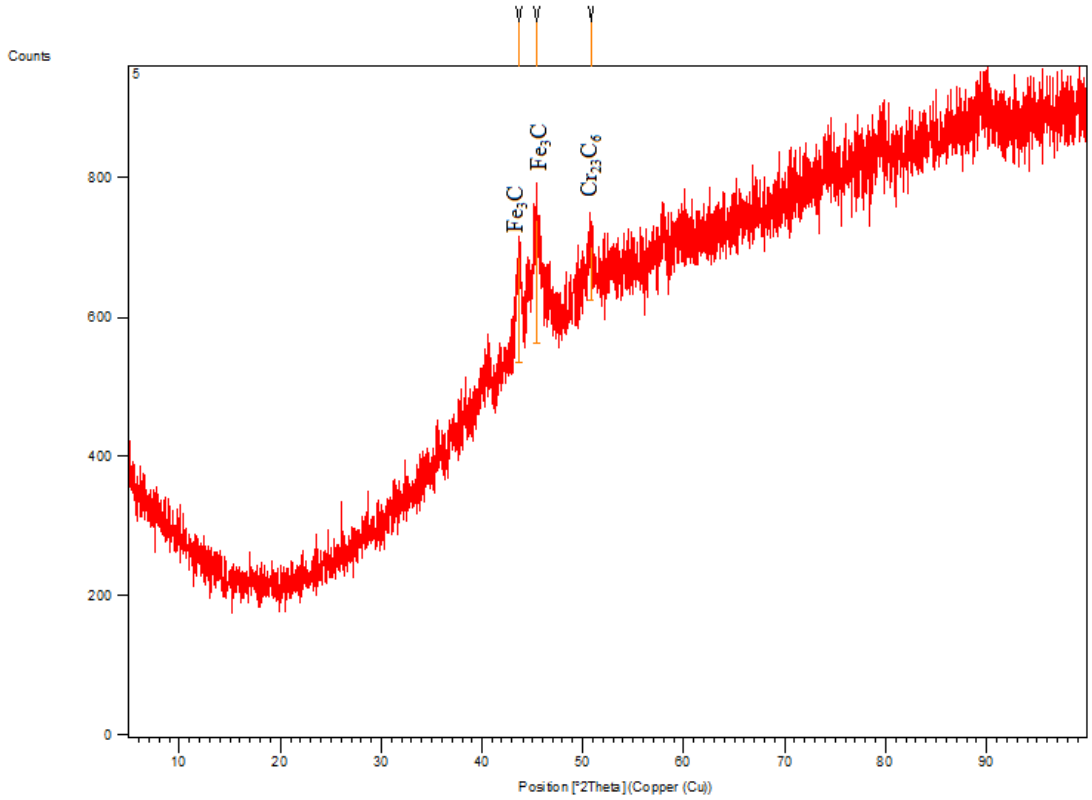

Figure 4.27: XRD pattern of HCHCr machined with W-Cu electrode in kerosene with silicon powder mixing. (I 7Amp, Pulse on time 100µs, Powder concentration 5g/l)

The XRD pattern of HCHCr machined with graphite electrode in edm oil with 5g/l powder concentration of tungsten powder mixed in dielectric medium is shown in the Figure 4.25. The pattern shows the traces of iron carbide (Fe_5C_2),chromium carbide ($Cr_{23}C_6$) and carbon (C60). Iron carbide consists of orthorhombic crystal structure whereas chromium carbide carbon (C60) has a cubic crystal structure. The presence of Fe_5C_2 compound increases the hardness of the surface. Corrosion resistance of steels improved and hardenability improved with chromium carbide. The carbon improves the strength, wear resistance and hardness but reduces the toughness and ductility. The bulk increase in carbon percentage from 1.59% to

15.82% might be due to transfer of carbon from graphite electrode. Percentage of chromium is decreased from 11.6% to 10.03%.

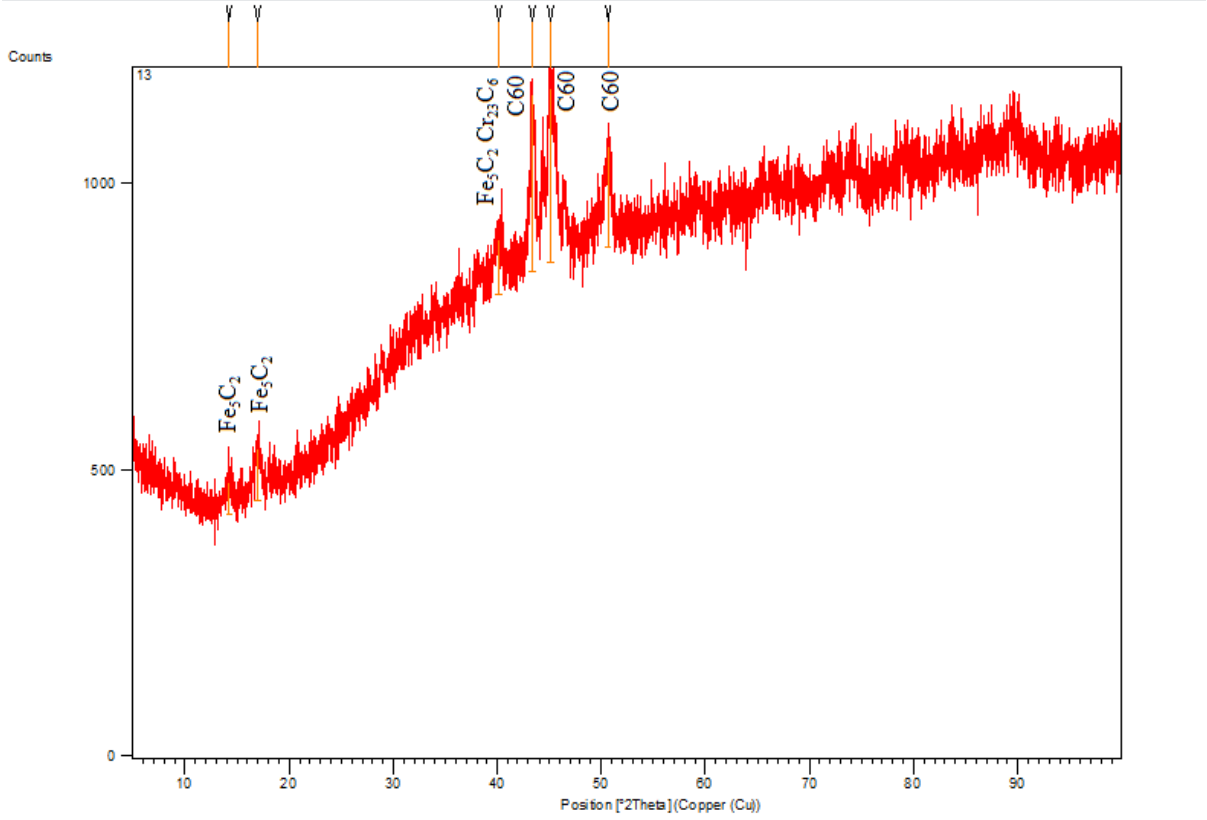

Figure 4.28: XRD pattern of HCHCr machined with graphite electrode in edm oil with tungsten powder mixing. (I=7Amp, Pulse on= 20µs, Powder concentration 5g/l)

4.8.2.3 XRD Analysis of (AISI 1045)

The XRD pattern of AISI 1045 machined with W-Cu electrode in kerosene with 10g/l powder concentration of tungsten powder mixed in dielectric medium is shown in the Figure 4.26. The pattern shows the presence of iron carbide (Fe_2C) and manganese carbide (Mn_7C_3). Iron carbide consists of orthorhombic crystal structure whereas manganese carbide has a cubic crystal structure. The presence of Fe_2C compound increases the hardness of the surface. The bulk increase in carbon percentage from 0.518% to 9.49% might be due to transfer of carbon from the kerosene. The carbon improves the strength, wear resistance and hardness but reduces the toughness and ductility. Percentage of manganese is increased from 0.749% to 0.80%.The increase in percentages of manganese as well as carbon indicate that the formation of manganese carbide is taking place in the sparking channel which gets deposited on the work surface after the sparking channel collapses.

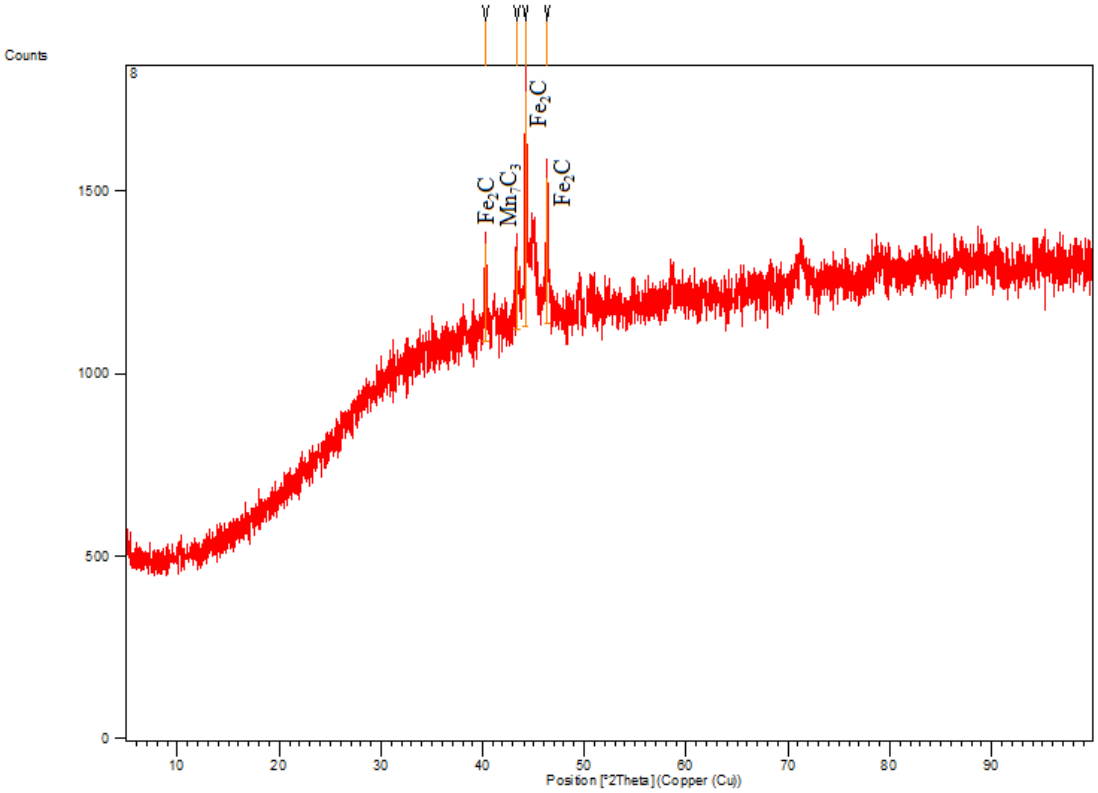

Figure 4.29: XRD pattern of AISI 1045 machined with W-Cu electrode in kerosene with tungsten powder mixing. (I=5 Amp, Pulse on= 20µs, Powder concentration 10g/l)

The XRD pattern of AISI 1045 machined with graphite electrode in edm oil with 10g/l powder concentration of silicon powder mixed in dielectric medium is shown in the Figure 4.27. The pattern shows the presence of iron carbide (Fe_3C) and carbon(C). Iron has an orthorhombic crystal structure. The presence of cohenite (Fe_3C compound) increases the hardness of the surface. The bulk increase in carbon percentage from 0.518% to 9.02% is due to transfer of carbon from the graphite electrode or kerosene. The carbon improves the strength, wear resistance and hardness but reduces the toughness and ductility. The percentage of manganese is increased from 0.749% to 0.85%. Manganese contributes to the strength and hardness (but to a lesser degree than carbon).

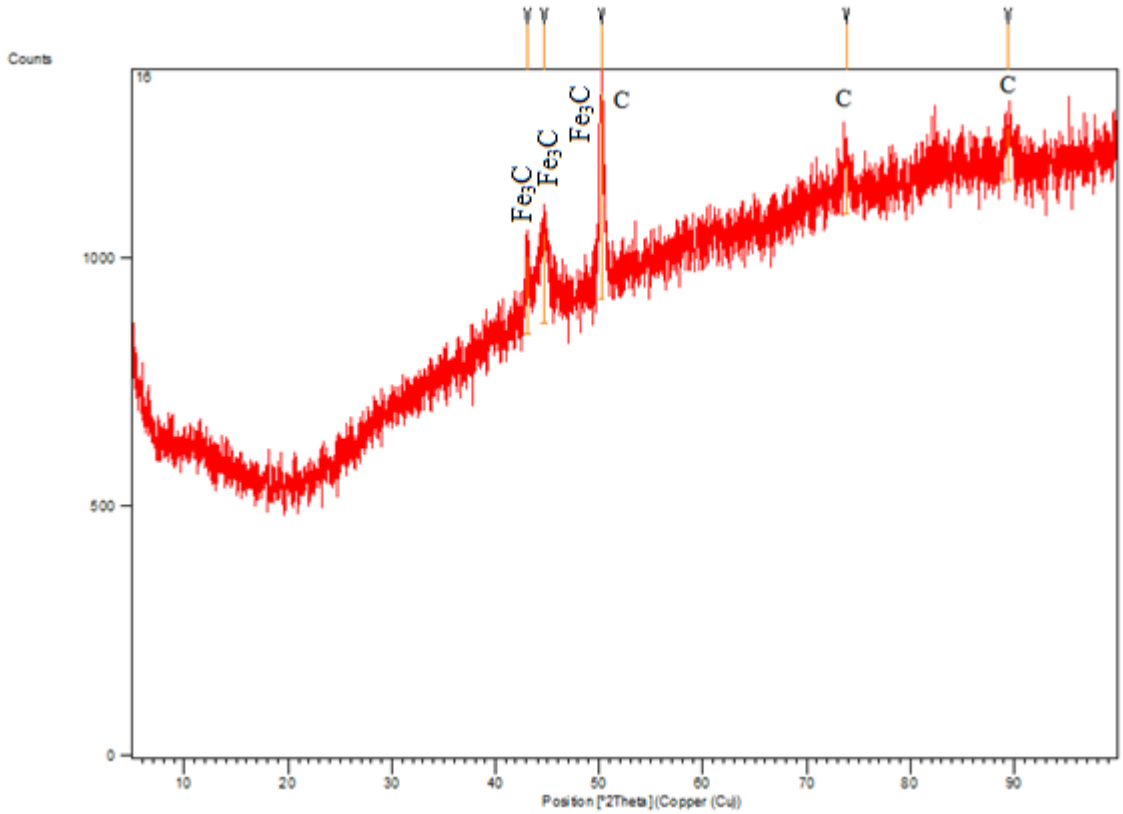

Figure 4.30: XRD pattern of AISI 1045 machined with graphite electrode in edm oil with silicon powder mixing. (I=5 Amp, Pulse on= 100µs, Powder concentration 10g/l)

4.8.3 SUMMARY OF XRD ANALYSIS

The summary of the XRD analysis is tabulated in Table 4.56.

Table 4.56: Summary of XRD analysis

Workpiece	Electrode	Powder	Dielectric	Results
H11	W-Cu	Graphite	Kerosene	• Shows the traces of Cohenite, synthetic (Fe_3C), chromium carbide and chromium. • Reduce the mechanical stress at the boundary layer. • Improves the hardness, corrosion resistance, hardenability. and strength of the surface.

H11	Brass	Silicon	edm oil	• Shows the traces of cohenite, synthetic (iron carbide, Fe_3C), copper and synthetic carbon (C8). • Increase the corrosion resistance and hardenability. • The increase in carbon content improves the hardness and strength of the surface. • Copper has not form any compound.
HCHCr	W-Cu	Silicon	Kerosene	• Shows the traces of cohenite, synthetic (iron carbide, Fe_3C) and chromium carbide ($Cr_{23}C_6$) • Iron carbide improves the hardness of the surface. • Improves strength and hardenability of the surface. • Temperature properties and corrosion resistance improved. • Reduce the mechanical stress at the boundary layer.
HCHCr	graphite	tungsten	edm oil	• Shows the traces of iron carbide (Fe_5C_2), chromium carbide ($Cr_{23}C_6$) and carbon (C60). • Iron carbide improves the hardness of the surface. • Corrosion resistance and hardenability improved with chromium carbide.

AISI 1045	W-Cu	tungsten	Kerosene	• The pattern shows the presence of iron carbide (Fe_2C) and manganese carbide (Mn_7C_3). • Iron carbide improves the hardness of the surface. • Significant increase in carbon improves the strength, wear resistance and hardness but reduces the toughness and ductility.
AISI 1045	graphite	silicon	edm oil	• Shows the presence of iron carbide (Fe_3C) and carbon(C). • Iron carbide improves the hardness of the surface. • The carbon improves the strength, wear resistance and hardness but reduces the toughness and ductility. • Manganese contributes to the strength and hardness (but to a lesser degree than carbon).

4.8.4 MICROSTRUCTURE ANALYSIS

Microstructure analysis was carried out on six selected samples using Scanning Electron Microscope to study the change in the microstructure after machining. The samples were prepared as per standard before SEM analysis on three different magnifications namely, 200×, 500× and 1000×.

4.8.4.1 Preparing Sample for Scanning Electron Microscope

The steps for the preparation of sample for SEM are given below:

All the samples of size are cut into size of 10 ×12mm

Clean the surface of sample with wire brush.

Clean the samples with acetone using cotton so as to remove debris from the machined surface.

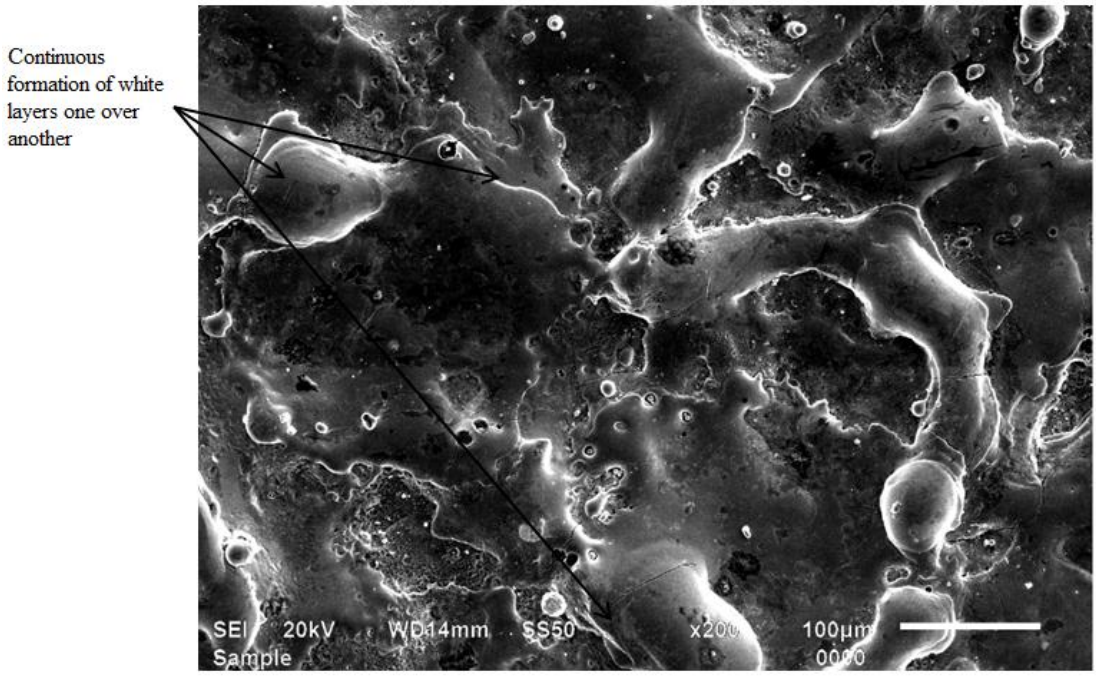

Figure 4.31: SEM micrograph at 200× of HDS machined with W-Cu electrode in kerosene with Graphite powder mixing. (I 5Amp, Pulse on time 50µs, Powder concentration 5g/l)

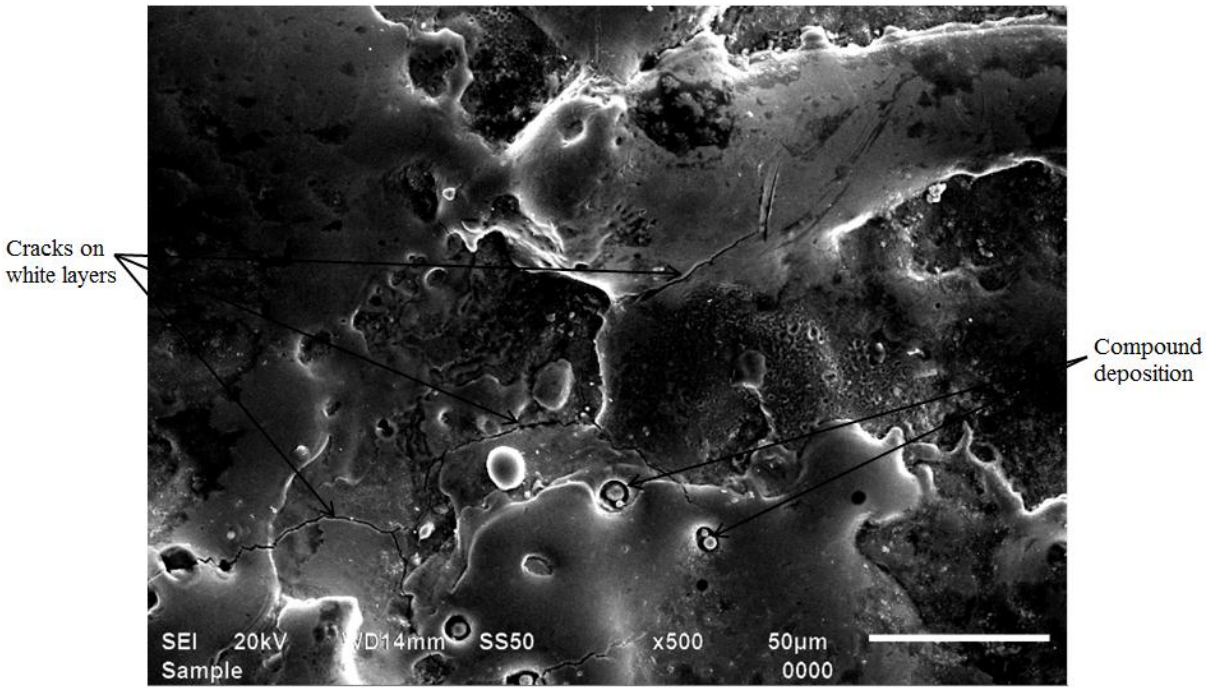

Figure 4.32: SEM micrograph at 500× of HDS machined with W-Cu electrode in in kerosene with Graphite powder mixing. (I 5Amp, Pulse on time 50µs, Powder concentration 5g/l)

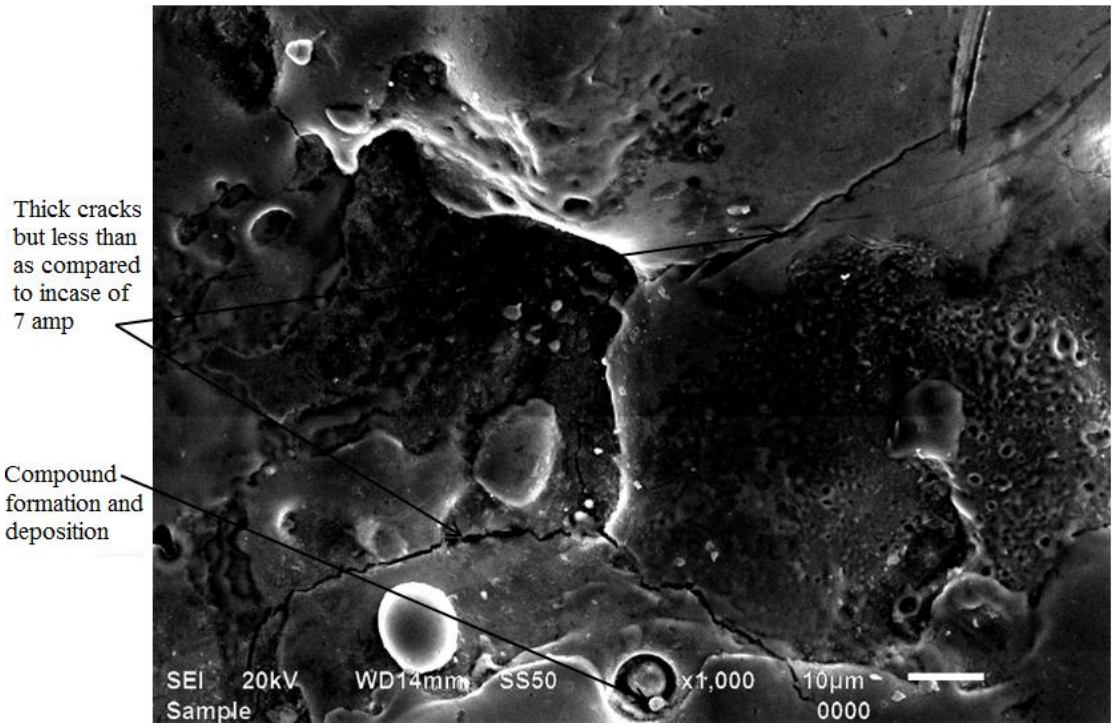

Figure 4.33: SEM micrograph at 1000× of HDS machined with W-Cu electrode in in kerosene with Graphite powder mixing. (I 5Amp, Pulse on time 50µs, Powder concentration 5g/l)

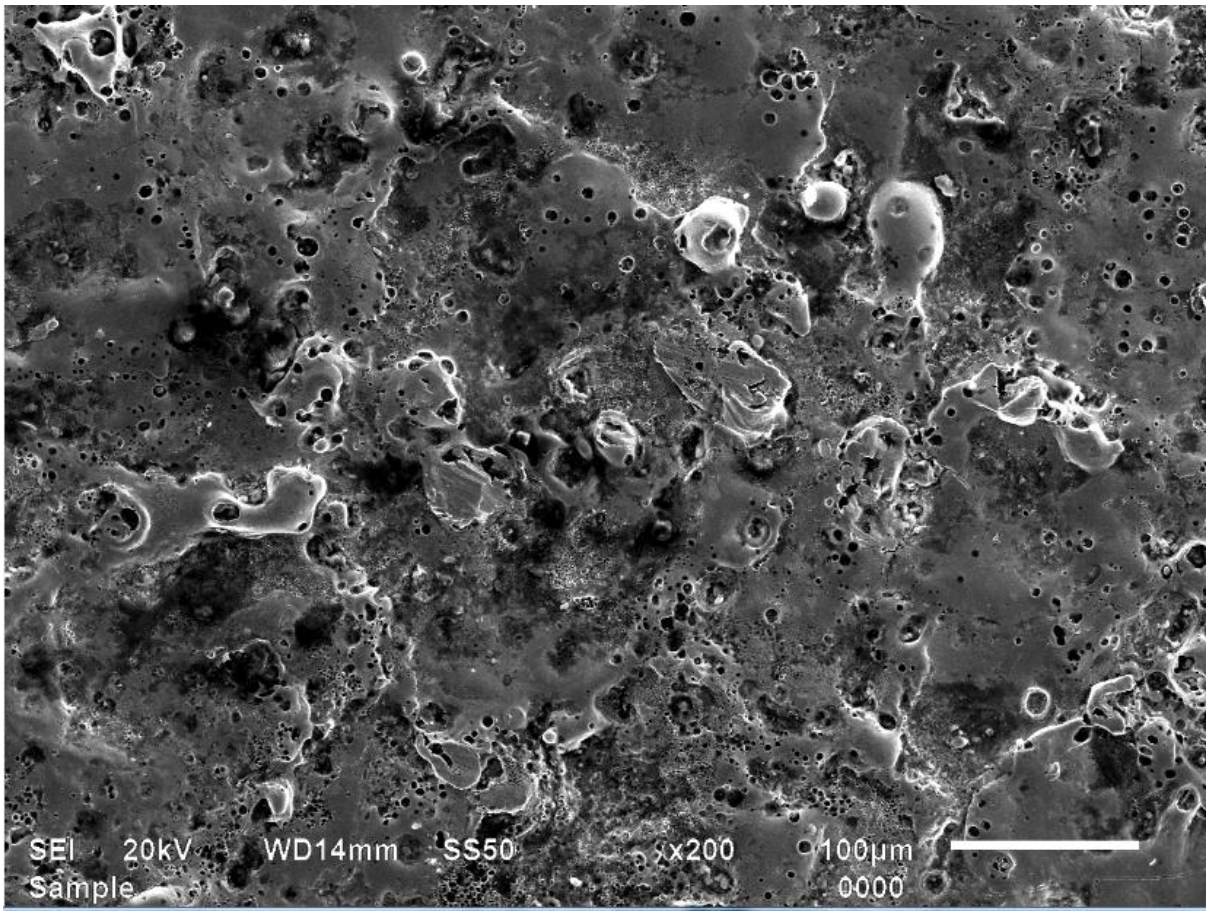

Figure 4.34: SEM micrograph at 200× HDS machined with Brass electrode in edm oil with silicon powder mixing. (I=5 Amp, Pulse on= 20µs, Powder concentration 5g/l)

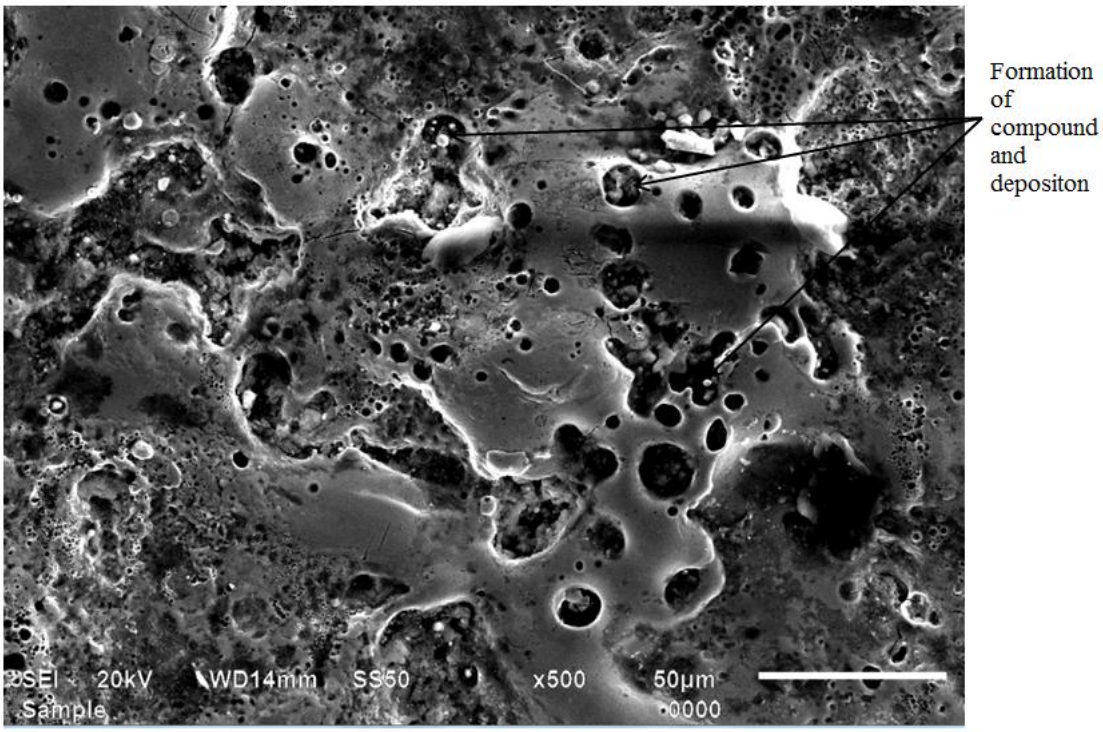

Figure 4.35: SEM micrograph at 500× HDS machined with Brass electrode in edm oil with silicon powder mixing. (I=5 Amp, Pulse on= 20µs, Powder concentration 5g/l)

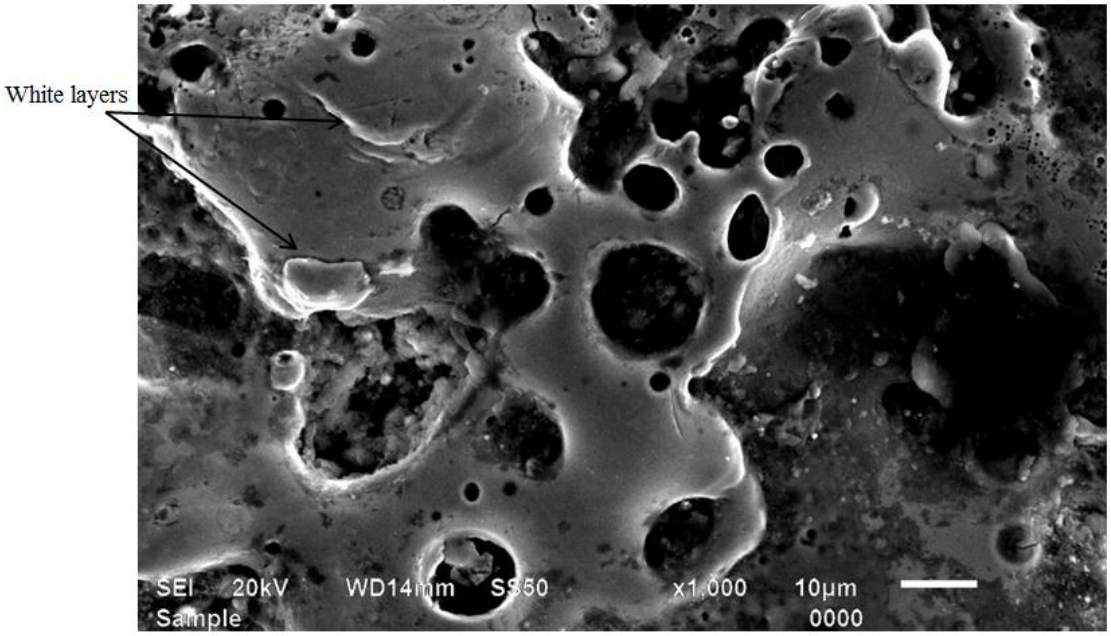

Figure 4.36: SEM micrograph at 1000× HDS machined with Brass electrode in edm oil with silicon powder mixing. (I=5 Amp, Pulse on= 20µs, Powder concentration 5g/l)

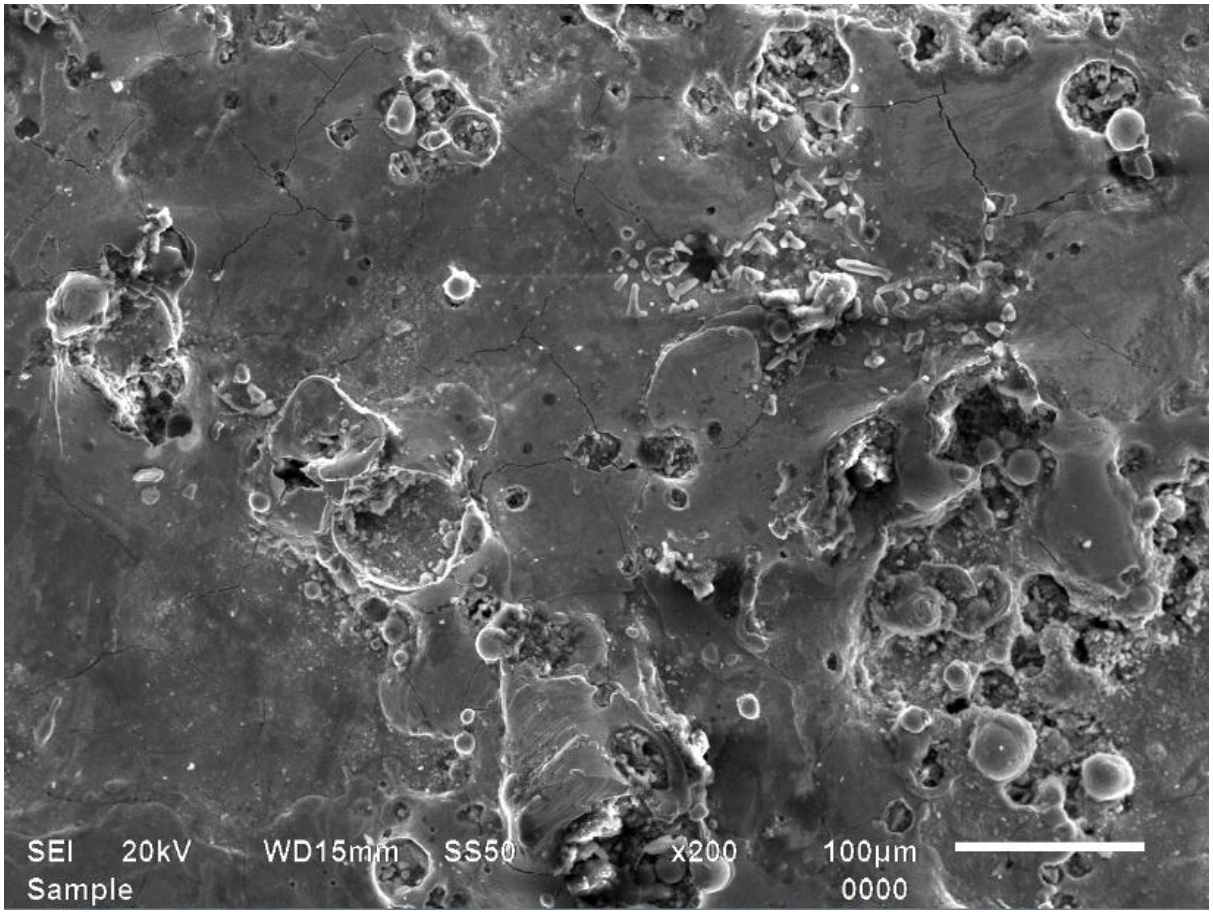

Figure 4.37: SEM micrograph at 200× HCHCr machined with W-Cu electrode in kerosene with silicon powder mixing. (I 7Amp, Pulse on time 100µs, Powder concentration 5g/l)

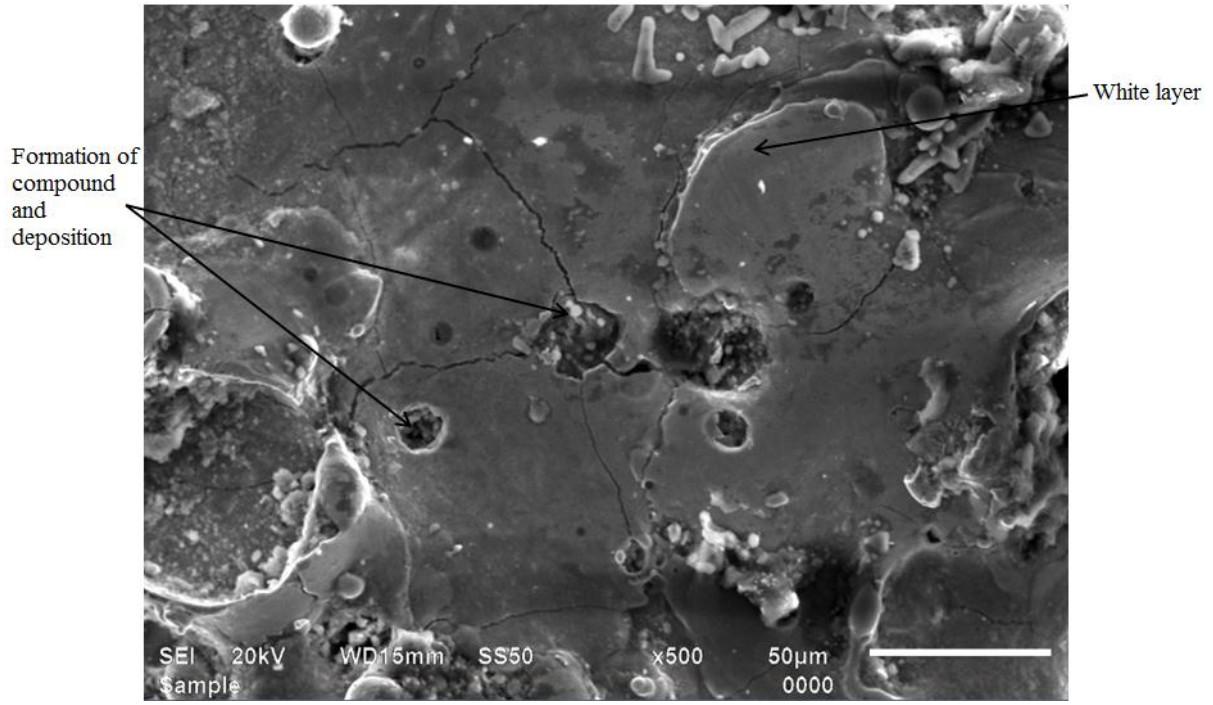

Figure 4.38: SEM micrograph at 500× HCHCr machined with W-Cu electrode in kerosene with silicon powder mixing. (I 7Amp, Pulse on time 100µs, Powder concentration 5g/l)

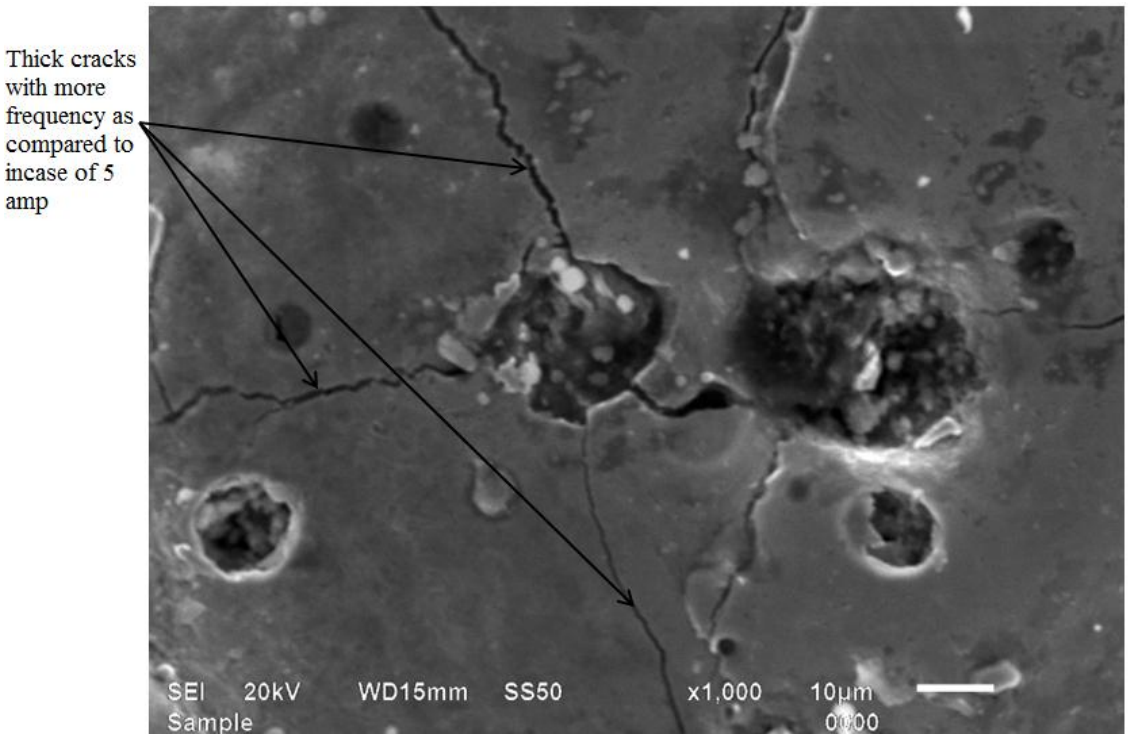

Figure 4.39: SEM micrograph at 1000× HCHCr machined with W-Cu electrode in kerosene with silicon powder mixing. (I 7Amp, Pulse on time 100µs, Powder concentration 5g/l)

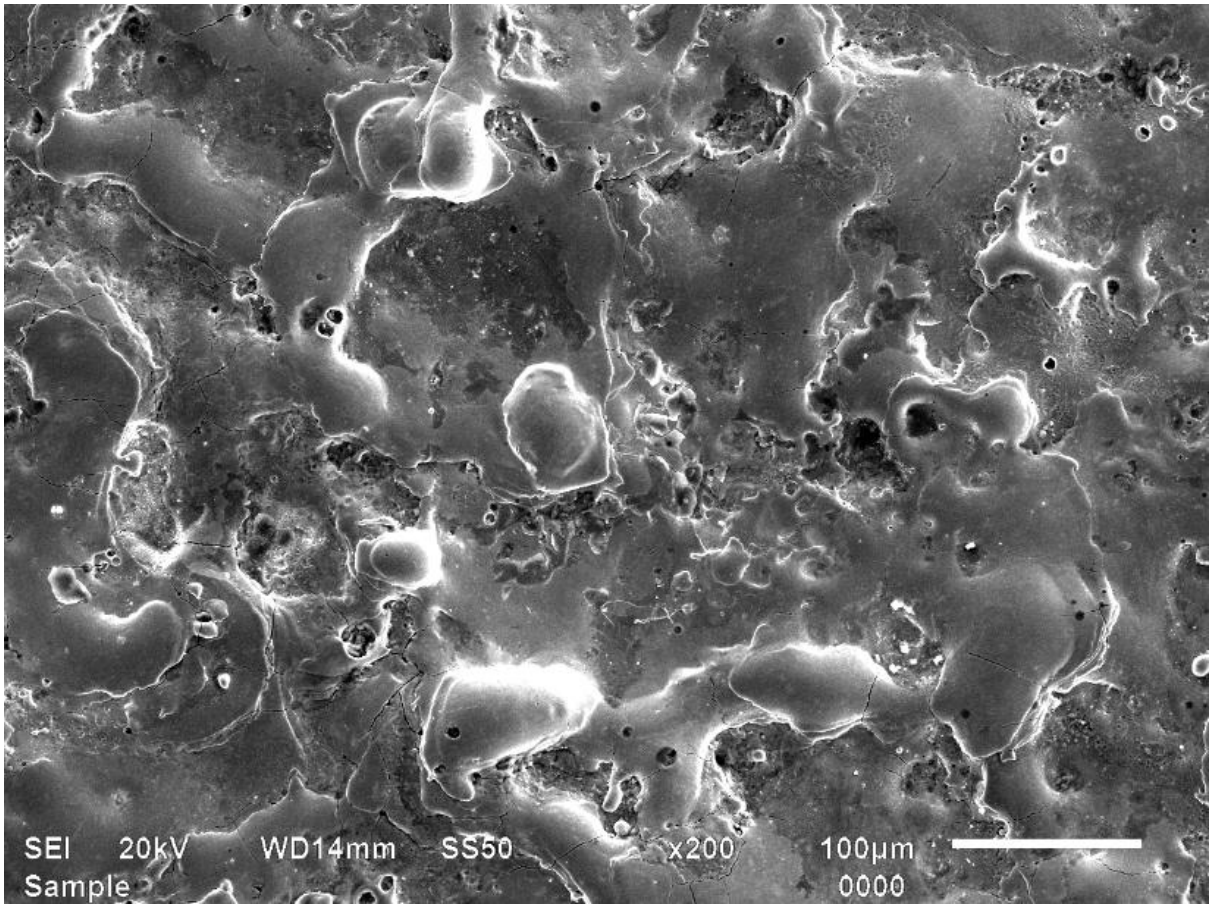

Figure 4.40: SEM micrograph at 200× HCHCr machined with Graphite electrode in edm oil with tungsten powder mixing. (I=7Amp, Pulse on= 20µs, Powder concentration 5g/l)

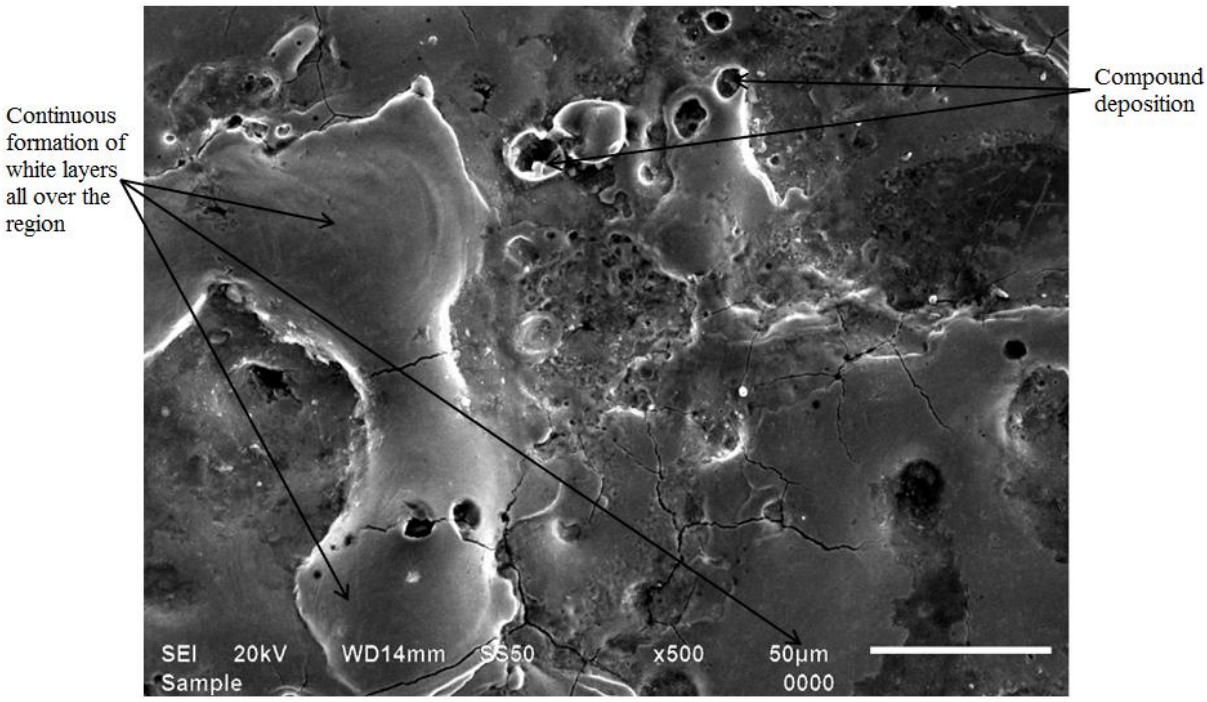

Figure 4.41: SEM micrograph at 500× HCHCr machined with Graphite electrode in edm oil with tungsten powder mixing. (I=7Amp, Pulse on= 20µs, Powder concentration 5g/l)

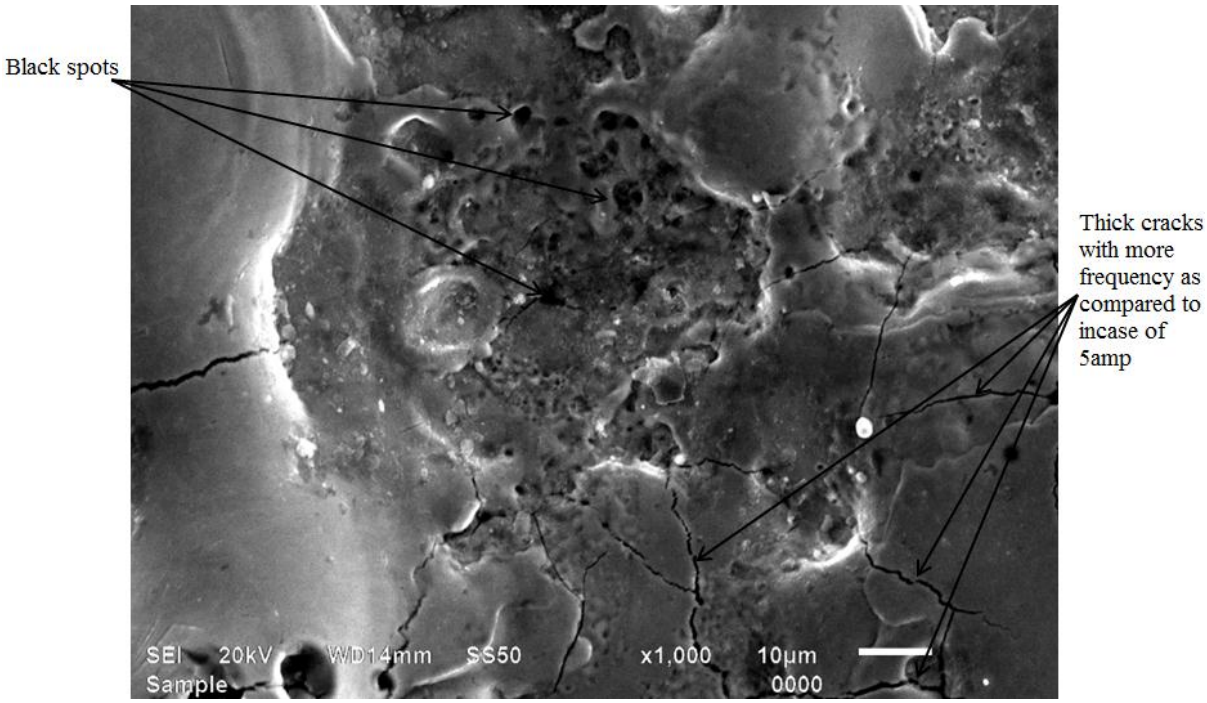

Figure 4.42: SEM micrograph at 1000× HCHCr machined with Graphite electrode in edm oil with tungsten powder mixing. (I=7Amp, Pulse on= 20µs, Powder concentration 5g/l)

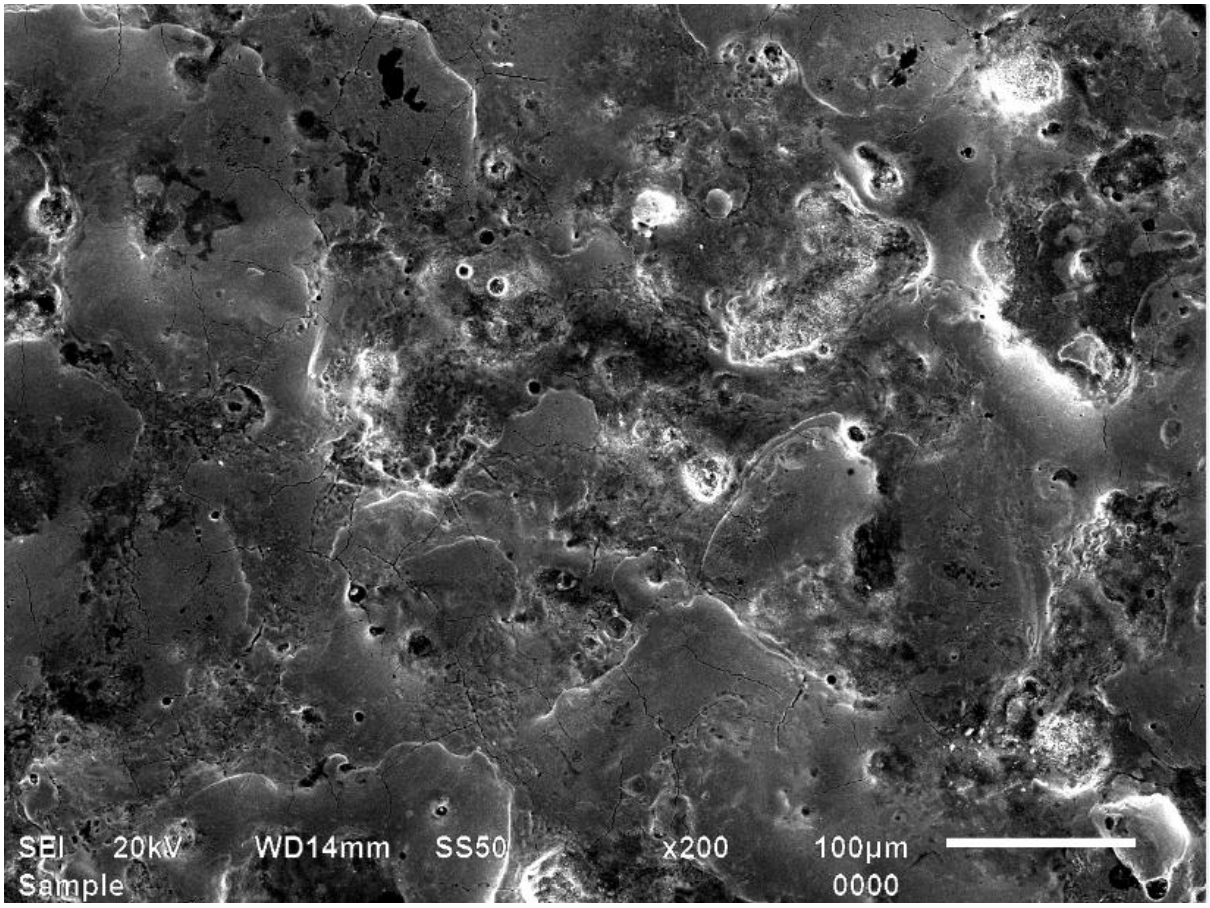

Figure 4.43: SEM micrograph at 200× AISI 1045 machined with W-Cu electrode in kerosene with tungsten powder mixing. (I=5 Amp, Pulse on= 20µs, Powder concentration 10g/l)

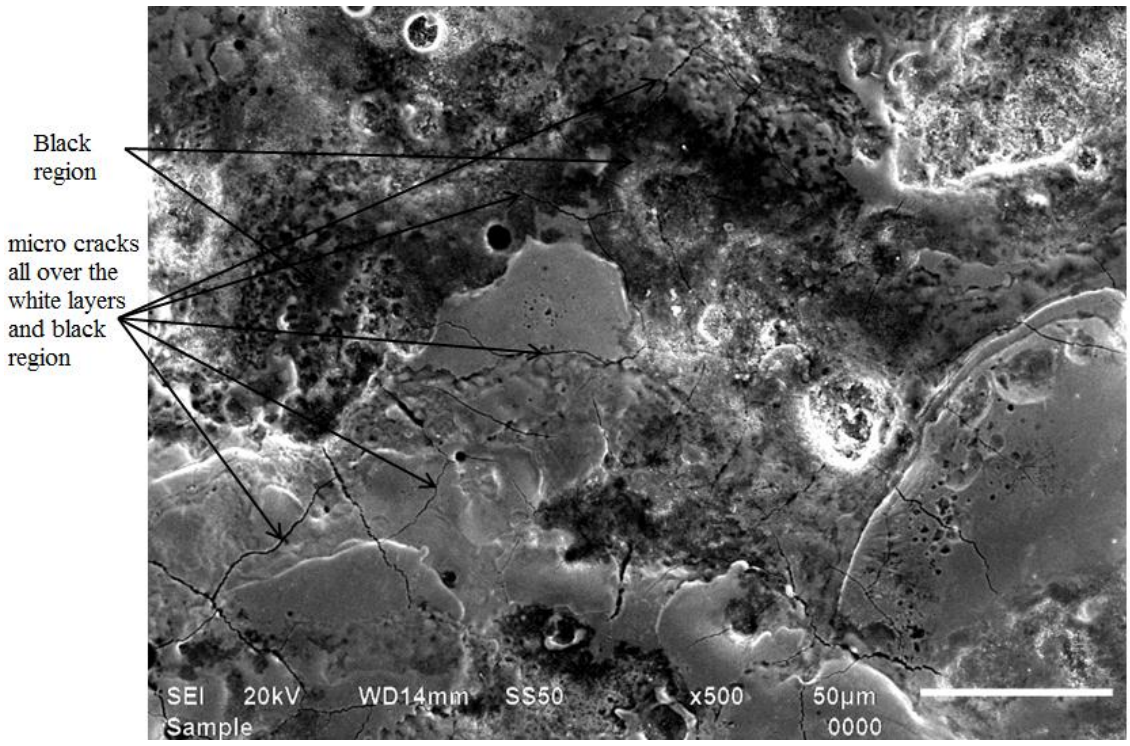

Figure 4.44: SEM micrograph at 500× AISI 1045 machined with W-Cu electrode in kerosene with tungsten powder mixing. (I=5 Amp, Pulse on= 20µs, Powder concentration 10g/l)

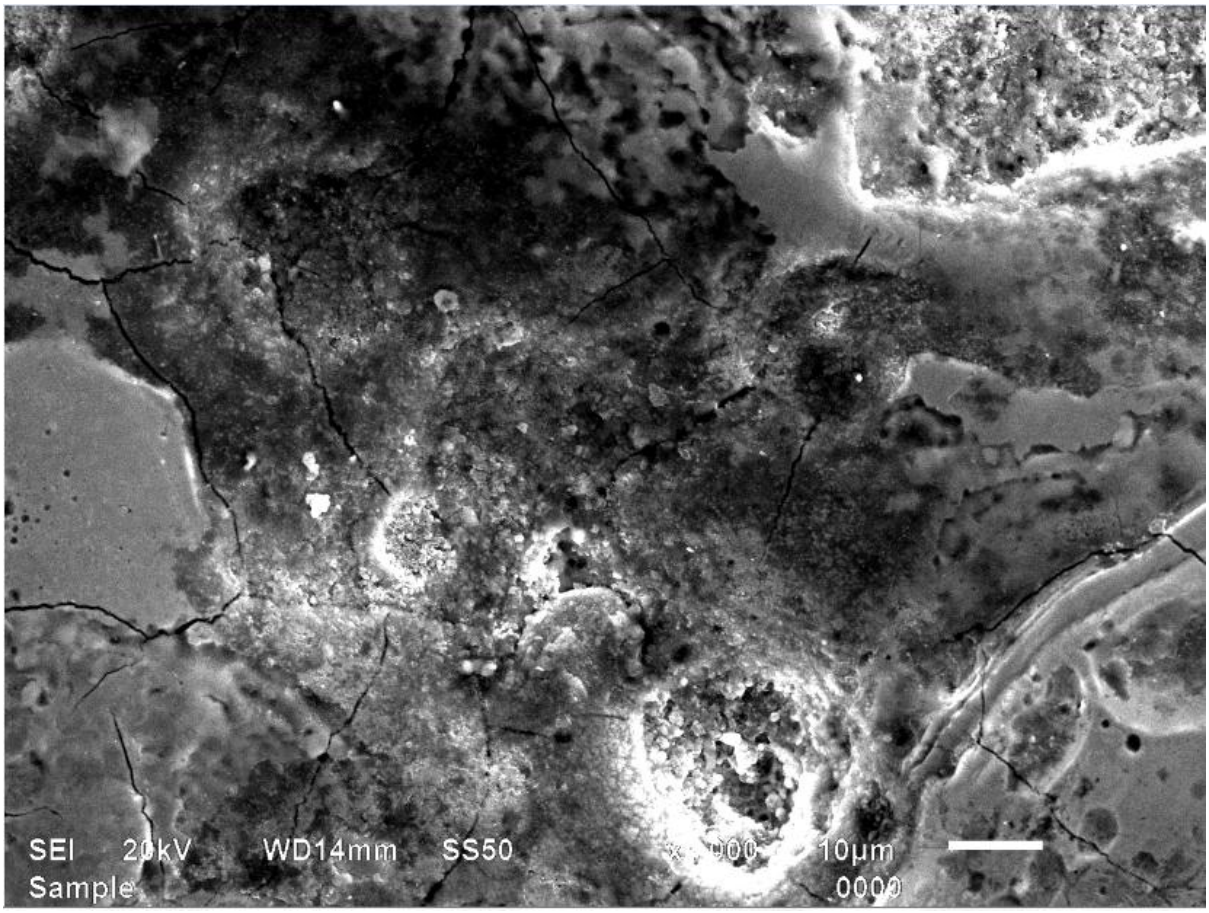

Figure 4.45: SEM micrograph at 1000× AISI 1045 machined with W-Cu electrode in kerosene with tungsten powder mixing. (I=5 Amp, Pulse on= 20µs, Powder concentration 10g/l)

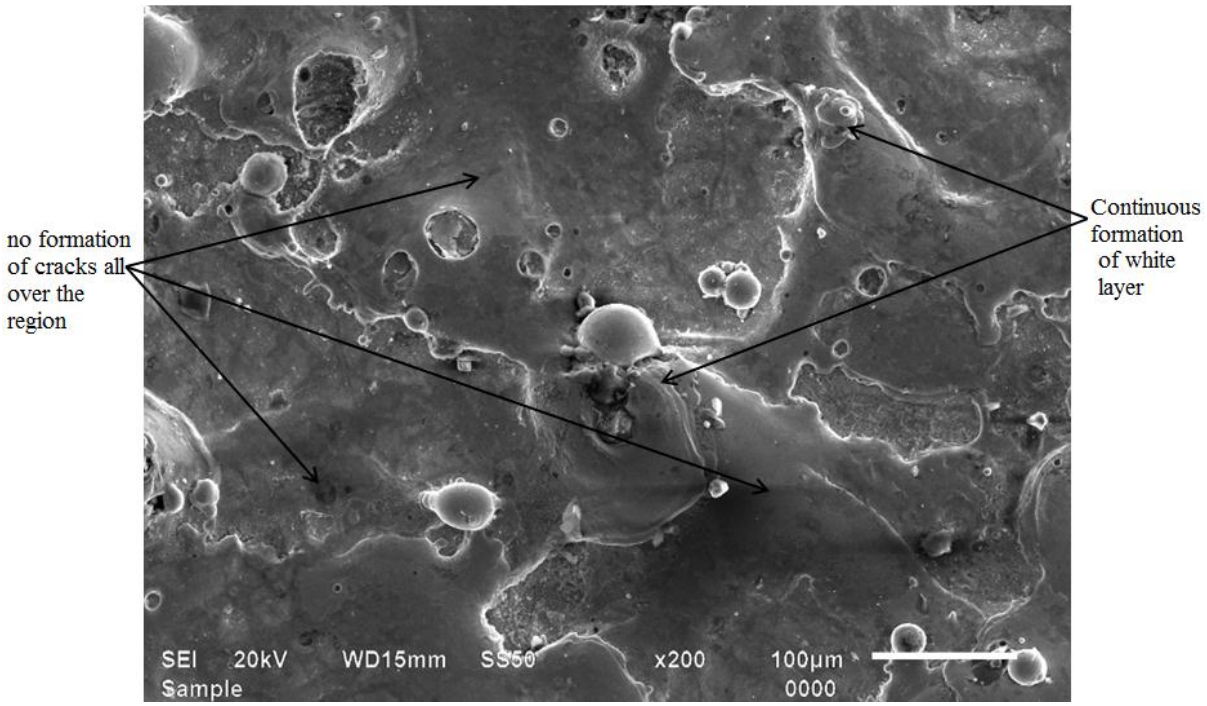

Figure 4.46: SEM micrograph at 200× AISI 1045 machined with Graphite electrode in edm oil with silicon powder mixing. (I=5 Amp, Pulse on= 100µs, Powder concentration 10g/l)

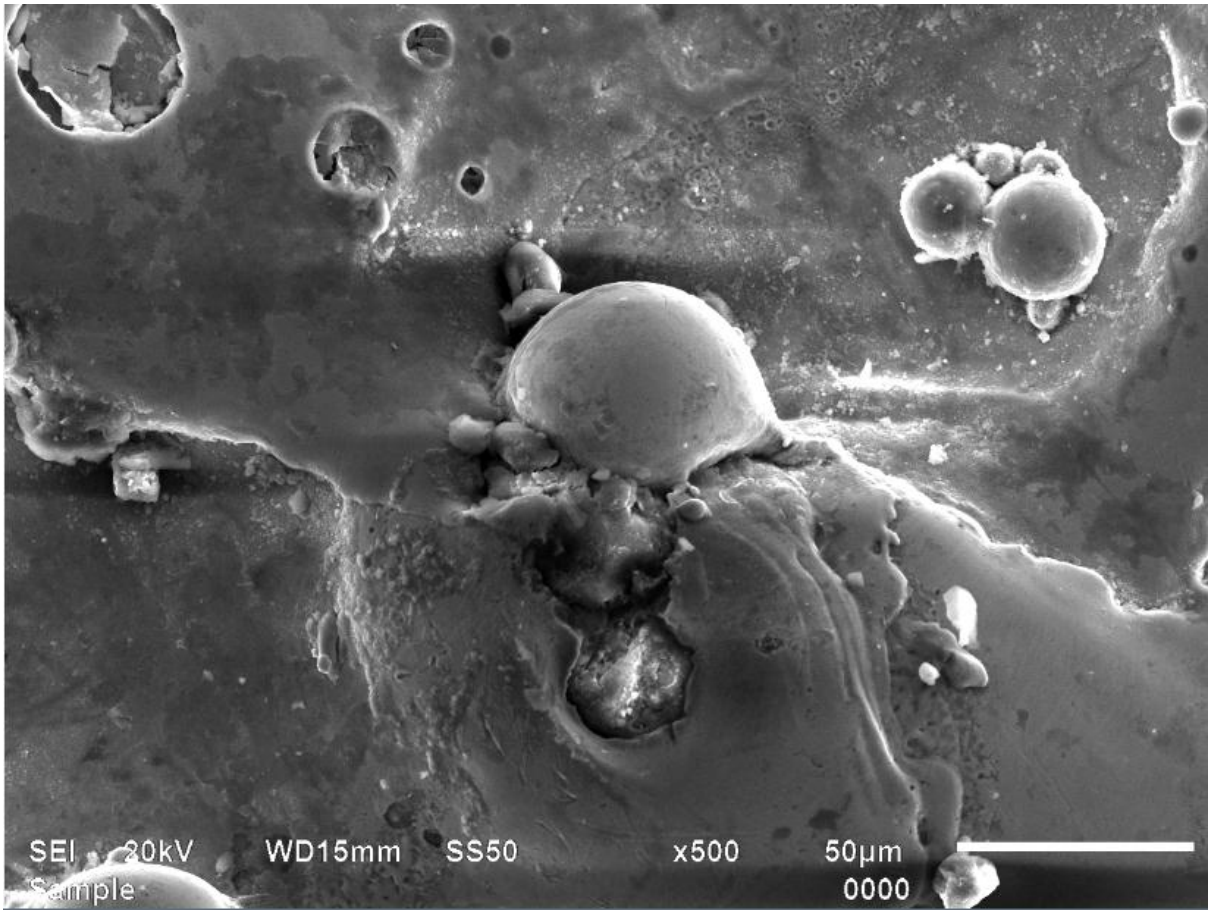

Figure 4.47: SEM micrograph at 500× AISI 1045 machined with Graphite electrode in edm oil with silicon powder mixing. (I=5 Amp, Pulse on= 100µs, Powder concentration 10g/l)

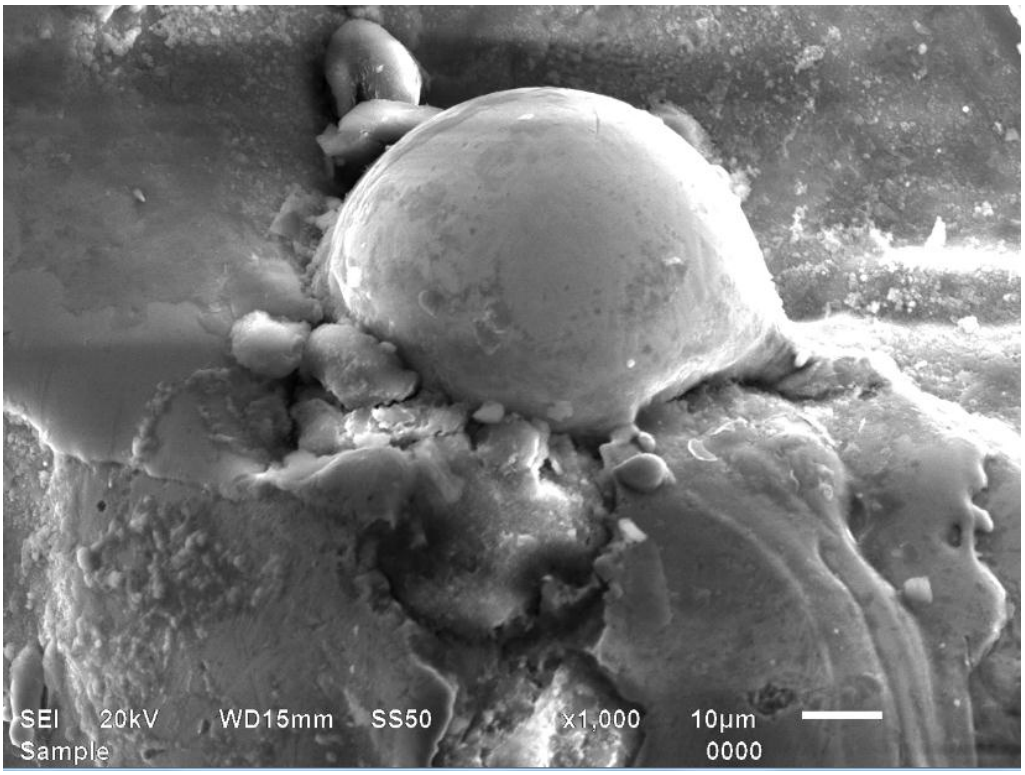

Figure 4.48: SEM micrograph at 1000× AISI 1045 machined with Graphite electrode in edm oil with silicon powder mixing. (I=5 Amp, Pulse on= 100µs, Powder concentration 10g/l)

SEM micrograph at 200×, 500× and 1000× of (hot die steel) with tungsten--copper electrode in kerosene with 5g/l powder concentration of graphite powder mixed in dielectric medium is shown in the Figure 4.31 -4.33. It shows the continuous formation of white layers one over another and cracks are present on these white layers. The reason for the continuous formation of white layers is high peak current and pulse on time. High peak current means more heat energy and high pulse on time means spark energy is continuously available for large period of time. Hence both the factors cause an impulsive force on the machined surface during sparking due to which materials are dispersed around the point where sparking takes place and thus white layers are formed. As spark energy is available for longer period of time, hence continuous formation of white layers occurs. The discharge between the tool and workpiece melts the material and material vaporises which in turn create altered layers of the cavity. The white layers are readily formed and it is stable on the surface. The white layers has fine grains and hard as it consists of some carbides. At high peak current and pulse on time, spark energy available is high and continuous. This produces thermal stress due to which cracks occurs on the machined surface or it might be due to large thickness of white layer because as the thickness of white layer increases, brittleness increases and thus fracture occurs more readily. The carbon transferred to the white layer is available from the graphite powder electrode or from the kerosene (dielectric) in case where HDS machined with W-Cu electrode in kerosene with Graphite powder mixing. (I 5Amp, Pulse on time 50µs, Powder concentration 5g/l). In case where HDS machined with Brass electrode in edm oil with silicon powder mixing (I=5 Amp, Pulse on= 20µs, Powder concentration 5g/l), it was observed that it has a good surface finish. Brass emerges as an electrode material which gives the desired surface finish. It can be seen in Figure 4.34–4.36, that there is no formation of cracks and crater size is small. The performance of graphite powder was found to be better than silicon powder in improving the surface roughness. The white spot are iron carbide (Fe_3C). It was also found that when Brass is used as electrode as compared to graphite and W-Cu, surface roughness improves. Figure 4.37-4.39 shows the SEM micrograph at HCHCr machined with W-Cu electrode in kerosene with silicon powder mixing. (I 7Amp, Pulse on time 100µs, Powder concentration 5g/l). It can be seen that cracks are present in more frequency as compared to that in case of 5 Amp. Further, Crater size is large. This is the reason why it has very rough surface. However; the micro hardness is quite good due to the formation of iron carbide (Fe_3C), manganese carbide (Mn_7C_3) and increase in carbon percentage. Figure 4.40-4.42 shows the SEM micrograph at 200× HCHCr machined with Graphite electrode in edm oil with tungsten powder mixing. (I=7Amp, Pulse on= 20µs,

Powder concentration 5g/l). Formation of white layers occurred all over the region on the surface. However pulse on time is less, frequency of crack is quite high as it is clear from the figure. It is because of high peak current. Figure 4.43-4.45 shows the SEM micrograph at AISI 1045 machined with W-Cu electrode in kerosene with tungsten powder mixing. (I=5 Amp, Pulse on= 20μs, Powder concentration 10g/l).In this case, the large number of micro cracks occurred all over the white region as well as black region. The SEM analysis shows the traces of Fe_2C and Mn_7C_3. However; manganese does not easily form carbides. But here it has replaced some atoms of iron to form compound with carbon. Figure 4.46-4.48 shows the SEM micrograph at 1000× AISI 1045 machined with graphite electrode in edm oil with silicon powder mixing. (I=5 Amp, Pulse on= 100μs, powder concentration 10g/l). In this case all the region is covered with almost white region and no formation of micro cracks are present on the machined surface. The white region represents the formation of iron carbide (Fe_3C). A bulk increase in carbon forms compound with iron but due to excess amount of carbon, the remaining carbon remains in the form of free graphite. As manganese is a weak carbide former thus it has formed any compound and remains as free manganese.

CHAPTER 5

RESULTS, CONCLUSIONS AND RECOMMENDATIONS

5.1 RESULTS

The effect of parameters i.e. workpiece, dielectric, electrode, pulse on time, current, powder concentration and powder were evaluated using ANOVA and factorial design analysis. The purpose of the ANOVA was to identify the important parameters in prediction of MRR, TWR, WR, micro hardness, surface roughness and measurement of overcut size. Some results amalgamated from ANOVA and plots are given below.

5.1.1 MRR

- Pulse on time was found the most significant factor with F value 24.08 and its contribution to MRR was 38.77% and followed by current (F value 12.78), electrode (F value 9.29), powder concentration (F value 6.11), powder (F value 5.45) were the factors that significantly affected the MRR which had contribution to MRR was 20.009%, 14.221%, 8.93956%, 7.845% and 4.5% respectively.
- Others two factors namely dielectric and workpiece material were found to be insignificant.
- In S/N ratio Current, pulse on and electrode are the factors which are found to be significant.
- The estimated mean value of MRR when six factors, namely, electrode material (W-Cu), Powder Concentration (10gm/l), current (7Amp), pulse on time (100μs), powder (silicon) were considered with 95% confidence interval was found to be 31.53 ± 0.5305mm^3/min.

5.1.2 TWR

- Powder concentration was found the most significant factor with F value 24.08 and its contribution to TWR was 20.358%.
- Powder Concentration (F value 10.23), pulse on (8.69), current (F value 7.76), powder (F value 6.44) and electrode (F value 6.39) are the factors that significantly affecting the TWR.
- Other factors such as workpiece material, dielectric were found to be insignificant.
- In S/N ratio, powder concentration was found to be the most significant factor affecting the TWR, followed by Pulse on time, current and electrode.

- The estimated mean value of TWR when four factors, namely, electrode (W-Cu) Powder Concentration (10g/l), Pulse on time (20µs) and powder (tungsten) were considered with 95% confidence interval was found to be 1.2 ± 0.112mm^3/min.

5.1.3 WR

- In S/N ratio, powder concentration was found to be the most significant factor affecting the WR, followed by electrode.
- In S/N ratio, all other factors except powder concentration and electrode were found to be insignificant.
- The estimated mean value of WR when two factors, namely, electrode (W-Cu) and Powder Concentration (0g/l) were considered with 95% confidence interval was found to be 0.18835 ± 0.0271.

5.1.4 SURFACE ROUGHNESS

- At centre position, powder concentration was found the most significant factor with F value 23.34 and its contribution to SR was 34.32413%.
- The other factors such as current (F value 12.15), pulse on time (F value 9.52), powder (F value 7.82) and electrode (F value 7.10) were found to be significant in surface roughness at centre position.
- All other factors such as workpiece and dielectric were found to be insignificant for surface roughness at centre position.
- The estimated mean value of surface roughness at centre position when current (3Amp), pulse on time (10µs), electrode (brass), powder concentration (10g/l) and powder (silicon) were considered with 95% confidence interval was found to be 4.651 ± 0.34 microns.
- At left position, powder concentration was found was found the most significant factor with F value 24.08 and its contribution to SR was 34.23%.
- The other factors such as current (F value 13.22), pulse on time (F value 9.38), electrode (F value 7.34) and powder (F value 7.29) were found to be significant in surface roughness at left position.
- All other factors such as workpiece and dielectric were found to be insignificant for surface roughness at left position.
- The estimated mean value of surface roughness at left position when current (7Amp), pulse on time (100µs), electrode (brass), powder Concentration (10g/l) and powder

(tungsten) were considered with 95% confidence interval was found to be 4.1128 ± 0. 23 microns.

- At right position, powder concentration was found was found the most significant factor with F value 24.08 and its contribution to SR was 34.23%.
- The other factors such as powder concentration (F value 23.34), current (F value 12.15), pulse on time (F value 9.52), powder (F value 7.82) and electrode (F value 7.10) were found to be significant in surface roughness at right position.
- All other factors such as workpiece and dielectric were found to be insignificant for surface roughness at left position.
- The estimated mean value of surface roughness at right position when current (7Amp), pulse on time (100μs), electrode (brass), powder Concentration (10g/l) and powder (tungsten) were considered with 95% confidence interval was found to be 4.4356 ± 0. 2186microns.

5.1.5 MICRO HARDNESS

- Powder concentration was found the most significant factor with F value 36.48 and its contribution to micro hardness was 35.61%
- The factors such as, current (F value 24.94), pulse on time (F value 16.46), electrode (F value 10.62) and powder (F value 7.15) are the factors that significantly affect the micro hardness at non-deposited region.
- All other factors such as workpiece and dielectric were found to be insignificant for micro hardness at non-deposited region.
- The estimated mean value of micro hardness at non-deposited region when current (7amp), pulse on time (100μs), electrode (W-Cu), powder concentration (10g/l) and powder (tungsten) were considered with 95% confidence interval was found to be 880.18 ± 3.813 HVN.
- The factors such as powder concentration (F value 34.74), current (F value 30.39), pulse on time (F value 19.64), electrode (F value 11.56) and powder (F value 8.09) were found to be significant for micro hardness at deposited region and all other factors studied in trials were found to be insignificant.
- The estimated mean value of micro hardness at deposited region when current (7amp), pulse on time (100μs), electrode (W-Cu), powder concentration (10g/l) and powder (tungsten) were considered with 95% confidence interval was found to be 1080.16 ± 3.6991HVN.

5.1.6 XRD ANALYSIS

HDS

- When HDS workpiece material was machined with W-Cu electrode in kerosene with graphite powder mixing (I 5Amp, Pulse on time 50µs, Powder concentration (5g/l), Cohenite synthetic (Fe_3C) was formed which increases the corrosion resistance and hardenability and reduce the stresses. Formation of chromium carbide reduces the mechanical stress build-up at the layer boundary. The increase in carbon content improves the hardness and strength of the surface. The increase in chromium reduces the stresses and improves the corrosion resistance.
- When HDS workpiece material was machined with brass electrode in kerosene with graphite powder mixing (I 5Amp, Pulse on time 50µs, Powder concentration 5g/l). Cohenite, synthetic (iron carbide), Cohenite synthetic (Fe_3C) was formed which increases the corrosion resistance and hardenability and reduce the stresses. The presence of cohenite increases the hardness of the surface. The increase in carbon content improves the hardness and strength of the surface. The increase in copper improves the resistance to corrosion. However copper has not formed compound with other elements. Silicon improves the oxidation resistance and strengthens the surface.

High Carbon High Chromium (HCHCr)

- When HCHCr workpiece material was machined with tungsten – copper electrode in kerosene with silicon powder mixing (I 7Amp, Pulse on time 100µs, Powder concentration 5g/l), the formation of cohenite, synthetic (iron carbide, Fe_3C) and chromium carbide ($Cr_{23}C_6$) takes place. The presence of cohenite (Fe_3C compound) increases the hardness of the surface. Corrosion resistance of steels improved and hardenability improved with chromium carbide. Formation of chromium carbide reduces the mechanical stress build-up at the layer boundary.
- When HCHCr workpiece was machined with graphite electrode in edm oil with tungsten powder mixing. (I=7Amp, Pulse on= 20µs, Powder concentration 5g/l), iron carbide (Fe_5C_2), chromium carbide ($Cr_{23}C_6$) and carbon (C60)was formed. The presence of Fe_5C_2 compound increases the hardness of the surface. Corrosion resistance of steels improved and hardenability improved with chromium carbide. The carbon improves the strength, wear resistance and hardness but reduces the toughness and ductility.

AISI 1045

- When AISI 1045 workpiece was machined with W-Cu electrode in kerosene with tungsten powder mixing (I=5 Amp, Pulse on= 20μs, Powder concentration 10g/l), Iron carbide (Fe_2C) and manganese carbide (Mn_7C_3) was formed. The presence of Fe_2C compound increases the hardness of the surface. The carbon improves the strength, wear resistance and hardness but reduces the toughness and ductility. Manganese does not easily form carbides. But here it has replaced some atoms of iron to form compound with carbon.
- When AISI 1045 workpiece was machined with graphite electrode in edm oil with silicon powder mixing. (I=5 Amp, Pulse on= 100μs, Powder concentration 10g/l), iron carbide (Fe_3C) and carbon(C) was formed. The presence of cohenite (Fe_3C compound) increases the hardness of the surface. The carbon improves the strength, wear resistance and hardness but reduces the toughness and ductility. Manganese contributes to the strength and hardness (but to a lesser degree than carbon).

5.1.7. MICROSTRUCTURE ANALYSIS

SEM micrograph carried out on 6 selected samples at three different magnifications, namely at 200×, 500× and 1000×. The continuous formation of white layers one over another can be observed and cracks are present on these white layers. The reason for the continuous formation of white layers is high peak current and pulse on time. Both the factors cause an impulsive force on the machined surface during sparking due to which materials are dispersed around the point where sparking takes place and thus white layers are formed. The white layers are readily formed and it is stable on the surface. It is observed that with increase in current and pulse on time, micro cracks on the white layer also increased. The reason of cracking is the existence of the internal stresses which were created at the time of the machining operation. Brass emerges as an electrode material which gives the desired surface finish. The performance of graphite powder was found to be better than silicon powder in improving the surface roughness. It is also observed that when current is increased, the crater size also increased.

5.1.8. MEASUREMENT OF OVERCUT

- Pulse on time was found the most significant factor with F value 32.23 and its contribution to SR was 43.65%.

- The factor such as powder concentration (F value 15.54) and current (F value 9.21) are the factors that significantly affect the overcut.
- All others factors such as dielectric, workpiece material electrode and powder were found to be insignificant.
- It is observed that overcut increases with increase in pulse on time, increase in current and powder concentration.
- In S/N ratio pulse on time was found to be the most significant factor affecting the overcut, followed by powder concentration and current.
- The estimated mean value of overcut when current (3amp), pulse on time (100μs), and powder concentration (0g/l) were considered with 95% confidence interval was found to be 0.123734 ± 0.0068398mm.

5.1.9. MEASUREMENT OF GEOMETRIC ACCURACY

- It is observed that the angle generated on the workpiece by the 90° tool front angle is more as compared to 120°.
- It is observed that when the tool front angle is small then more variation occurs in sparking at different places between the tool and workpiece and thus the angle generated on the workpiece is less accurate.

5.2. CONCLUSIONS

The following conclusions were drawn from the present study:

- The MRR are mainly affected by the pulse on time, current, electrode, powder concentration and powder.
- The TWR are mainly affected by the powder concentration, pulse on time, current, powder and electrode.
- In WR, powder concentration was found to be the most significant factor affecting the WR, followed by electrode.
- In micro hardness, powder concentration, current, pulse on, electrode and powder are the factors that significantly affect the micro hardness.
- Micro hardness increases with the addition of silicon, graphite and tungsten powder.
- Surface roughness was mainly affected by the powder concentration, current and pulse on time. When current increases, it causes more surface roughness.
- The factor such as powder concentration (F value 15.54) and current (F value 9.21) are the factors that significantly affect the overcut. It is observed that overcut

increases with increase in pulse on time, increase in current and powder concentration.

- It is observed that the angle generated on the workpiece by the 90° tool front angle is more as compared to 120°. It is observed that when the tool front angle is small then more variation occurs in sparking at different places between the tool and workpiece and thus the angle generated on the workpiece is less accurate.
- It is observed that when powder such as silicon, graphite and tungsten are added into the dielectric medium by varying powder concentration or different electrodes are used then it causes change in microstructure and different types of compounds or carbides are formed which enhances the surface properties of the workpiece.
- Thickness of cracks increased with increase in current.
- When current decreases, the surface finish increases. Brass electrode can be used to achieve high surface finish.
- Tungsten increases the hardness of the workpiece material to higher extent as compared to silicon and graphite.

TECHNICAL SPECIFICATION OF EDM MACHINE

The experiment has been conducted on Electrical Discharge Machine model T-3822M, Victory
Electromech, Kolhapur, India. Technical data of machine is as under:

1. Electrical Data

Supply voltage	415V, 3Ø, 50 Hz
Connected load	3 KVA
Open gap voltage output	135±5% V
Max. Machine current	12Amp
Current range	3 ranges of 4Amp each
Current adjustment	0-4Amp in each current range

2. *Machine Tool*

Height	1300mm
Width	730mm
Depth	840mm
Net weight	325 kg
Quill travel	150mm

3. Work Tank

Length	600mm
Width	350mm

SPECIFICATIONS OF MEASURING INSTRUMENTS

1. *OPTICAL EMISSION SPECTROMETER*

Make and model	Baird, DV-6, USA
Base	Iron, Aluminium, Copper
Medium	Argon gas
Accuracy	0.0001%

2. *PERTHOMETER*

Make and model	Mahr. M4Pi, Germany
Measurement method	Stylus
Profile resolution	100nm
Cut-off wavelength	0.8mm
Tracing length	4.8mm

3. *MICRO HARDNESS TESTER*

Make and model	Metatech, MVH-2, Pune, India,
Software used	Quantimet
Load	1 kg
Dwell time	20 sec

4. *SCANNING ELETRON MICROSCOPE*

Make and model	JSM-840A Joel, Japan
Magnification range	10× to 3,00,000×

5. *X-RAY DIFFRACTION TESTER*

Make and model	ME 210 LA 2, Rigaku corporation
Scan speed	5°/minute
Range of 2θ	5° to 100°

SPECIFICATIONS OF DIELECTRIC MEDIUM

1. Kerosene oil

Appearance	Clear, transparent, light
Density (kg/m^3)	817.28
Flash Point (°C)	40
Boiling Point (°C)	600
Viscosity (centistokes)	2.71

2. EDM oil

Appearance	Clear, light
Density (kg/m^3)	835
Flash Point (°C)	130
Viscosity (centistokes)	3.12
Specific gravity	0.78±0.04
Dielectric strength	45 kv

[1] Fuller J.E. (1996), "Electrical Discharge Machining", ASM Machining handbook, Vol. 16, pp. 557-564.

[2] Pandey P.C. and Shan H.S. (1995), "Modern Machining Processes", Tata McGraw Hill, New Delhi, India, ISBN 0-07-096553-9.

[3] Jain V.K. (2004), "Advanced Machining processes", Allied Publishers, New Delhi, India, ISBN 81-7764-294-4.

[4] Ho, K.H., Newman and S.T., (2003). "State of the art electrical discharge machining", International Journal of Machine Tools & Manufacture, Vol. 43, pp. 1287–1300.

[5] Jeswani, M.L. (1981), "Effect of addition of graphite powder to kerosene used as a dielectric fluid in electrical discharge machining", Wear, Vol.70, pp. 133-139.

[6] Zeid, A., O.A., (1997). "On the effect of electrod ischarge machining parameters on the fatigue life of AISI D6 tool steel", Journal of Materials Processing Technology, Vol. 68, No. 1, pp. 27–32

[7] McGeough, J.A., (1988). "Advanced Methods of Machining", 1st edition Chapman and Hall, USA ISBN 0-412-31970-5.

[8] Kunieda, M., Lauwers, B., Rajurkar, K. P. and Schumacher, B. M. (2005), "Advancing EDM through Fundamental Insight into the Process", Journal of Materials Processing Technology, Annals of CIRP, Vol. 54(2), pp. 599-622.

[9] Kumar, S., Singh, R., Singh, T.P. and Sethi,B.L.(2009). "Surface modification by electrical discharge machining: A review," Journal of Materials Processing Technology, Vol. 209, pp. 3675-3687.

[10] Lee, S.H. and Li,X.P. (2001)."Study of the effect of machining parameters on the machining characteristics in electrical discharge machining of tungsten carbide", Journal of materials processing Technology, Vol. 115, pp.344-358.

[11] Crookall, J R and Heuvelman, C J (1971), “Electro-discharge machining – the state of the art”, Annals of the CIRP, Vol. 20 (1), pp. 113-120

[12] Heuvelman, C.J. and Horn, B.L. (1974), “Review of Co-operative work on EDM in STCE of CIRP”, Annals of the CIRP, 23/2, 213.

[13] Lee, L. C., Lim, L. C. and Wong, Y. S. (1992), “Towards crack minimization of EDMed surfaces”, Material Processing Technology, Vol. 32, pp. 45-54.

[14] Longfellow, J.D., Wood, J.D. and Palme R.D. (1968), “Effect of Electrode Material Properties on Wear Ratio in Spark Machining”, Institute of Metals Journal, Vol. 96, No. 2, pp. 43.

[15] Zhao, W.S., Meng, Q.G. and Wang, Z.L. (2002). “The application of research on powder mixed EDM in rough machining”, Journal of Materials Processing Technology,Vol. 129, pp. 30-33.

[16] Wong, Y.S., Lim, L.C., and Tee, R.I. (1998). “Near mirror finish phenomenon in EDM using powder mixed dielectric.” Journal of Materials Processing Technology, Vol. 79, pp. 30-40.

[17] Kansal, H.K., Singh, S. and Kumar, P., (2007), “Effect of silicon powder mixed EDM on machining rate of AISI D2 die steel”, Journal of Manufacturing processes, Vol. 9, pp. 13-21.

[18] Kruth, J.P., Stevens, L., Froyen, L. and Lauwers, B. (1995). “Study on the white layer of a Surface machined by die sinking electro-discharge machining”, Annals of the CIRP, Vol. 44 (1), pp. 169–172.

[19] Narumiya, H., Mohri, N., Saito, N., Otake, H., Tsnekawa, Y., Takawashi, T. and Kobayashi,K. (1989). “EDM by powder suspended working fluid.” Proceedings of 9th ISEM, pp. 5-8.

[20] Mohri, N. Saito, N. and Higash, M. (1991). “A new process of finish machining on free surface by EDM methods”, Annals of the CIRP, Vol. 40, pp. 207-210.

[21] Pecas, P. and Henriques, E.A. (2003). “Influence of silicon powder mixed dielectric on conventional electrical discharge machining”, International Journal of Machine Tools and Manufacture, Vol. 43, pp. 1465-1471.

[22] Uno, Y. and Okada, A. (1997). “Surface generation mechanism in electrical discharge machining with silicon powder mixed fluid.” International Journals of Electrical machining No. 2, pp. 13–17.

[23] Klocke, F., Lung, D., Antonoglou, G. and Thomaidis, D., (2004). “The effects of powder suspended dielectrics on the thermal influenced zone by electro discharge machining with small discharge energies”, Journal of Materials Processing Technology,Vol.149, pp. 191–197.

[24] Wu, K.L., Yan, B.H., Huang, F.Y. and Chen, S.C. (2005). “Improvement of surface finish on SKD steel using electro-discharge machining with aluminium and surfactant added dielectric”, International Journals of Machining Tools Manufacturing, Vol. 45, pp. 1195–1201.

[25] Pecas, P., Henriques, E. (2008). “Effect of powder concentration and dielectric flow in the surface morphology in electrical discharge machining with powder mixed dielectric (PMDEDM)”, International Journal of Advanced Manufacturing Technology, Vol. 37, pp. 1120-1132.

[26] Kobayashi, K., Magara, T., Ozaki, Y. and Yatomi, T. (1992). “The present and future Developments of electrical discharge machining”, Proceedings of 2nd International Conference on Die and Mould Technology, Singapore, pp. 35-47.

[27] Sano, M., Yatsushiro, K., Okada, K. and Hihara, M, (2007) “Study of Surface modification by electrical discharge machining”, International Journal of Electrical Machining,Vol.12, pp. 9–15.

[28] Furutani, K., Sanetoa, A.,Takezawaa, Mohria, N. and Miyakeb, H. (2001). “Accretion of titanium carbide by electrical discharge machining with powder suspended in working fluid”, Journal of International Societies for Precision Engineering and Nano technology, Vol. 25, pp. 138-144.

[29] Simao, J., Lee, H.G, Aspinwall, D.K, Dewes, R.C and Aspinwall, E.N. (2003). "Work piece surface modification using electrical discharge machining", International Journal of Machine Tools & Manufacture, Vol. 43, pp. 121-128.

[30] Erden, A. and Bilgin, S. (1980). "Role of impurities in electric discharge machining", Proc. of 21st International Machine Tool Design and Research Conference, pp. 345-350.

[31] Kozak, J., Rozenek, M., Dabrowski, L. (2003). "Study of electrical discharge machining using powder suspended working fluid", Journal of Engineering Manufacture, Vol. 217, pp. 1597-1602.

[32] Chow,H.M., Yan B.H., Huang, F.Y. and Hung, J.C. (2000), "Study of added powder in kerosene for the micro slit machining of titanium alloy using electrical discharge machining", Journal of Materials Processing Technology, Vol. 101, pp. 95-103.

[33] Uno, Y., Okada, A. and Cetin, S., (2001), "Surface modification of EDMed surface with powder mixed fluid", 2nd International Conference on Design and Production of dies and molds.

[34] Ming, Q.Y. and He, L.Y. (1995). "Powder suspension dielectric fluid for EDM", Journal of Materials Processing Technology, Vol. 52, pp. 44-54.

[35] Jeswani, M.L. (1981). "Effects of the addition of graphite powder to kerosene used as the dielectric fluid in electrical discharge machining", Wear, Vol.70, pp. 133-139.

[36] Tzeng, Y., Chen,F.(2005)."Investigation into some surface characteristics of electrical discharged machined SKD-11 using powder suspension dielectric oil", The International Journal of Material Processing Technology, Vol. 170, pp. 385-391.

[37] Tzeng and Lee, C.Y.(2001). "Effects of Powder Characteristics on Electro discharge Machining Efficiency", The International Journal of Advanced Manufacturing Technology, Vol.17, pp. 586–592

[38] Kibria, G.,Sarkar, B.R., Pradhan, B.B. and Bhattacharyya, B. (2010). "Comparative study of different dielectrics for micro-EDM performance during micro hole machining of Ti-6Al-4V alloy", International Journal of Advanced Manufacturing Technology, Vol. 48, pp. 557–570

[39] Yeo, S.H., Tan, P.C. and Kurnia, W.(2007). "Effects of powder additives suspended in dielectric on crater characteristics for micro electrical discharge machining", Journals of Micro mechanics Micro engineering, Vol. 17, pp. N91–N98

[40] Wong, Y.S., Lim, L.C. and Tee, R.I. (1998). "Near mirror finish phenomenon in EDM using powder mixed dielectric", Journal of Materials Processing Technology,Vol.79, pp. 30-40.

[41] Furutani, K. (2003) "Electrical Conditions of Electrical Discharge Machining with Powder Suspended in Working Oil for Titanium Carbide Accretion Process", ISBN No: 981-04-8484-4, pp. 532-545.

[42] Yan, B.H. and Chen, S.L. (1993). "Effects of dielectric with suspended aluminium powder on EDM", Journal of the Chinese Society of Mechanical Engineers, Vol. 14, pp. 307 312.

[43] Prihandana, G.S., Mahardika, M., Hamdi, M., Wong, Y.S. and Mitsui, K. (2009), "Effect of micro powder suspension and ultrasonic vibration of dielectric fluid in micro-EDM process- Taguchi approach", International Journal of Machine Tools & Manufacture, Vol. 49, pp. 1035-1041.

[44] Kung, K.Y., Horng, J.T. and Chiang, K.T. (2009) "Material removal rate and electrode wear ratio study on the powder mixed electrical discharge machining of cobalt-bonded tungsten carbide" Int J Adv Manuf Technol ,Vol. 40, pp. 95–104.

[45] Mohri, N., Satio, N., Tsunekawa, Y. and Kinoshtia, N. (1993), "Metal surface modification by electrical discharge machining with composite electrode", CIRP Annals Manufacturing Technology, Vol 42, pp. 219-222.

[46] Singh, S., Maheshwari, S. and Pandey, P.C. (2004) ,"Some investigations into the electric discharge machining of hardened tool steel using different electrode materials", Journal of Materials Processing Technology, Vol.149, pp. 272–277.

[47] Marfona, J. and Wykes, C. (2000), "A new method of optimizing material removal rate using EDM with tungsten electrode", International Journal of Machine Tools & Manufacture, Vol. 40, pp. 153-164.

[48] Muttamara, A., Fukuzawa, Y., Mohri, N. and Tani, T. (2009), "Effect of electrode material on electrical discharge machining of alumina", Journal of Materials Processing Technology,Vol. 209, pp. 2545-2552.

[49] Mohri, N., TakeZawa, H., Furutani, K., Ito, Y. and Sata, T., (2000), "A new process of additive and removal machining by EDM with a thin electrode", CIRP-Annals-Manufacturing Technology, Vol. 40, pp. 123-126.

[50] Jeswani, M.L., Basu, S., (1976), "Electron microprobe study of deposition and diffusion of tool material in electrical discharge machining", International Journal of Production Research, Vol. 17, pp. 1-14.

[51] Pec¸as, P.,Henriques, E. (2008) "Electrical discharge machining using simple and powder-mixed dielectric: The effect of the electrode area in the surface roughness and topography" jo5rnal of materials processing technology 250–258 IDMEC, Instituto Superior T´ecnico, TULisbon, Av. RoviscoPais, 1049-001 Lisbon, Portugal.

[55] Roy, R.K., (1990), "A primer on the Taguchi method", Van Nostrand Reinhold, New York.